The Effects of Body Mass Index and Gender on Pelvic Stiffness and Peak Impact Force During Lateral Falls

by

Iris Levine

A thesis
presented to the University of Waterloo
in fulfillment of the
thesis requirement for the degree of
Master of Science
in
Kinesiology

Waterloo, Ontario, Canada, 2011

AUTHOR'S DECLARATION

I hereby declare that I am the sole author of this thesis. This is a true copy of the thesis, including any required final revisions, as accepted by my examiners.

I understand that my thesis may be made electronically available to the public.

Abstract

Fall-related hip fractures are a substantial public health issue. Unfortunately, little is known about whether the effective stiffness of the pelvis, a critical component governing impact force during lateral falls, differs substantially across different segments of the population. The objective of this thesis was to enhance the knowledge base surrounding pelvis impact dynamics by assessing the influence of gender and body mass index (BMI) on the effective stiffness of the pelvis, and on resulting peak loads applied to the hip, during sideways falls. Towards this end I conducted pelvis release trials (in which the pelvis was suspended and suddenly released onto a force plate) with males and females with low (<22) and high (>28) BMIs.

One resonance-based (k_{vibe}), and three force-deflection based (k_{1st}, $k_{combo\ 300}$, and $k_{combo\ opt}$) methods of effective pelvic stiffness estimation were examined. The resulting stiffness estimates, and peak forces sustained during the pelvis release experiments, were compared between each BMI and sex group.

The optimized force-deflection stiffness estimation method, $k_{combo\ opt}$ provided the strongest fit to the experimental data. Strong main effects of BMI ($f(1,13) = 10.87$, $p = 0.003$) and sex ($f(1,13) = 5.97$, $p = 0.022$) were found for this stiffness estimation method. Additionally, a significant BMI-sex interaction was observed ($f(3,6) = 5.31$, $p = 0.030$), with low BMI males having much higher stiffness estimates than any other group. Normalized peak forces were higher in low BMI participants than in high BMI participants ($f(1,13)=24.9$, $p<0.001$). Linear regression demonstrated that peak impact force was positively associated with effective pelvic stiffness ($\beta = 0.550$, $t(25) = 3.110$, $p=0.005$), height ($\beta = 0.326$, $t(25) = 2.119$, $p=0.045$) and soft tissue thickness ($\beta = 0.785$, $t(25) = 4.573$, $p<0.001$).

This thesis has demonstrated that body habitus and sex have significant effects on the stiffness of the pelvis during lateral falls. These differences are likely related to a combination of soft tissue and pelvic anatomical differences between BMI and sex groups. Pelvic stiffness, along with other easily collected variables, may be helpful in predicting peak forces resulting from lateral falls in the elderly. Differences in pelvic stiffness estimates between BMI and sex groups, and estimation method, necessitate careful consideration. These data will aid in selecting the most appropriate pelvic stiffness parameters when modeling impact dynamics for higher energy falls.

Acknowledgements

I am finishing my Master's degree in a pit of debt.

First I owe thanks to those who inspired me to try in the first place. Kelly Meyers and Christine Rieger, who showed me how much I loved puzzles and how little I loved patients. Drs. Carol Sames and Moshe Marko, who showed me you can use your passion for science to drive your life. Drs. Scott White, Dan Ramsey and David Mandeville, who taught me to examine the details, trust myself, and be my own advocate. Waterloo or bust, you encouraged me to strive for the best.

Second, I'd like to thank those who opened doors for me. Dr. Jennifer Durkin, for bringing me here, and instilling the importance of a work-life balance. Dr. Andrew Laing, who took me in when I was lab-less. You've seen me through my worst, and I can't think of anyone else who would have put up with me the way you did. My thesis committee, Drs. Clark Dickerson and Jack Callaghan, for providing perspective and breadth of experience.

And last, I am eternally indebted to those who provided so much emotional support during my time at Waterloo. My officemates, who got me through coursework, coffee runs and quarter-life crises. My labmates, for supporting me and serving my every whim. Lauren for sticking through countless ultrasounds. Mike and Jeff for building my contraptions. Shivam, Johnny and Kelly for doing the heavy lifting. My family, for sticking through the long phone calls, missed holidays and personal struggles.

Table of Contents

List of Figures

List of Tables

Chapter 1 Introduction

1.1 Falls in Obese and Aged Population

Older adults in North America are enjoying both increased life expectancy and booming population. The rate of hip fracture, however, has increased at a rate beyond that expected based on population statistics (Cummings and Melton 2002). Projections for the year 2050 indicate that hip fractures could occur at a rate of more than 21 million globally per year (Cummings and Melton 2002). From the age of 55 to 85, the incidence of hip fracture increases tenfold (Melton 1990). The population of active older adults can be expected to increase on-par with population growth, resulting in a large percentage of the population at greater risk of hip fracture (Cummings and Melton 2002). The number of obese older adults, however, is also increasing (Belanger-Ducharme and Tremblay 2005). While a large amount of body mass is generally seen as protective against osteoporosis-specific injuries such as proximal femoral fractures, the change in risk of hip fractures due to amount of body mass has not been mechanically quantified.

1.2 Scope of the Problem: Life Expectancy, Quality of Life and Economic Considerations

In the first year following vertebral or hip fracture, older adults are more likely to die than those who suffered no fractures, or a fracture of the rib, forearm or wrist (Ioannidis, Papaioannou et al. 2009). The hazard ratio (adjusted for frequency of fracture type) for prediction of death following a fracture is highest for hip fracture (3.52, 95% CI 1.54-8.03), followed by vertebral fracture (3.0, 95% CI 1.10-8.17) (Ioannidis, Papaioannou et al. 2009). The next highest indicators of likelihood of death are having four or more diseases, smoking status, and lack of physical activity, none of which have a hazard ratio above 2.0. Hip fractures are independent predictors of mortality; while co-morbid conditions might hasten death following a hip or vertebral fracture, a hip fracture alone can put an otherwise healthy patient at a higher risk for death. The proposed mechanism underlying these results is related to the immobility associated with a hip fracture, which increase the likelihood of infection,

as well as sparking a decline in overall physical and mental health. These figures suggest that something as common and unpredictable as a trip, slip or loss of balance can have a much greater effect on life expectancy than the many diseases of old age that are the focus geriatric medicine.

While the increased risk of death post-fracture decreases over time since the original hip fracture, the rate of co-morbid conditions and decreased quality of life remains higher than controls (Pande, Scott et al. 2006; Ioannidis, Papaioannou et al. 2009). Hip fracture patients scored more poorly than controls on both the Health Assessment Questionnaire (HAQ) and Short Form 36 (SF-36) at two years post-fracture ($p<0.04$) (Pande, Scott et al. 2006). Both the HAQ and SF-36 assessments are used to evaluate the physical and mental state of a disabled person, including their ability to problem-solve, live independently and move around their environment, all of which contribute to a quantitative assessment of quality of life. While some co-morbid conditions such as frailty or disease were frequent at baseline (prior to fracture) in hip fracture patients relative to controls, hip fracture patients were more likely to require residential or nursing home care in the years following the incident than controls. Two years post-fracture, only 34% of patients were able to walk independently, while 85% of controls were able to do so.

Economic analysis of the per-patient burden of hip fracture indicates that while the first hospitalization immediately following the incident ranges from $9,275 for long-term care residents to $12,675 for a community-dwelling resident forced to long-term care, these expenses increase greatly when extended care is included (Wiktorowicz, Goeree et al. 2001). The cost of re-hospitalization, rehabilitation, physician visits and home care add to a total of up to $50,000 in the first year post-fracture. Age, gender and living situation all contributed significantly to the determination of first-year costs. Of the patients studied, 13.8% were re-hospitalized within the first year, and 5.6% suffered a second hip fracture, both of which would increase the first-year costs of a hip fracture. Of those who initially lived independently, 15.5% were transferred to a long-term care facility, to a cost of $23,000

per year. In total, the approximate annual cost of care for all hip fractures in Canada was estimated at $650 million in the year 2001.

1.3 Thesis Purpose and Goals

One theory that has been proposed to explain the higher frequency of hip fracture in low body mass individuals is the positive correlation between BMI and BMD (Hayes, Myers et al. 1996; Gjesdal, Halse et al. 2008). However, other factors may play a role in this relationship. Soft tissue overlying the hip, the thickness of which co-varies with BMI, has been shown to be negatively correlated with effective pelvic stiffness and peak force following a sideways fall (Robinovitch, Hayes et al. 1991). The study of pelvic stiffness, therefore, may be an important factor in understanding how factors other than BMD influence the mechanical risk of lateral falls. However, as previous investigations have focused mainly on healthy, university aged participants with normal body mass composition, it is unclear whether existing data extends to segments of the population with low BMI (representing classic 'frail' older participants at high risk of hip fracture) or high BMI (representing a growing trend of obesity of older adults). Specifically, how much trochanteric soft tissue attenuates peak force during these falls has not been quantified for the low (<20) and high (>30) BMI population. Thus, the purpose of this thesis is to determine whether effective pelvic stiffness (calculated from both frequency response and force-deflection approaches) and peak force applied to the pelvis during low severity falls, is influenced by BMI and gender during low severity falls.

The first goal is to refine the pelvic stiffness estimation techniques previously used by Robinovitch et al. (Robinovitch, Hayes et al. 1991; Robinovitch, Hayes et al. 1997) and Laing et al. (Laing and Robinovitch 2010) by determining the optimal transition point (characterized by both force and deflection) between non-linear and linear stiffness regions. The first hypothesis is that the selection of a transition point based on the data from each trial will result in a better fitting model (as determined by improvement in r^2 value), which may be more sensitive to differences in BMI and gender. The

second hypothesis is that estimation of stiffness based on the free-vibration characteristics of the pelvis may also not be appropriate for the broader population. The complexity of the joints and mass segments of the effective pelvic mass may cause additional modes of oscillation that are not captured by an estimation which assumes only one mode of vibration. It is expected that the high BMI participants will have greater soft tissue damping of secondary vibrations. Therefore, poor estimation of secondary vibrations will be more apparent in low BMI participants than high BMI participants.

The second goal is to characterize pelvic stiffness (using the k_{1st} and $k_{combo\ opt}$ methods) and peak impact characteristics in low- and high-BMI fallers. It is hypothesized that participants with higher BMI will exhibit decreased effective stiffness of the pelvis. It is also hypothesized that female subjects will have lower effective pelvic stiffness than male subjects, which may be due to anatomical differences.

The third goal is to test whether or not the stiffness estimates derived in this study will be accurate for higher energy falls, and to see what factors can be used to predict peak force. Specifically, it is hypothesized that the stiffness estimates derived from the zero-centimeter force-deflection data will not differ from those based on the five-centimeter data. This will demonstrate that the stiffness estimates derived from the zero-centimeter data are appropriate for modeling higher energy impacts. The sixth hypothesis is that peak force, and peak force normalized to the effective mass of the pelvis will have significant differences between BMI groups. Specifically, the peak force will be higher in the high BMI group, but the normalized peak force will be higher in the low BMI group. The increased soft tissue depth of the high BMI participants will provide a greater reduction of effective pelvic stiffness than the low BMI group. When the effective mass of the pelvis is removed from the comparison, the low BMI participants will suffer higher peak forces related to the magnitude of their effective pelvic stiffness. The seventh hypothesis is that peak force can be predicted through a combination of easily collected variables, such as waist and hip circumference, height, weight and trochanteric soft tissue depth, as well as effective stiffness estimates.

Chapter 2 Literature Review

Only one in ten hip fractures results from an incident other than a fall from standing height (Grisso, Kelsey et al. 1991; Cummings and Melton 2002). While spontaneous fractures and fractures resulting from other causes such as automobile accidents do occur, the vast majority result from direct impacts to the lateral or posterolateral femur. While only 1-2% of all falls result in a fracture to the proximal femur, the high incidence of falls in older adults results in 24,000 hip fractures in Canada every year (Hayes, Piazza et al. 1991; Papadimitropoulos, Coyte et al. 1997).

2.1 Importance of Fall Mechanics

Directly lateral falls are commonly studied due to their real-life frequency and potential for hip fracture, though it has been argued that they are not associated with the highest impact force or velocity (Nankaku, Kanzaki et al. 2005). A study by Feldman and colleagues (2007), in which the floor underneath a participant was moved quickly in order to initiate a fall, resulted in lateral hip impacts in 93% of falls (N=44). This type of impact is associated with fracture of the femoral neck of the impacted femur. This is in contrast to the pelvic ring and ipsilateral acetabulum fractures associated with the lateral impact of an automobile crash (Beason, Dakin et al. 2003; Etheridge, Beason et al. 2005). This suggests that hip flexion angle, and the angle between the hip and the impact site (ground or car door) change the location of fracture, though the maximum load to fracture is similar.

While directly posterior falls are also frequent subjects of research, the highest fracture risk during this event is to the lumbar vertebrae rather than the hip or pelvis. Peak vertical force following a posterior fall from standing height have been reported to range from 3,250N (Nankaku, Kanzaki et al. 2005) to 7500N (Sran and Robinovitch 2008), with posterior falls accounting for 25% of vertebral fractures (Cooper, Atkinson et al. 1992). Only 17% of hip fractures, however, are the result of a

posterior fall, which is likely due to the increased thickness of soft tissues overlying the posterior aspect of the pelvis.

Nankaku and colleagues reported on a third fall direction of even greater potential for injury than either directly posterior or lateral falls (Nankaku, Kanzaki et al. 2005). Impact velocity and force have been reported to increase as a fall shifts from a directly lateral to an oblique landing position, putting the average impact velocity (SD) of an oblique (45° from posterior) direction fall at 2.25 (0.35) m/s, higher than either directly lateral (1.99 (0.32) m/s) or directly posterior (1.86 (0.21) m/s) falls . Possible explanations for this increase in velocity during oblique falls include a reduced ability to control the center of mass and limb movement when falling in the posterolateral direction, particularly in subjects with a higher proportion of fat mass (i.e. mass that does not contribute to muscular control of descent) (Corbeil, Simoneau et al. 2001). The resulting mean impact force of 2,497(457) N is higher than that observed for sideways (2,251 (442) N) (Nankaku, Kanzaki et al. 2005). In addition, a posterolateral directed load vector is associated with a low-fracture tolerance (Keyak, Skinner et al. 2006). However, the majority of hip fracture patients able to recall the direction of fall report falling sideways rather than posterolaterally (Lauritzen and Askegaard 1992; Nevitt and Cummings 1993).

The overwhelming majority of hip fractures, as determined by post-fracture patient reports, are caused by a directly lateral fall which impacts the hip (56%) (Nevitt and Cummings 1993). This injury and fall mechanism is associated with a population with lower BMI and weight, slower walking speed, lower bone mineral density (BMD) and poor triceps strength, all of which are characteristics of a frail older adult (Nevitt and Cummings 1993; Lloyd, Williamson et al. 2009). With the projected growth in this particular population, it is essential to assess impact biomechanics during sideways falls.

2.2 Types of Hip Fractures

Fractures of the proximal femur can be categorized as occurring at the femoral neck (cervical), between the greater and lesser trochanter (intertrochanteric), or distal to both trochanters (subtrochanteric)(Figure 2.1) (Marks, Allegrante et al. 2003). Studies by Pulkkinen and colleagues exposed which variables are associated with each type of fracture (Pulkkinen, Eckstein et al. 2006; Pulkkinen, Jämsä et al. 2008). Women more frequently suffer cervical fractures than men ($p=0.002$), and the relative significance of structural variables such as neck-shaft angle and femoral head and neck diameters differs between males and females. In most cases, some form of open reduction and fixation is required, particularly for older adults. In cases where the proximal end of the femur is displaced, total hip arthroplasty is typically required.

2.3 Factors that Effect the Mechanics of Proximal Femur Fractures

The way in which patients fall varies widely—the type of fall and angle of impact are both important factors in determining the risk of hip and vertebral fracture. While bone mineral density (BMD) is a consistent indicator of possibility of fracture (Marshall, Johnell et al. 1996), fall mechanics (i.e. the way in which a person falls) have a much stronger association with hip fracture risk. These factors include starting height and activity (sitting, standing, walking, etc.), ability to react (cognitive state and reaction time), and environmental factors which all contribute to impact velocity, impact force and area of body exposed to fracture risk (Nevitt and Cummings 1993; Hayes, Myers et al. 1996; Frick, Kung et al. 2010).

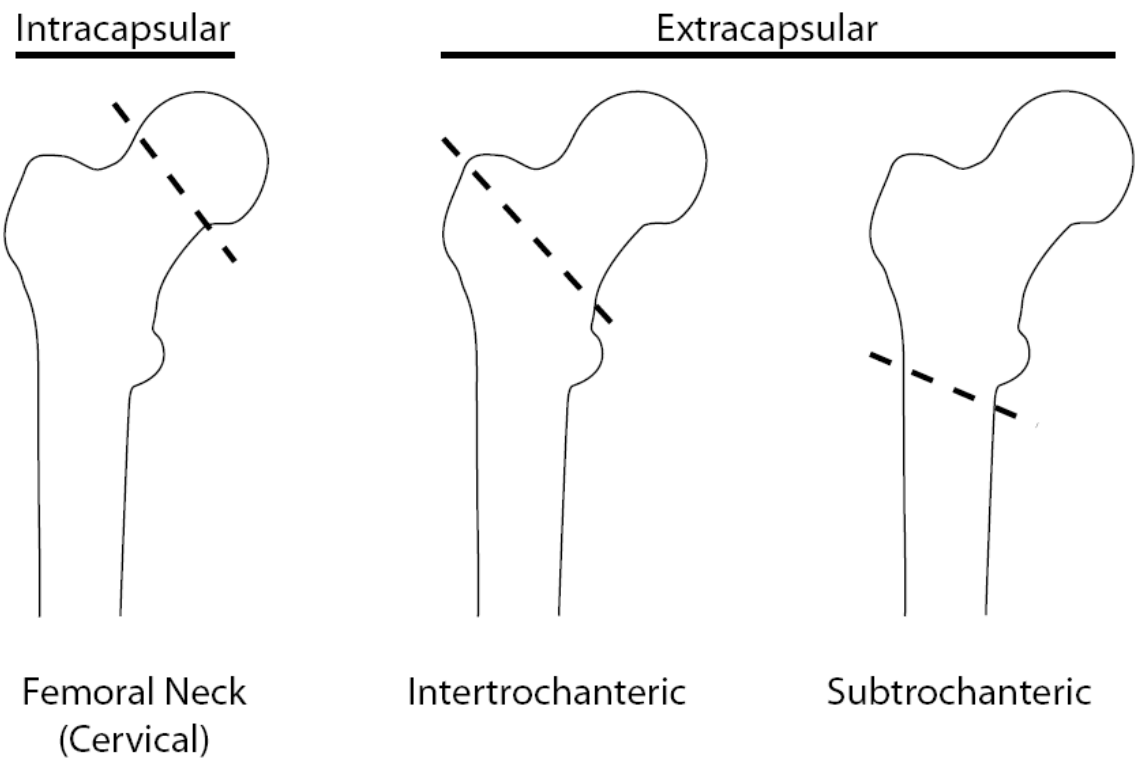

Figure 2.1 Proximal Femur Fracture Classes

Fractures of the proximal femur can be categorized as occurring at the femoral neck (cervical), between the greater and lesser trochanter (intertrochanteric), or distal to both trochanters (subtrochanteric) (Marks, Allegrante et al. 2003). Studies by Pulkkinen and colleagues exposed which variables are associated with each type of fracture (Pulkkinen, Eckstein et al. 2006; Pulkkinen, Jämsä et al. 2008). Women more frequently suffer cervical fractures than men ($p=0.002$), and the relative significance of structural variables such as neck-shaft angle and femoral head and neck diameters differs between males and females.

2.4 Hayes Risk Assessment Score

There are two components necessary to determine whether or not a fracture will result from a fall: tissue tolerance and applied loads. Tissue tolerance refers to the force sustainable by a tissue, such as a bone, prior to failure. Typically, this is the point at which catastrophic damage occurs (factors such as loading rate, direction, and bone material and structural properties influence how great the impact a bone can undergo prior to fracture. These factors will not be addressed in this thesis). The second factor required for estimating fracture risk is the load applied to the bone in question during a fall.

Hayes and colleagues devised a tool for fracture-risk prediction based on these two components (Hayes, Piazza et al. 1991; Hayes, Myers et al. 1996). The “factor of risk” is determined by the ratio of the expected service load to the failure load (the magnitude of the impact during a fall compared to the known fracture threshold of a bone). In the elderly population, climbing stairs has a risk factor as high as 0.6, while lifting heavy loads or falling on the hip can have a risk factor greater than 1.0 (Hayes, Piazza et al. 1991).

2.4.1 Tissue Tolerance

The fracture tolerance of the proximal femur has been examined experimentally in two primary load directions: vertical and lateral. Vertical loading corresponds to day-to-day expected activities such as walking and stair climbing, where the greatest amount of force is directed through the shaft of the femur. The fracture tolerance for older adults has been tested in cadaveric specimens. At a loading rate of 6.5 mm/sec, the average vertical fracture load is 4,420 (1,680) N in men and 2,910 (930) N in women (Lochmüller, Groll et al. 2002). Side-impact loads represent an impact configuration that may occur during an automobile crash or sideways fall. At the same loading rate, the average side-impact fracture tolerance for older adults is 4,230 (1,530) N in men, and 3,070 (1,060) N in women.

The load sustainable by the proximal femur and pelvis following lateral impact can be directly related to bone mineral density (Hayes, Piazza et al. 1991; Bouxsein, Courtney et al. 1995). Bone mineral density (BMD) can be easily determined via imaging techniques such as quantitative computed tomography (QCT) or dual-energy X-ray absorbtiometry (DXA). The results of such a test are commonly used to estimate the fracture risk of a patient by predicting tolerance of a bone for stress and strain. Compressive fracture loads at the proximal femur have been shown to strongly correlate with BMD determined by DXA (r^2=0.88 for BMD at the femoral neck, r^2=0.76 for total BMD) (Cheng, Lowet et al. 1998).

Gender and age are the strongest predictors of BMD ($p<0.001$) (Gjesdal, Halse et al. 2008). Male cadaveric proximal femur specimens have, in several studies, endured 1.5 kN more force prior to fracture than female specimens ($p<0.01$) (Cheng, Lowet et al. 1998; Lochmüller, Groll et al. 2002). The amount of lean mass is the next strongest determinant of femoral fracture risk ($p<0.001$) (Gjesdal, Halse et al. 2008). A one kilogram increase in lean mass across both gender and age groups studied (range 47-50 and 71-75 years of age) consistently correlated with BMD and bone mineral apparent density (BMAD, bone mineral content corrected for apparent bone size). This suggests that level of lean mass is predictive of fracture risk, regardless of skeletal size. A low level of fat mass (<20 kg) was also a significant indicator for increased risk of fracture in women of both age groups ($p<0.001$). Loss of more than 10% of body weight (from lifetime maximum weight to study baseline weight) has been shown to increase risk of hip fracture by twice in women aged 50 – 64 years(Langlois, Mussolino et al. 2001). In women older than 65, even a 5% reduction in body weight over the lifetime increased the risk of hip fracture by 50%.

Although low body mass is a classic risk factor for hip fracture risk, there are several cases in which BMI is not the most accurate tool for predicting fracture risk based on a BMI-BMD correlation. The correlation between fat mass and BMD is weaker in men (Kuwahata, Kawamura et al. 2008). Only trunk fat mass or limb (non-dominant arm) lean mass, and not limb fat mass can be used to accurately predict BMD. The BMD decrease after extreme weight loss is generally thought to correlate highly with the amount of weight lost (Fleischer, Stein et al. 2008), however, other research suggests that the BMD loss associated with extreme weight loss, gastric bypass surgery or cyclic weight gain and loss exceeds the amount expected for the body fat loss (Meyer, Tverdal et al. 1998; Carrasco, Ruz et al. 2009). Therefore, there are situations where estimation of BMD based solely on BMI is not reliable. Further, determination of BMD via QCT or DXA is not a practical test for all older adults that may be at risk for hip fracture following a fall.

2.4.2 Applied Loads

In order to predict the risk of fracture during a fall the loads applied to the tissues must be known. Towards this end, Robinovitch and colleagues developed “lateral pelvis release experiments” to evaluate the impact response of the pelvis to a short free-fall (Robinovitch, Hayes et al. 1991). The pelvis of a participant is gently suspended in a thin sling, then released suddenly onto an impact surface mounted to a force plate. An additional benefit to pelvis release experiments is the stabilization of the pelvis, which allows for controlled observation of pelvic deflection. The major drawback to the experiment is the low maximum height from which participants can be dropped in the interest of safety and repeatability of falling position.

Mathematical models have been developed to transform the free-fall data from pelvis release experiments into conditions that represent a realistic fall from standing height. The original model reported by Robinovitch et al. (1991) involves a mass, spring and damper, allowing the stiffness of the pelvis to be characterized as an oscillatory system, with force amplitude decreasing after the initial impact. The peak force predicted by this model, following a sideways fall from standing height (a free-fall of 0.7m), was 5,600-8,600 N across participants. Activation of the muscles of the trunk, which was theorized to increase the mass of the pelvis acting on the impact point (the effective mass) was later shown to have no effect either the experimental or predicted impact forces (Robinovitch, Hayes et al. 1997). An upright trunk position, involving lateral flexion of the spine and bracing with one arm, was also expected to increase the effective mass. However, no difference was found between the relaxed and upright postures, suggesting that either the mass and position of the trunk has no effect on peak force during a fall, or that the bracing arm reduces the contribution of the torso to effective mass.

A later mathematical model including not only a spring and damper associated with the central pelvic mass, but also two peripheral spring-damper pairs associated with the torso and lower body,

resulted in peak force predictions averaging 2,850 N, and ranging from 1150 N to 5288 N (Robinovitch, Hayes et al. 1997). This later investigation by Robinovitch and colleagues reports much lower predicted forces than the earlier (1991) study, which is due to the way in which the effective mass of the pelvis was determined. The earlier study estimated this value from the force of the pelvis contacting the force plate in a muscle-contracted state; this resulted in high effective mass approximations from the participants actively pushing on the force plate with their hip, rather than simply resting. This was corrected in later investigations, reducing both the effective mass of the pelvis and the predicted fall-from-standing-height forces.

There is some debate over the peak loads generated during the impact phase of a sideways fall. A finite element model produced by Majumder et al. (2007) estimated a peak force of 8331 N following a sideways fall from standing height. In contrast, experimental testing using a surrogate pelvis (simulated trochanteric soft tissue and proximal femur) at an impact velocity consistent with a fall from standing height produced total peak hip impact forces of 4,000 N and femoral neck impact forces of 2,500 N (Robinovitch, Hayes et al. 1991; Majumder, Roychowdhury et al. 2007). Comparing the low impact forces (1800-2600 N) reported by Nankaku et al. (2005) and the consistently higher values from the investigators discussed above, it is generally accepted that the force applied to the hip during a sideways fall in an elderly person is likely in the range of 3-8,000 N.

The use of mathematical models for the prediction of hip impact following a sideways fall from standing height requires the input of several variables. The magnitude of peak force is dependent on the velocity at impact, which is most simply dependent by the pre-fall height of the pelvis. Accordingly, free-fall dynamics have been used to estimate the impact velocity by equating potential energy ($PE=mgh$) with the kinetic energy at impact ($KE=1/2mv^2$). With the height of the pelvis ranging from 0.7 to 1.3 m, the impact velocity would range from 3.7 to 5.1 m/s. However, these values are not consistent with *in vivo* experiments because this estimation does not account for

eccentric muscle contractions of the trunk and lower limb (which would be utilized to maintain balance and reduce the velocity of descent). Bending at the hip, knee and ankle joints prior to, and during a fall, and bracing with the upper limbs are also neglected. From *in vivo* experiments, impact velocities of 2.0-5.0 m/s can be expected (Robinovitch, Hayes et al. 1991; Van den Kroonenberg, Hayes et al. 1995; van den Kroonenberg, Hayes et al. 1996; Feldman and Robinovitch 2007). Consequently, a lateral pelvis release drop height associated with an impact velocity of 1.0 m/s (for a 5 cm drop height) can be considered a model of low-severity, but clinically relevant falls. The impact forces resulting from the pelvis release experiments can be extrapolated to predict the impact resultant from a fall from standing height.

2.5 Factors that Influence Applied Loads

While the effect of soft tissues overlying the hip on the attenuation of impact force has been investigated in several studies, the results are not particularly relevant for clinical use. Bouxsein et al. (2007) reported that older women (mean 74.5 years) were more likely to suffer fracture if the layer of soft tissue overlying the hip was thinner ($p=0.04$). The trochanteric soft tissue thickness in this study, however, was determined via DXA, which may not be practical for clinicians without access to the appropriate equipment, and may not be indicated for some patients. The reduction in risk of hip fracture associated with an increase in soft tissue thickness was characterized as a 1.8-fold increase in epidemiological risk for fracture for a one-standard-deviation-decrease in soft tissue thickness. More recent research has found that trochanteric soft tissue depth did was not related to incidence of hip fracture in men (Nielson, Bouxsein et al. 2009). A relationship between soft tissue depth and location of fracture (men with lower soft tissue depth were more likely to have intertrochanteric fractures than femoral neck fractures) was found in this second study. The mechanical benefit of increased soft tissue thickness was not investigated in either case.

Robinovitch and colleagues quantified and modeled the mechanical properties of trochanteric soft tissue (Robinovitch, McMahon et al. 1995). The experiment found that for every 1 mm increase in soft tissue thickness, a 70 N reduction of peak force resulted. This translates to a theoretical 2450 N decrease in peak force from the specimen with the thinnest soft tissue thickness (8 mm) to the thickest (43 mm). Increased soft tissue padding also increased the time to peak load during *in vivo* experiments, and decreased the rate of loading (Robinovitch, Hayes et al. 1991). However, the generalizability of these results is limited as only a slim range of body sizes was investigated (BMI range of 21-28, determined from the heights and weights reported). Currently, 33.3% of Canadian adults can be described as overweight (BMI>24.5 but less than 30); additionally, 14.9% of Canadian adults have a BMI greater than 30, classifying them as obese (Belanger-Ducharme and Tremblay 2005). While the relationship between soft tissue thickness and peak femoral force was linear in the Robinovitch investigation, whether this relationship remains at greater soft tissue thicknesses has not been confirmed.

2.5.1 Pelvic Stiffness

Stiffness is a critical component of all models of impact for sideways falls. Stiffness can be characterized from the magnitude of force and deflection following impact, as well as the post-impact vibration characteristics of the structure. These values vary based on material and structural properties. Effective pelvic stiffness represents the in-series compliance of soft tissues overlying the proximal femur, the femur itself, the soft tissues in the articulations between the femur and acetabulum, and in the pelvic ring. The effective stiffness has been found experimentally to range up to 70,000 N/m (Robinovitch, Hayes et al. 1991). However, little research has evaluated how effective stiffness varies across different segments of the population

Low pelvic stiffness could reduce the risk of hip fracture for several reasons. Hooke's law describes the relationship between a spring (k), the amount of displacement of a structure (x), and the

restoring force (F_s). This relationship takes the form $F_s=-kx$. In the pelvis, this deflection is the medial-lateral compression of the pelvis between the tissue overlying the contacting hip and the contralateral hip (Figure 2.2). *In vitro* cadaveric studies have placed the deformation tolerance of the de-fleshed pelvis at 19.77% in a hip-flexed (e.g. automobile side impact) position, and up to 25% in a hip-extended position (Beason, Dakin et al. 2003; Etheridge, Beason et al. 2005). The spring constant, k, also has an elastic potential energy, $PE_{s,}$ which is the amount of energy that can be absorbed by the pelvis before causing plastic changes to the structure. This second relationship takes the form $PE_s=1/2kx^2$. Through *in vitro* testing (porcine soft tissue over a rigid metal anvil), thicker soft tissue samples (29 mm), have been shown to absorb up to 60% more energy from a fall height of 25-40 cm than thinner samples (20 mm) (Lauritzen and Askegaard 1992).

The effective stiffness of the pelvis during impact can be calculated if the stiffness of both the bony pelvis and soft tissue in series over the greater trochanter are known. This relationship takes the form $k_{total}=(k_{skeletal} \cdot k_{soft\ tissue})/((k_{skeletal} + k_{soft\ tissue})/2)$. The stiffness of the soft tissue is dependent on the contact area between the impact surface and the soft tissue (A), and the depth of the soft tissue (L). This is determined by the equation $k_{soft\ tissue} = AE/L$. Assuming no change in contact area, or the material-specific elastic modulus (E), the increased thickness of the soft tissue overlying the hip, for high BMI persons, would be associated with a decrease of the effective stiffness of the pelvis.

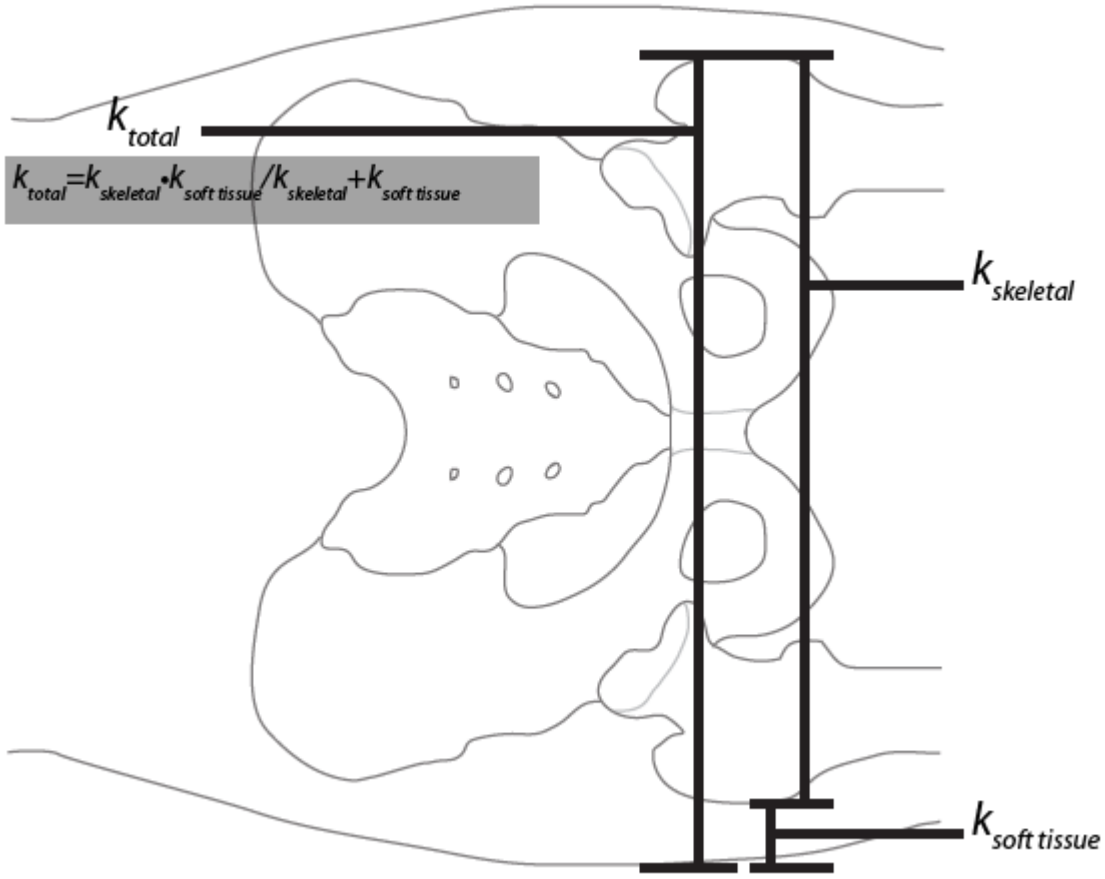

Figure 2.2 Effective Pelvic Stiffness Components

Effective pelvic stiffness is a term that describes the stiffness of the pelvis and surrounding soft tissues, as a system, during impact. The two major components of this system are $k_{skeletal}$ and $k_{soft\ tissue}$. The more dominant component, $k_{skeletal}$ is much stiffer, and has been found in previous studies to not be force-dependent (Robinovitch, Hayes et al. 1991; Laing and Robinovitch 2010). The second component, $k_{soft\ tissue}$, is associated with much lower stiffness values, and varies non-linearly with force. Effective pelvic stiffness is found by combining the component stiffnesses, $k_{total} = k_{skeletal} * k_{soft\ tissue} / k_{skeletal} + k_{soft\ tissue}$.

The magnitude of BMI is highly positively correlated with ultrasound measures of trochanteric soft tissue thickness (Maitland, Myers et al. 1993). The soft tissue thickness, in turn, is associated with a negative correlation with effective pelvic stiffness, i.e. as soft tissue thickness overlying the greater trochanter increases, it contributes to a reduction in pelvic stiffness. The stiffness of muscle varies non-linearly with rate of loading and magnitude of deflection, and reaches a maximum around 0.4

N/m (Best, McElhaney et al. 1994). Relative to the bony components of the pelvis, both muscle and fat, as well as connective tissues, have lower stiffness values. These soft tissues therefore contribute to a reduction in the overall effective stiffness of the pelvis.

The relationship between magnitude of force applied and stiffness is reported to be exponential below 250 N in females, and 200 N in males (Robinovitch, Hayes et al. 1991). Stiffness is relatively constant above this threshold. Several factors, including the effective mass of the pelvis, and trochanteric soft tissue thickness could contribute to the exponential increase in the low force region. One possible explanation is that the effective stiffness at the high force region is dependent on the stiffness of the skeletal components, which are much less compressible than soft tissue. A change in the magnitude of the area contacting the ground is another possible factor. Using the relationship $k = AE/L$, if the area increases from minimal contact (when the soft tissue first impacts the force plate) to an area equal to the height and width of the pelvis in the sagittal plane, this would result in increased stiffness. A 'bottoming-out' effect could also account for the maximal stiffness. Whether or not this transition point is a factor of gender, or simply the depth of soft tissue overlying the hip is not clear.

Other gender differences in effective pelvic stiffness are apparent. The men studied by Robinovitch and colleagues had an overall higher stiffness value than women at all impact magnitudes (Robinovitch, Hayes et al. 1991). Both females and males exhibited a decrease in pelvic stiffness with increased soft tissue thickness, though the correlation was stronger in women than men (R^3=0.828 in women, r^2=0.387 in men).

There are also skeletal and joint components which could influence pelvic stiffness. These include several ligaments connecting the femur to the pelvis, and the synovial membrane separating the two bones. The iliofemoral, pubofemoral and ischiofemoral ligaments surround the acetabulum, widening the contact area for the head of the femur while not restricting hip flexion, extension or internal and external rotation. The synovial membrane within the acetabulum, provides cushioning to the femoral

head and facilitates movement of the proximal femur. Collagen rich soft tissues such as cartilage and ligaments increase in tensile stiffness and strength, with both factors peaking in young adulthood and decreasing quickly after age 60 (Kempson 1982; Woo, Ohland et al. 1990). The stiffness and modulus of elasticity of the anterior cruciate ligament are 35.4% and 22.5% lower in ten females than ten males, respectively (Chandrashekar, Mansouri et al. 2006). It can be expected that similar effects on stiffness due to aging and gender occur in the pelvis, as well.

2.6 Estimating Pelvic Stiffness and Impact Characteristics

There are several methods that can be used to estimate the effective stiffness of the pelvis, and peak force following impact. The stiffness estimation methods used in this thesis are based on those described below. This thesis will also address the influence of gender and BMI on the estimation of effective pelvic stiffness, and the relationship between effective pelvic stiffness and peak lateral force on the hip resulting from an un-braced sideways fall.

2.6.1 Vibration Response of the Pelvis Following Peak Impact Force

Four models have been tested as possible predictors of the vibration response (spring and damping components) of the pelvis during sideways impacts. Mass-spring, Voight support, Maxwell support and standard linear solid support models (Figure 2.3) (Robinovitch, McMahon et al. 1995). The mass spring model, governed solely by effective mass and a spring constant, is the simplest model, though its lack of damping reduces its force prediction accuracy after the first half-period of oscillation. While all of the models over-predict peak force at low impact velocities, and under-predicted force at high impact velocities, the mass spring model satisfactorily predicted the initial peak force (the first oscillation of force post-impact) to within a mean (SD) difference from the experimental values of 2.2 (14.0) %, and time to peak force to within -12.8 (6.4) %. This indicates that the mass spring model is a fair predictor of the initial components of impact during a lateral fall.

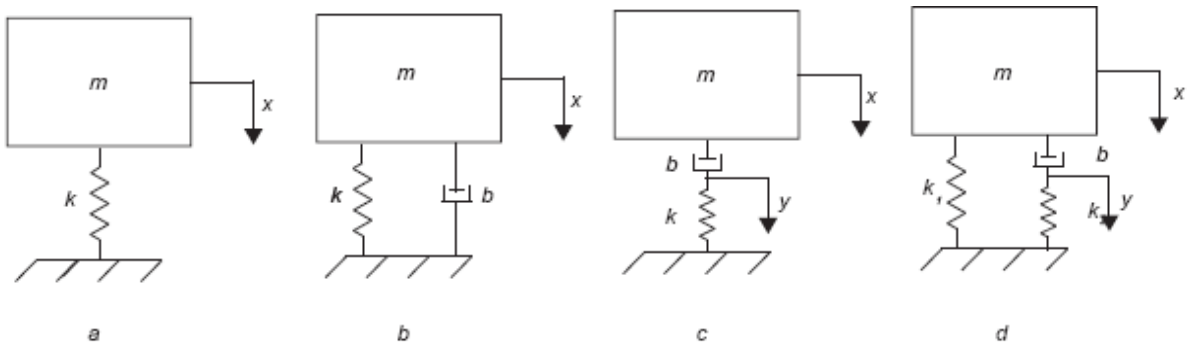

Figure 2.3 Mathematical Models for Support Structures that have been Investigated as Systems to Model that Impact Response of the Pelvis

The simplest model to explain the stiffness of the pelvis during impact is the mass-spring model (diagram a). While this model does not account for the decrease in magnitude of force oscillations after the initial impact, it provides a more accurate estimation of stiffness than the other models at higher impact velocities (2.2-2.6 m/s)(Robinovitch, Hayes et al. 1991). Two models include a damper, which more accurately matches the force oscillations after impact. The Voigt support model (diagram b) includes a damper (b) in parallel with the spring (k), while the Maxwell support model; (diagram c) includes a damper in series with the spring. While the Voigt model provides the best prediction of peak force at low impact velocities (1.0-1.4 m/s), it predicts much lower forces at high impact velocities when compared to experimental data. This could have a dangerous effect on models which predict the peak force associated with lateral falls. The Maxwell model provided more accurate force predictions at higher impact velocities than the Voigt model, but did not perform as well as the simpler Mass-spring model. The final model, the standard linear support model (diagram d) provided similar results to the mass-spring model, however, the difference was not consistently better or worse, and not different enough from the simpler model to justify the use of the more complex model. The focus of this study is the peak impact force rather than the force oscillations following the peak impact. For this purpose, the mass-spring model provides the best estimates while also having the simplest approach.

Inclusion of a damper in the Voigt model only improved force prediction at low impact velocities (<1.88m/s), but over-estimated the initial rate of loading. Experimental data indicates that a model capable of a step-response should be used, as the inclusion of a damper would provide. However, in practice, the more complex model has not proved useful for predicting impact responses at velocities consistent with a fall from standing height. The remaining Maxwell and standard linear solid models are more complicated still, including in-series damping components, but have been shown not to sufficiently improve peak force and rate of loading predictions. Majumder and colleagues have similarly found that the inclusion of damping components provide very minimal benefit (Majumder,

Roychowdhury et al. 2007). While an ideal model might mimic the step-response of true pelvic impacts, a model which accurately characterizes the initial impact characteristics (where applied loads and energy inputs are highest) would be better for the prediction of injury using a factor of risk approach (expected service load/failure load).

A limitation of the mass spring model, however, is that it has not been validated *in vivo* for populations outside of the normal body composition range (BMI <18.5 or >24.5). Excess soft tissue padding seen in the obese population could reduce the initial impact force and rate of loading, or increase the damping characteristics after the initial impact. It has been assumed in the development of protective hip padding products that the soft tissue padding over the greater trochanter of obese patients provides a degree of natural protection during fall-related impacts, but the amount of force attenuation and changes in effective stiffness have not been quantified.

The mass-spring models tested by Robinovitch and colleagues (Robinovitch, Hayes et al. 1997) estimate the stiffness of the pelvis assuming a single mode of vibration. The body segment impacting the ground during a lateral fall, however, is much more complex. The two hip joints, with three degrees of freedom each, may allow the pelvis and thigh segments to act as separate masses. This could result in multiple degree-of-freedom vibration, which is more complex than those modeled by the simple vibration-based technique used previously.

2.6.2 Force-Deflection Response of the Pelvis During Initial Impact

A second method of determining pelvic stiffness is based on the force-deflection properties of the pelvis between the start of impact and the point of peak force. Three methods are proposed by Laing and Robinovitch (Laing and Robinovitch 2010). The first is a first-order polynomial, fit through data points between the start of impact and the peak force using a least-squares regression approach. This produces a single estimate of pelvic stiffness, equal to the first derivative of the polynomial. This method is the simplest to compute, and would therefore be the easiest to apply to a force-prediction

method. A second approach fits a second-order polynomial for all deflection values between the start of impact and peak force using a least squares regression approach. The first derivative of this polynomial produces an infinitely force-varying stiffness estimate. This method accounts for non-linearities in stiffness as force increases. A third method applies a second-order polynomial to deflections between the start of impact and a transition of 300 N. This transition point is based on an observation by Robinovitch et al. that stiffness varies with force below 300 N, but plateaus at forces higher than this value(Robinovitch, Hayes et al. 1991). A first-order polynomial is applied to the remaining deflection values, the slope of which is tangential to the slope of the second-order polynomial at the transition point. This produces a force-varying stiffness value for deflections corresponding to forces less than 300 N, and a single stiffness estimate for forces above this transition. These values are determined by taking the first derivative of each piece of the composite polynomial.

The third force-deflection approach provided the most accurate force predictions, with a mean error of -0.3 (11.6)%. This approach also follows what is known about the elastic properties of biological tissues. An initial non-linear (toe) region smoothly transitions to a linear elastic region, which is followed by a plastic region at high levels of force and deflection. Similar piece-wise approaches have been applied in order to characterize the material properties of other deformable biological tissues (Chandrashekar, Hashemi et al. 2008).

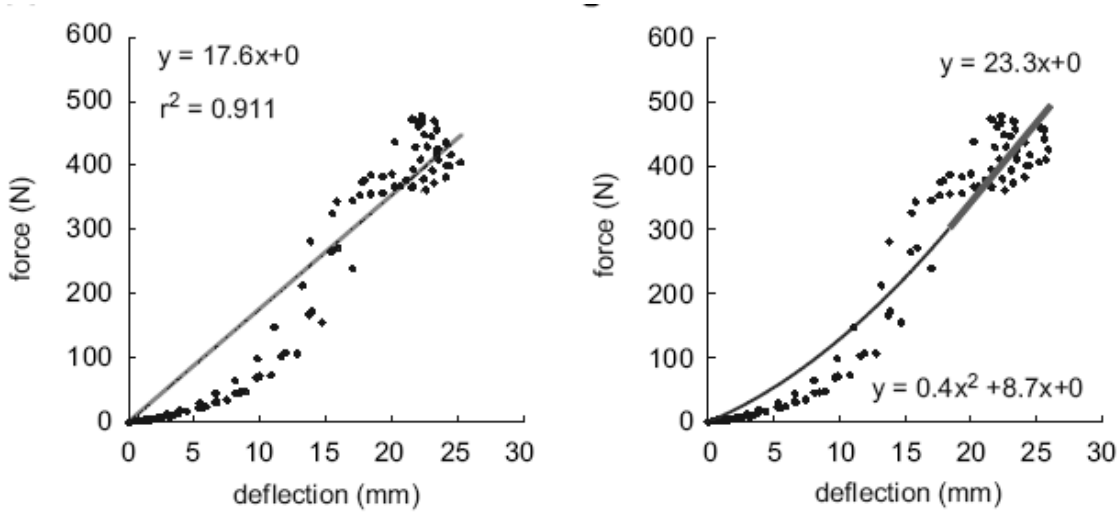

Figure 2.4 Force-Deflection Methods for Estimating Pelvic Stiffness

Two force-deflection based approaches for the estimation of pelvic stiffness are represented above. The approach on the left uses a first-order polynomial, fit through data points between the start of impact and the peak force. This produces a single estimate of pelvic stiffness, equal to the first derivative of the polynomial. In this case, the stiffness is estimated to be 17600 N/m. The method on the right fits a second-order polynomial for all deflection values between the start of impact and peak force. This polynomial is applied to deflections between the start of impact and a transition, which is 300 N in this case. A first-order polynomial is applied to the remaining deflection values, the slope of which is tangential to the slope of the second-order polynomial at the transition point. This produces a force-varying stiffness value for deflections corresponding to forces less than 300 N, and a single stiffness estimate for forces above this transition. These values are determined by taking the first derivative of each piece of the composite polynomial. In the case shown above, the peak stiffness is estimated to be 23300 N/m (Laing and Robinovitch 2010).

2.7 Peak Force Estimation

The effective pelvic stiffness calculated with these methods can then be used as an input into predictive models of impact force. Most simply, the theoretical relationship of energy conservation between the kinetic energy associated with the freefall of the pelvis and the potential energy of the pelvis (modeled as a simple mass-spring system) is the following:

$$KE = \tfrac{1}{2} mv^2 = \tfrac{1}{2} kx^2 \quad (1)$$

If the function relating force to stiffness, *F = -kx (rearranged to take the form x=F/k)* is substituted for *x* in equation one, an impact-velocity dependent relationship between applied force and stiffness can be found:

$$F_{peak} = v_{impact}\sqrt{mk} \quad (2)$$

This relationship can be used to find the force associated with a system with constant mass and constant stiffness, and an impact velocity dependent on freefall height. Several other factors (discussed in Section 0) can also modify peak force.

2.8 Current Methods to Reduce Hip Fracture Risk

There are several methods in clinical use for decreasing hip fracture risk, however, these may be influenced by body habitus. Several studies have indicated that increased soft tissue thickness over the greater trochanter may be useful in reducing the force on, and energy absorbed by the proximal femur during lateral falls (Lauritzen and Askegaard 1992; Lauritzen, Petersen et al. 1993; Robinovitch, McMahon et al. 1995). This is supported by theory. According to the relationship $k = AE/L$, an intervention which increases L of the pelvis during impact, while maintaining or decreasing A and E will reduce the effective stiffness. The effective stiffness of the pelvis and intervention, together, can be found using the relationship $k_{total} = (k_{pelvis} \cdot k_{pad})/(k_{pelvis} + k_{pad})$.

As a result, many manufacturers have developed wearable protective hip padding (PHP) in order to reduce hip fracture risk during a sideways fall. The most current investigations have shown that use of soft-shell PHP can decrease the peak pressure of a lateral, anterolateral or posterolateral fall by up to 80% (Choi, Hoffer et al. 2009; Cameron, Robinovitch et al. 2010). However, user compliance with PHP is not high for several reasons. Hayes et al. reported overall compliance (wearing hip protectors at morning, noon, and evening check-in sessions over length of subject hospital stay) of fall-risk subjects as 53% overall, and 23% at night (Hayes, Close et al. 2008). Reasons for non-compliance

included discomfort, loss or damage to hip protectors, lack of appropriate size or fit, or psychological factors such as body image.

Distribution of soft tissue around the pelvis may affect the protective capacity of PHP. For example, Laing et al. (2008) found that force attenuation decreases as BMI increases for oval soft shell hip protectors. In addition, Choi et al. (2010) found that low BMI (<18.5) women experienced twice the normalized peak pressure than high BMI (>25) women in an unpadded condition, though the normalized peak pressure was similar between BMI groups in a padded condition. Additionally, regardless of pad structure (i.e. soft, hard, or hybrid), multiple impacts reduced the effectiveness by at least 25%, and high variability in effectiveness and resilience existed in all brands of PHP tested. The data presented in this study suggests that PHP may not be resilient enough to provide daily protection for a high fall-risk patient, particularly when potential pad degradation due to cleaning procedures and frequent falls are considered.

The surface onto which a patient falls can have a large effect on the force applied to the proximal femur. Similarly to the effect of trochanteric soft tissue, low-stiffness floors in-series with the pelvis would reduce the total stiffness of the system during a sideways fall. Using a hip drop simulator with a free-fall of 0.7 m, Maki and Fernie (Maki and Fernie 1990) ranked several common floor types by their ability to reduce the impact to the hip during a fall. Thick, padded carpet topped the list as the most mechanically effective, however, a thick carpet pile can be a trip hazard. Other short pile carpets and unpadded carpets were also effective at reducing the peak impact, while wood, terrazzo, vinyl and linoleum were ranked least effective. The peak impact reduction between the most compliant surface (thick pile padded carpet) and least compliant surface is nearly 25%. However, all surfaces produced impacts well above the fracture threshold. Similarly, Sran and colleagues performed tether-release experiments, in which a subject falls from a tether-supported standing position (with a slight lean angle of 15º posterior) (Sran and Robinovitch 2008). The foam samples used represent a range of

stiffness consistent with that of commonly used floor types. Foams of 95, 67, and 59 kN/m stiffness produced force attenuations of 15.4% (2.2%), 20.3% (3.0%) and 34.4% (1.8%) from the rigid floor condition. Consistent with the research of Maki and Fernie, the force attenuation provided by traditional compliant surfaces may not be sufficient to prevent a fracture. However, novel compliant flooring systems may be more effective at attenuating impact force whilst having minimal effects on balance and mobility (Laing and Robinovitch 2009).

Similar to the results from Laing et al. (2008), the magnitude of force attenuation provided by low-stiffness floors would be expected to be decreased for high-BMI fallers relative to low-BMI fallers. With thick soft tissue contributing to a low pelvic stiffness, the change between impact surface stiffness of, for example, 67,000 and 59,000 N/m (as studied by Sran et al. 2008) would have a negligible effect on the effective stiffness of the system during impact. For example, for a low BMI faller with effective pelvic stiffness of 70,000 N/m, the 67,000 N/m surface would provide a 2,500 N/m reduction in effective stiffness, while the 59,000 N/m floor would provide a 6,000 N/m reduction in effective stiffness. For a high BMI faller with pelvic stiffness of 40,000 N/m, these surfaces would provide no decrease in effective stiffness. Using a hypothetical floor with a stiffness of 20,000 N/m, a 56% reduction in effective stiffness would be achieved for the low BMI faller, while only a 35% reduction in effective stiffness would occur for the high BMI faller.

Chapter 3 The Influence of BMI and Gender on Pelvic Stiffness and Peak Loads During Sideways Falls

3.1 Introduction

With the incidence of hip fracture reaching 21 million per year, globally, investigations into the mechanics of the injury are becoming increasingly important (Melton 1993; Cummings and Melton 2002). At the same time, however, the population at greatest risk for hip fracture is changing. The incidence of obesity is increasing amongst Canadians as a whole (Belanger-Ducharme and Tremblay 2005), and the mechanics of falls in the obese elderly have not been widely investigated. While a large amount of body mass is generally seen as protective against osteoporosis-specific injuries such as fractures of the proximal femur, the change in mechanical risk of hip and vertebral fracture due to amount of body mass has not been quantified. Understanding the effect of body mass on sideways falls, and consequent hip fractures, is therefore key to controlling the incidence of this injury.

Previous studies by Robinovitch and colleagues (1991) utilized a technique called "pelvis release experiments" to safely mimic the impact of a sideways fall in order to quantify impact characteristics such as peak force and loading rate, as well as pelvic stiffness. A one millimeter increase in trochanteric soft tissue thickness has been shown to reduce the peak impact of a sideways fall by 70 N (Robinovitch, McMahon et al. 1995). A negative correlation between soft tissue thickness and pelvic effective stiffness (r^2=0.828 in women, r^2=0.387 in men) likely contributes to this reduction in peak force, allowing more energy absorption by the soft tissue (Robinovitch, Hayes et al. 1991). Pelvic support systems have previously been modeled with four mathematical approaches (Figure 2.3), with the simple mass-spring model satisfactorily predicting the initial peak force (the first oscillation of force post-impact) and time to peak force. The mass-spring model is therefore a good predictor of the

initial components of impact during a lateral fall in normal-weight adults (Robinovitch, McMahon et al. 1995; Majumder, Roychowdhury et al. 2007).

Stiffness is a critical variable in determining force applied to the hip during a sideways fall, and defining how much energy can be absorbed by the system without damage. Hooke's law, which describes the relationship between a spring (k), the amount of displacement of a structure (x), and the restoring force (F_s), dictates how much deflection a structure is allowed while still maintaining an elastic state. This relationship takes the form $F_s=-kx$. In the pelvis, this deflection is the medial-lateral compression between the soft tissue overlying the contacting hip, and the contralateral hip. *In vitro* cadaveric studies have placed the deflection tolerance of the pelvis at 19.77% in a hip-flexed (e.g. automobile side impact) position, and up to 25% in a hip-extended position (Beason, Dakin et al. 2003; Etheridge, Beason et al. 2005). The spring constant, k, also has an elastic potential energy, PE_s, which is the amount of energy that can be absorbed by the pelvis before causing plastic changes to the structure. This second relationship takes the form $PE_s=1/2kx^2$. Through *in vitro* testing (porcine soft tissue over a rigid metal anvil), thicker soft tissue samples (29 mm), have been shown to absorb up to 60% more energy from a fall height of 25-40 cm than thinner samples (20 mm) (Lauritzen and Askegaard 1992).

Effective pelvic stiffness represents the in-series compliance of soft tissues overlying the proximal femur, the femur itself, the soft tissues in the articulations between the femur and acetabulum, and in the pelvic ring. The effective stiffness has been found experimentally to range between 16,000 and 70,000 N/m, (Robinovitch, Hayes et al. 1991; Robinovitch, Hayes et al. 1997; Laing and Robinovitch 2010). While it has been previously shown that increased trochanteric soft tissue depth is associated with a decrease in pelvic stiffness(Robinovitch, Hayes et al. 1991), none of the participants included in the studies represented members of the overweight or underweight population.

Two methods of effective pelvic stiffness estimation have been previously been explored: the first estimates a pelvic stiffness dependent on the resonant characteristics of the pelvis after peak impact force(Robinovitch, Hayes et al. 1991; Robinovitch, Hayes et al. 1997; Laing and Robinovitch 2010). The second method of estimation is dependent on the force-deflection properties of the pelvis between the start of impact and peak impact force. Three force-deflection methods have been studied by Laing and colleagues (2010). The first utilizes a first-order polynomial, fit through data points between the start of impact and the peak force. This produces a single estimate of pelvic stiffness, equal to the first derivative of the polynomial. The second method fits a second-order polynomial for all deflection values between the start of impact and peak force. This provides a force-dependent stiffness estimate with no plateau. A third uses the same second-order polynomial for all deflections between the start of impact and a transition point of 300 N. A first-order polynomial is applied to the remaining deflection values, the slope of which is tangential to the slope of the second-order polynomial at the transition point. This produces a force-varying stiffness value for deflections corresponding to forces less than 300 N, and a single stiffness estimate for forces above this transition. These values are determined by taking the first derivative of each piece of the composite polynomial. Previously, the third force-deflection (utilizing a piece-wise polynomial fit with a transition of 300 N) provided the most accurate predictions of peak force (Laing and Robinovitch 2010).

While these pelvic methods have produced similar effective stiffness estimates in the normal-weight population, it is unknown how the results of each method will be affected by the depth of soft tissue and pelvic mass associated with low and high BMI fallers. It is also unknown whether the gender differences in pelvic stiffness observed in normal BMI fallers also exist for high and low BMI patients. Finally, it is unclear whether the relationship between effective pelvic stiffness and peak force is maintained in patients outside the ‘normal’ BMI range.

My hypotheses are that:

1. (a)The methods of characterizing pelvic stiffness by fitting the force-deflection data with a piecewise-polynomial fit will match more strongly with the actual data than a simpler, first-order approach, with the quality of fit measured as mean squared error. (b)Further, a piecewise-polynomial fit that optimizes the transition point to the actual data will provide a better fit than one that has a singular transition point for all participants.
2. Using k_{1st} as a gold standard comparator, the estimation of stiffness based on the free-vibration characteristics of the pelvis will not be appropriate for low BMI participants. The complexity of the joints and mass segments of the effective pelvic mass in this low BMI population may cause additional modes of oscillation that are not captured by an estimation that assumes only one mode of vibration.
3. Members of the high BMI group will have lower pelvic effective stiffness than the low BMI group.
4. The female subjects will have lower effective pelvic stiffness than the male subjects. This may be due to differences in soft tissue thickness, or other in-series compliant tissues.
5. The optimal transition point (measured in centimeters of deflection, and Newtons of force) will be influenced by gender and BMI.
6. The stiffness estimates derived from the zero-centimeter force-deflection data will not differ from those based on the five-centimeter data. This would demonstrate that the stiffness estimates derived from the zero-centimeter data are appropriate for higher energy impacts.
7. Absolute peak force during pelvis release trials will be higher in the high BMI group, but the peak force normalized by the effective mass of the pelvis will be higher in the low BMI group.

8. Peak impact force can be predicted through a combination of easily collected anthropometric variables in addition to effective mass, and stiffness of the pelvis.

3.2 Methods

A list and explanation of all variables used in this study is presented in Table 1.

3.2.1 Participants

Twenty-eight participants were recruited for classification into either a low Body Mass Index (BMI) (<22) or high BMI (>28) group, with seven men and seven women in each group (Table 2). The mean (SD) BMI for each group was: high BMI females, 34.1 (4.7); low BMI females, 19.5 (1.8); high BMI males, 33.2 (2.3); low BMI males, 20.5 (1.5). These BMI groups represent portions of the population for which no data regarding impact characteristics and pelvic stiffness has been reported(Robinovitch, Hayes et al. 1991; Laing and Robinovitch 2010), and represent significantly different populations from one another ($f(1,13) = 166.821$, $p < 0.001$). Young adult participants with a mean age of 22.4 (2.7) years were recruited because of their lower risk of osteoporosis related injury compared to their older adult counterparts. Participants were excluded for reasons including musculoskeletal injury in the past year that could affect their ability to complete the experimental trials, lifetime hip, pelvic or spinal fracture, or other health conditions which would make participation unsafe. All participants provided written informed consent. This study was approved by the Office of Research Ethics at the University of Waterloo.

3.2.2 Instrumentation and Experimental Protocol

After providing written informed consent, the participants changed into loose athletic shorts. Participant height, weight, hip and waist circumferences were recorded, to the nearest 0.5 centimeters. Only height was significantly different between gender groups ($f (1,13) = 34.35$, $p<0.001$), while weight ($f (1,13) = 86.16$, $p<0.01$), waist circumference ($f (1,13) = 100.20$, $p<0.001$), and hip circumference ($f (1,13) = 118.60$, $p<0.001$) were significantly different between BMI and not gender

groups. Participants completed a short health questionnaire regarding medical history and current health status, confirming the information provided to the researcher via telephone conversation prior to the data collection session. At this point, the collection session for one participant was delayed due to slight bruising over the hip due to recreational sports. No other participant reported any current or past injury to the femur, pelvis or spine.

Table 1 Variables

	Variable Name	Variable Description
Independent Variables	Gender	A categorical between-subjects factor with two levels (male, female)
	BMI	A categorical between-subjects factor with two levels (low, high)
Potential Covariates (continuous variables)	Height	The height of the participant, in meters
	Body Mass	The mass of the participant, in kilograms
	$BMI_{continuous}$	Body mass index, BMI = Body mass/(Height^2)
	Waist	The waist circumference of the participant, in centimeters
	Hip	The hip circumference of the participant at the level of the greater trochanter, in centimeters
	Waist-Hip Ratio	WHR = W/H
	Soft Tissue Thickness	The depth of trochanteric soft tissue, determined via two-dimensional ultrasound, in centimeters
	Effective Mass of the Pelvis ($M_{neutral}$)	The force of the resting pelvis, in the position described in Section 3.2.2.1
Dependent Variables (continuous variables)	T_{imp}, F_{imp}, D_{imp}	The time (s), force (N) and deflection (mm) at the beginning of impact
	T_{max}, F_{max}, D_{max}	The time (s), force (N) and deflection (mm) at peak impact force
	F_{min}	The force (N) at the first minimum of oscillation following peak force.

	F_{end}	The force (N) at the end of the pelvis release trial. This is not significantly different from the effective mass of the pelvis
	$k_{1st\ est}$	The stiffness estimate (N/m) determined using the k_{1st} stiffness estimation method
	$k_{combo\ 300\ peak}$	The stiffness estimate (N/m) in the high-deflection region determined using the $k_{combo\ 300}$ stiffness estimation method
	$k_{combo\ peak}$	The stiffness estimate (N/m) in the high-deflection region, determined using the $k_{combo\ opt}$ stiffness estimation method
	$L_{deflection}$	The transition point, in centimeters of deflection
	L_{force}	The transition point, in Newtons of force
	$L_{normmax}$	L_{force}, normalized by the effective mass of the pelvis
	$L_{normpelvis}$	$L_{deflection}$, normalized by the peak trial deflection
	k_{vibe}	The stiffness estimation method based on the resonant characteristics of the pelvis following peak impact force
	k_{1st}	The stiffness estimation based on the force-deflection properties of the pelvis between the start of impact and peak force, using a linear least-squares regression fit
	$k_{combo300}$	The stiffness estimation based on the force-deflection properties of the pelvis between the start of impact and peak force, using a piecewise-polynomial least-squares regression fit with a transition of 300 N
	$\boldsymbol{k_{combo\ opt}}$	The stiffness estimation based on the force-deflection properties of the pelvis between the start of impact and peak force, using a piecewise-polynomial least-squares regression fit with an optimized transition

Table 2 Participants and Associated Ancillary Measures

Participant	Gender	Group	Age	Height (m)	Weight (kg)	BMI	Waist (cm)	Hip (cm)	Hip-Waist ratio	Soft Tissue Thickness (cm)
CAT	F	H	19	1.63	84.0	31.6	86	109	0.8	9.2
CVB	F	H	22	1.60	75.0	29.3	88	112	0.8	8.8
MAA	F	H	19	1.63	97.0	36.5	103	123	0.8	11.5
DCM	F	H	21	1.62	89.0	33.9	94	118	0.8	10.4
CBM	F	H	23	1.59	110.0	43.5	113	134	0.8	10.0
KMD	F	H	20	1.74	96.0	31.7	95	109	0.9	8.5
MDC	F	H	19	1.62	85.0	32.4	90	116	0.8	10.1
EMB	F	L	23	1.75	64.0	20.9	69	103	0.7	6.5
FYC	F	L	22	1.64	48.0	17.8	63	90	0.7	2.1
TAL	F	L	23	1.67	47.0	16.9	61	83	0.7	4.1
LEM	F	L	21	1.65	50.5	18.5	64	86	0.7	5.5
JAC	F	L	22	1.63	57.0	21.5	73	90	0.8	2.4
TMT	F	L	19	1.53	49.5	21.1	66	93	0.7	5.2
JLH	F	L	21	1.68	56.0	19.8	68	93	0.7	6.5
BAL	M	H	26	1.74	98.0	32.4	92	111	0.8	6.6
KSC	M	H	23	1.81	115.0	35.1	103	117	0.9	6.4
YKJ	M	H	20	1.71	101.0	34.5	105	116	0.9	8.7
MEJ	M	H	27	1.80	108.0	33.3	107	112	1.0	7.3
ATH	M	H	23	1.83	120.0	35.8	108	113	1.0	9.7
ACC	M	H	21	1.76	99.5	32.1	94	117	0.8	9.8
BRP	M	H	26	1.94	109.0	29.0	94	111	0.8	6.5
TAS	M	L	24	1.86	66.0	19.1	69	89	0.8	3.1
AAY	M	L	31	1.79	65.0	21.5	80	94	0.9	3.1
NSF	M	L	22	1.94	80.0	21.3	82	97	0.8	1.0
MAD	M	L	23	1.88	66.0	18.7	70	95	0.7	5.2
ADT	M	L	23	1.74	67.5	22.3	76	90	0.8	4.3
KSL	M	L	24	1.73	64.5	21.6	74	92	0.8	5.4
DAT	M	L	22	1.69	55.0	19.3	68	88	0.8	5.0
Mean	F	H	20.4	1.63	90.9	34.1	95.6	117.3	0.814	9.79
SD			1.6	0.05	11.3	4.7	9.5	8.9	0.03	1.0
Mean	F	L	21.6	1.65	53.1	19.5	66.3	91.1	0.728	4.61
SD			1.4	0.07	6.1	1.8	4.1	6.4	0.04	1.8
Mean	M	H	23.7	1.80	107.2	33.2	100.4	113.9	0.882	7.84
SD			2.7	0.08	8.3	2.3	6.9	2.7	0.06	1.5
Mean	M	L	24.1	1.80	66.3	20.5	74.1	92.1	0.804	3.85
SD			3.1	0.09	7.3	1.5	5.5	3.3	0.04	1.6

An ultrasound device (M-Turbo Ultrasound System, SonoSite, Bothell, Washington, USA) with a C60x 5-2MHz, curved array (30cm scan depth), was used to determine the two-dimensional soft tissue depth in the coronal plane over the greater trochanter, to the nearest 0.1 centimeter. Participants were asked to stand with the medial edges of their calcaneus and first metatarsal fifteen centimeters apart. This foot position was marked on a tape affixed to the floor in order to maintain a consistent stance during and between ultrasound measurements. The participant was asked to stand with their weight evenly distributed through each foot, with their upper body braced against a wooden box (122 x 61 x 2zero-centimeters) to reduce movement of the hip and spine during the ultrasound collection Figure 3.1). This limited changes in angle of the femur with respect to the pelvis, as well as variation in the amount of soft tissue overlying the greater trochanter. After exposing the skin over the left hip by lifting up the leg of the participant's shorts, the greater trochanter was identified through palpation, and ultrasound gel was applied to the skin over the landmark. With the ultrasound transducer aligned perpendicular to the femur, three coronal plane ultrasound images were collected (Figure 3.2 Ultrasound Image for Participant MAAFigure 3.2).Care was taken to limit compression of the soft tissue by the transducer head. For each image, the built-in software caliper function was used to measure the distance between the surface of the skin and the greater trochanter. This method for measuring soft tissue thickness was used previously by Maitland et al. (Maitland, Myers et al. 1993). A pilot study (Appendix 2) found this technique to be strongly reliable (Inter-rater reliability, ICC = 0.779; intra-rater reliability, ICC = 0.942).

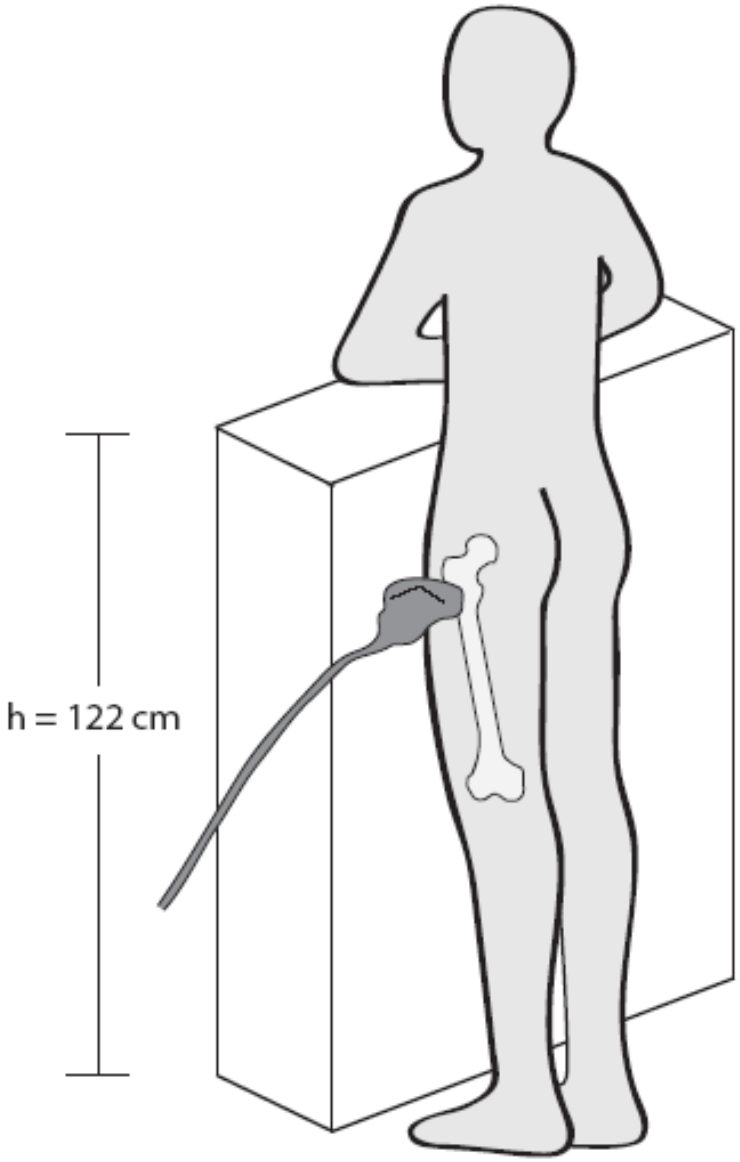

Figure 3.1 Position for Ultrasound Image

The participant was positioned in front of a large, wooden box (122 x 61 x 20 centimeters) to reduce movement of the hip and spine during the ultrasound measurements. Participants were asked to stand evenly, with the medial edges of their calcaneus and first metatarsal fifteen centimeters apart. This distance was marked by a piece of tape on the floor. An ultrasound device (M-Turbo Ultrasound System, SonoSite, Bothell, Washington, USA) with a C60x 2-5 MHz, curved array was used to determine the depth of soft tissue over the greater trochanter in the coronal plane.

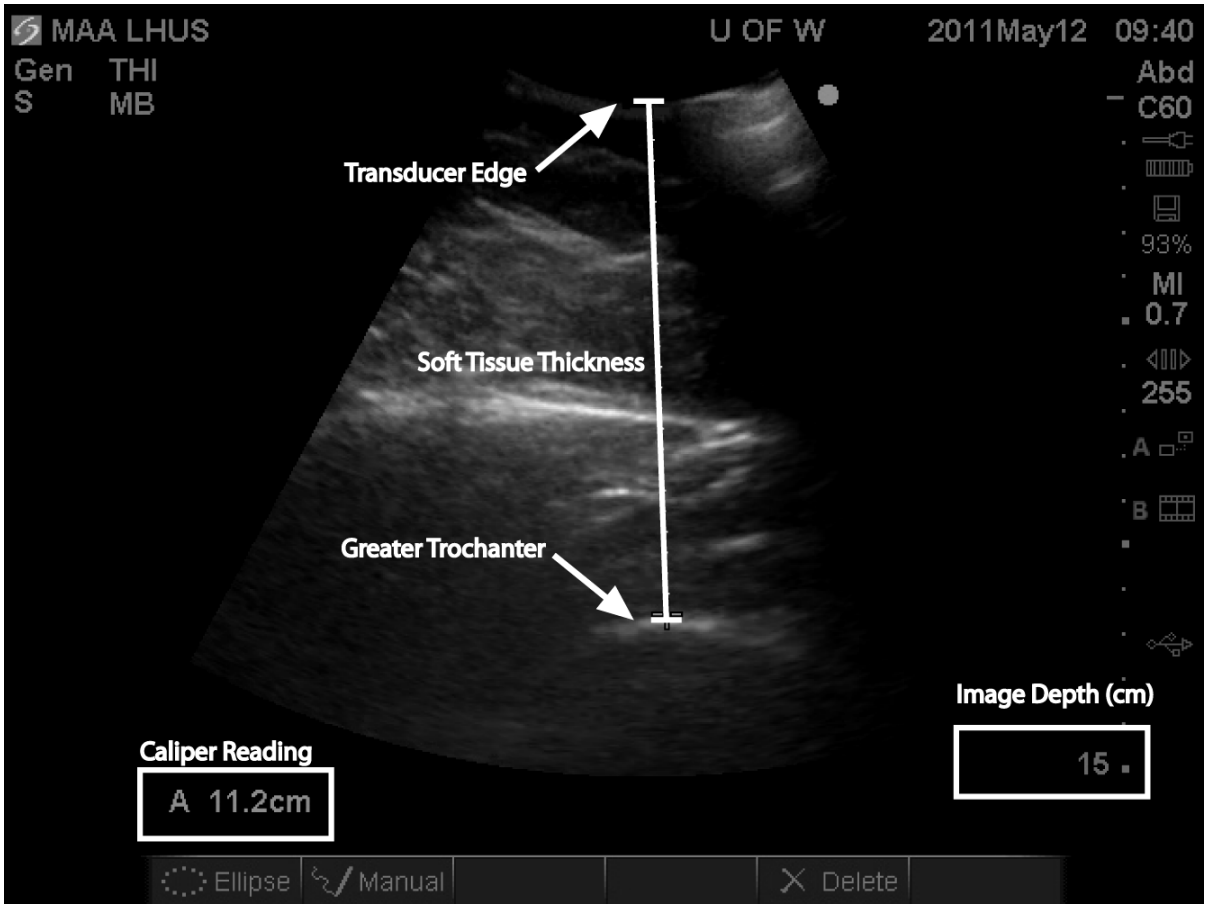

Figure 3.2 Ultrasound Image for Participant MAA

A coronal plane image of the soft tissue overlying the greater trochanter of participant MAA. This image was collected using the C60x curved array transducer, with an image depth of fifteen centimeters. The ultrasound device was set to balance the resolution-scan depth trade-off. The caliper function was used to determine the distance between the transducer edge and the greater trochanter. For this participant, a high BMI female, soft tissue depth was 11.2 centimeters.

3.2.2.1 Lateral Pelvis Release Technique

The "lateral pelvis release" technique was developed by Robinovitch et al. as a way to determine the peak impact force and effective stiffness characteristics of the pelvis (Robinovitch, Hayes et al. 1991). Validation studies for this technique showed strong agreement between theoretically calculated values of *k* and *b* and those based on the impact characteristics of a mechanical surrogate pelvis using the pelvis release apparatus. Peak force and time-to-peak-force also matched theoretical calculations within 4.5%.

The participant wore moderately tight-fitting spandex shorts for the lateral pelvis release trials (Figure 3.3). The size of spandex shorts was selected to limit migration of the hip marker, while also limiting pre-compression of the soft tissue or a binding effect at the waist or leg. Pilot work showed that the use of tight-fitting spandex shorts increased peak forces during lateral impact only marginally when compared to loose fitting athletic shorts (Appendix 2). Based on this limited influence on force, the benefit of reducing marker migration outweighed the potential tissue pre-compression.

Optotrak Smart Markers (Optotrak, Northern Digital, Waterloo, Ontario, Canada) were affixed to the right greater tubercle of the shoulder, greater trochanter and lateral femoral condyle for the duration of the investigation. All landmarks were palpated in a standing position. The greater tubercle was found by palpating the most lateral portion of the proximal humerus, inferior to the acromion. This landmark was selected because it would remain in a static position during an ideal collection. The greater trochanter was found by palpating the proximal femur during weight-bearing alternating internal-external rotation of the right leg with a bent knee. A prominent, lateral eminence, with a sharp superior edge was selected. The location of this landmark was confirmed between trials by palpating the femur of the participant in the impact position (detailed below). This step was taken to ensure that this critical marker did not migrate during or between trials. The lateral femoral condyle was selected as a landmark because of its location distal to the greater trochanter on the femur. This landmark was found by palpating the distal femur during weight-bearing alternating flexion-extension at the knee. The most prominent, lateral protuberance, superior to the lateral knee-joint space, was selected as the landmark. The markers for the greater tubercle of the humerus and the lateral femoral

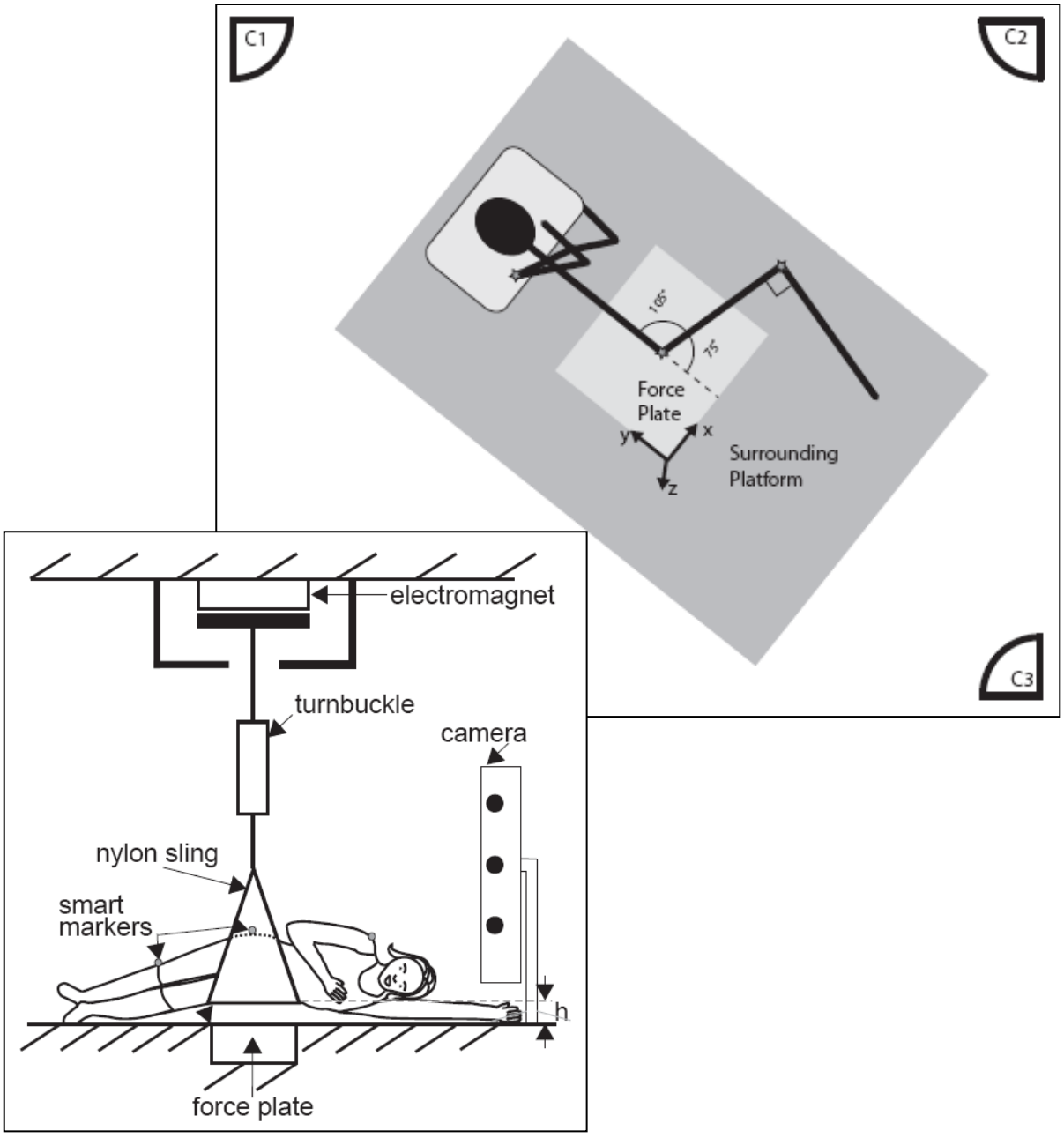

Figure 3.3 Lateral Pelvis Release Experiment

The participant was positioned on their left side with their pelvis supported by a sling above a force plate. Their upper torso and shoulder, and legs and lower legs were supported by a wooden platform flush with, and surrounding the force plate, positioned such that the left arm was flexed overhead at the shoulder, the right arm crossed the chest, the hips flexed to 75º, and the knees flexed to 90 º. Two cameras were arranged along the anteroposterior axis of the participant, while a third was positioned perpendicular to this axis.

condyle were attached directly to the skin. The marker for the greater trochanter of the femur was attached to the tight-fitting spandex shorts.

The participant was then asked to lie on their left side with their pelvis supported by a sling above a force plate. Their upper torso and shoulder, and legs and lower legs was supported by a wooden platform flush with, and surrounding the force plate, positioned such that the left arm was flexed overhead at the shoulder, the hips flexed at 75º, and the knees flexed at 90 º. This position approximates the position assumed following a fall from standing height and used in previous impact studies (Robinovitch, Hayes et al. 1991; Laing and Robinovitch 2010). One trial was collected with the participant resting in this position in order to determine the effective mass of the pelvis ($M_{neutral} = F_{neutral}/g$). For the pelvis release trials, the angles were confirmed prior to and after impact, and were monitored during impact via movement of the kinematic markers in order to maintain a standardized position throughout the trial. Trials were excluded if the hip flexion was not maintained (using a tolerance of approximately five degrees), or if notable rotation of the pelvis or spine about the anteroposterior axis occured.

The sling supporting the pelvis was made of a thin piece of rip-stop nylon, 51cm wide (corresponding to the distance from the waist to mid-thigh of the participant) by 137cm long (evenly cradling the pelvis. The sling was bordered by five-centimeter double-layer channels on each short end for the passage of a height-adjustable set of strong nylon climbing ropes and a turnbuckle. This unit was in turn connected to an electromagnet (custom model, AEC Magnetics, Cincinnati, Ohio, USA) affixed to the ceiling. This sling was selected on the basis of a set of pilot studies (Appendix 2).

With the magnet engaged, the participant's pelvis was raised to either a height of zero or five centimeters. The height was finely adjusted via the turnbuckle. For the zero-centimeter condition, the skin overlying the greater trochanter barely contacted the force plate. The zero-centimeter height was chosen based on the minimization of impact velocity and force, while still allowing for the quantification of pelvic deflection, and free-vibration characteristics (Robinovitch, Hayes et al. 1991;

Laing and Robinovitch 2010). This limits discomfort to the participant, which reduces guarding and bracing attempts that may alter the impact characteristics. From this minimal height condition, the pelvis is allowed to fall freely and impact the force plate, while maintaining control over impact position. The five-centimeter condition was included to determine whether the stiffness estimates derived from the zero-centimeter condition could be applied to higher energy impacts, such as a fall from standing height.

Both height conditions were confirmed by live force data (i.e. there was no force offset prior to impact) and a functional test (a thin card moved easily between the participant and force plate for the zero-centimeter condition; a five-centimeter block moved easily between the participant and the force plate for the five-centimeter condition). The left greater trochanter was positioned so that while the sling was suspended, the pelvis of the participant hung plumb beneath the electromagnet and so that the left greater trochanter would impact the center of the force plate. This positioning ensured that all soft tissue surrounding the pelvis, proximal femur and lower torso (i.e. those contributing to the effective mass of the pelvis) would impact the force plate, rather than the surrounding platform.

The participant was instructed to relax their core and extremity muscles in order to reduce muscle tension as a potential confounding variable. After the participant reports they are both ‘relaxed’ and ‘ready’ to begin a trial, the magnet was disengaged by the investigator following a delay of 1-3 seconds. This allowed the participant’s pelvis to fall and impact the force platform. The participant was warned that this event would occur, but was blinded to the timing of the event. The control box for the magnet was blocked from the line of sight of the participant, and care was taken to muffle the sound of the magnet release. These blinding precautions were taken to reduce the chance that the participant would brace or increase muscle activation during impact.

The time-varying loads applied to the pelvis were measured by a force plate (model OR6-3, Advanced Medical Technology, Inc., Watertown, Massachusetts, USA), sampled at 1200 Hz,

collected via NDI First Principles (Northern Digital, Waterloo, Ontario, Canada). A three-dimensional motion-capture system (Optotrak, Northern Digital, Waterloo, Ontario, Canada) was used to track the timing and positioning of impacts during the investigation at a sampling rate of 400 Hz. This sampling rate was 67% higher than previous sampling rates used for this purpose (Laing and Robinovitch 2010) in effort to maximize the number of data points available for analysis.

The participant began with four consecutive zero-centimeter trials, then four consecutive five-centimeter trials. Participants underwent four trials at each drop height condition. One minute was allowed between each trial for minimal tissue recovery. During this time, the participant was asked to stand quietly or kneel, without allowing contact between the hip and any surface (e.g. floor, wall, etc.). Five minutes were allowed between the two height conditions. Participants were notified that they could take longer recovery periods or stop the experiment if they felt any discomfort, bruising or other injury. No participant requested either of these accommodations.

3.2.3 Data Analysis

All signal conditioning and data processing was performed using a customized Matlab (Mathworks, Natick, Massachusetts, U.S.A.) routine. Force data was filtered with a fourth-order, dual-pass Butterworth filter, with a cut-off frequency of 100 Hz. Kinematic data was filtered with a fourth-order, dual-pass Butterworth filter, with a cut-off frequency of 10 Hz. Residual analysis was conducted to confirm the appropriateness of these cut-off values. Applied load (F) was down-sampled from 1200 Hz to 400 Hz to match the kinematic collection rate. For hypotheses one through five, all results are based on the zero centimeter condition. For hypotheses six and seven, results are based on both the zero and five centimeter conditions.

3.2.3.1 Methods of Indentifying Forces, Deflections, and Event Timing

A point-picking routine was created to select key data coordinates for further analysis. The coordinates for the beginning of impact (T_{imp}, F_{imp}), peak force (T_{max}, F_{max}), the minimum of the first force oscillation following impact (T_{min}, F_{min}), and the final resting pelvis (T_{end}, F_{end}) were manually selected (Figure 3.4) by one observer. The corresponding vertical position of the pelvis for the first two points was also selected. These points are D_{imp} and D_{max}. All kinematic values were subtracted from the starting vertical position of the greater trochanter marker to produce positive deflection values. These points were confirmed using an automated Matlab routine which selected T_{imp} and T_{max}, the two most critical points, based on the following criteria: The mean and standard deviation of force in the unloaded period at the beginning of the trial were calculated over the first 300 samples to determine the quiet noise and offset. T_{imp} was selected as the time at which the applied load exceeded two standard deviations of the force in the unloaded region. The maximum force recorded following T_{imp} was selected to be T_{max}. Both methods of point selection were compared to confirm that the correct points were determined, and not any erroneous fluctuations in load associated with voluntary movement of the participant prior to or after the impact. Such errors required removal of trials two trials each from two low-BMI females, and one low-BMI male, as well as one trial from one high-BMI male. The T_{max}, F_{max}, T_{min} and F_{min} coordinates were used to calculate the k_{vibe} stiffness estimate. The force and deflection data was selected between (and including) T_{imp} and T_{max} to calculate the force-deflection stiffness estimates. F_{end} was used to confirm the selection of $M_{neutral}$.

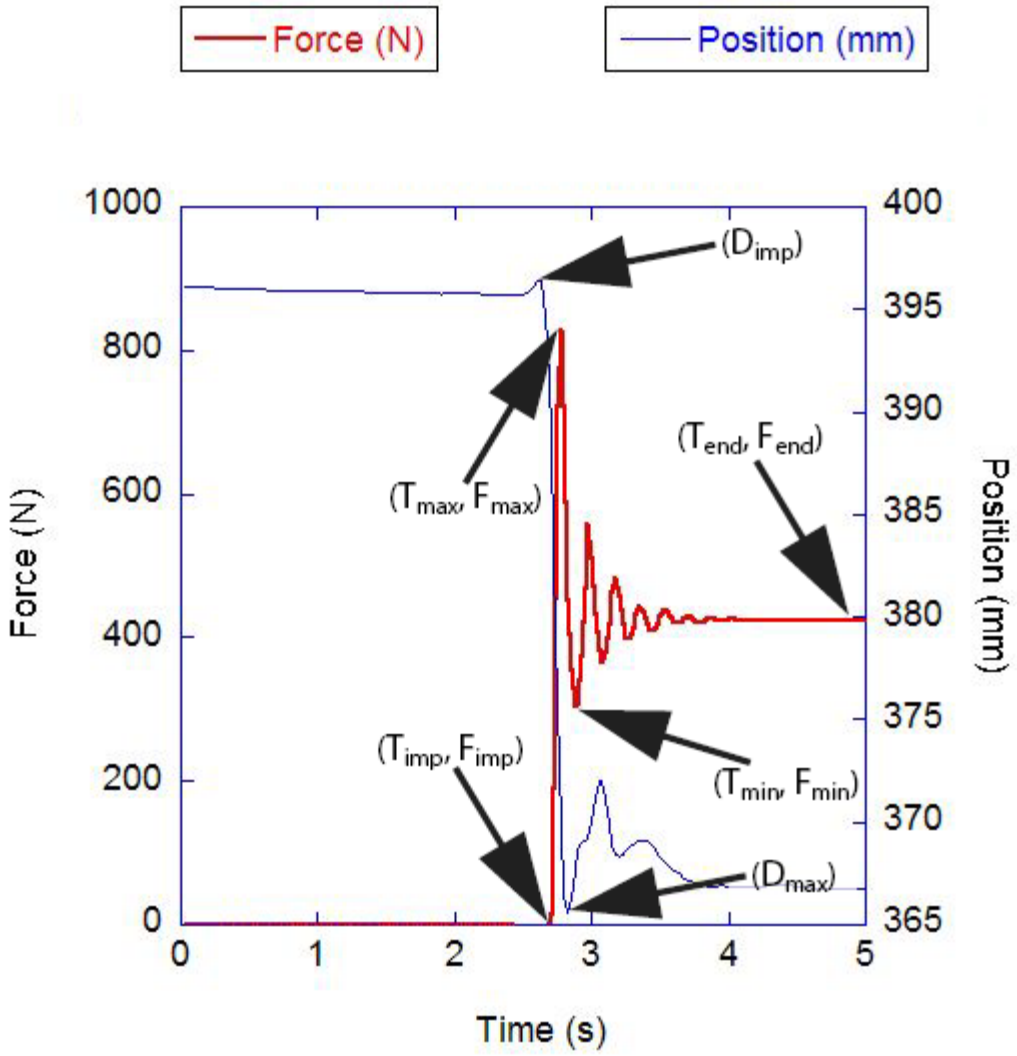

Figure 3.4 Force and Deflection Trace for Participant CAT, Zero-Centimeter Condition

The points selected by the point-picking routine are indicated on the figure. The coordinates for the start of the impact are indicated by (T_{imp}, F_{imp}). The coordinates for peak force are indicated by (T_{max}, F_{max}). The coordinates for the minimum of the first oscillation following impact are indicated by (T_{min}, F_{min}). The coordinates for final resting pelvis are indicated by (T_{end}, F_{end}). The corresponding vertical position of the pelvis for the first two points was also selected. These points are D_{imp} and D_{max}.

3.2.4 Methods of Estimating Effective Pelvic Stiffness

Pelvic stiffness was characterized based on the free-vibration models of impact used previously during pelvis release experiments and low energy impacts with mechanical fall simulators (Robinovitch, Hayes et al. 1991; Laing and Robinovitch 2010). This process involves an analysis of

the time-varying oscillation in ground reaction force to calculate natural frequency and then effective stiffness of the pelvis (Figure 3.5). Specifically, the period of oscillation (T) was determined via the identification of time of peak force (T_{max}) and time of minimum force (T_{min}); this was calculated as $T=2*(T_{min}-T_{max})$. The natural frequency of the impact was then determined by the relationship $\omega_n=2\pi/T$. The effective stiffness (k_{vibe}) was then determined by the relationship $k_{vibe}= \omega_n m$, where m is the effective mass of the pelvis at rest, determined by the division of the force of the pelvis at rest (F_{m-}) by gravity (g), $m=F_m/g$.

In addition to using the observed natural frequency of oscillation, effective stiffness was characterized based on the force-deflection properties of the pelvis during each trial. The time-varying deflection of the pelvis (x) was defined as the change in vertical distance between the impact surface and the marker overlying the greater trochanter between the time of impact (T_{imp}) and T_{max}. The force data for four separate trials was combined and re-sorted from low to high force magnitude. These values were plotted against pelvic deflection (x), also combined and sorted low to high. This maximized the number of data points available to build the models, and did not produce significantly different results from estimations based on the data from only one trial. This step was particularly important for low BMI participants, who, due to extremely low time-to-peak-force values, had as few as seven data points in one trial that occurred between T_{imp} and T_{max}. For example, a participant with four trials, seven data points per trial, would have twenty-eight data points in the combined data set. This would provide an increase in statistical power when correlating the calculated polynomial with the experimental data. This step was particularly important for the two piece-wise polynomial methods, for which the number of total data points was divided based on a transition point. Basing a piece-wise polynomial on a small data set would result in a higher probability that either of the two regions (the second-order toe region, and the linear-elastic region) would contain only one or two data points. This would increase the error associated with the transition point. The combination of trials

into one data set reduces these errors. A comparison of all three force-deflection methods is provided in Figure 3.5.

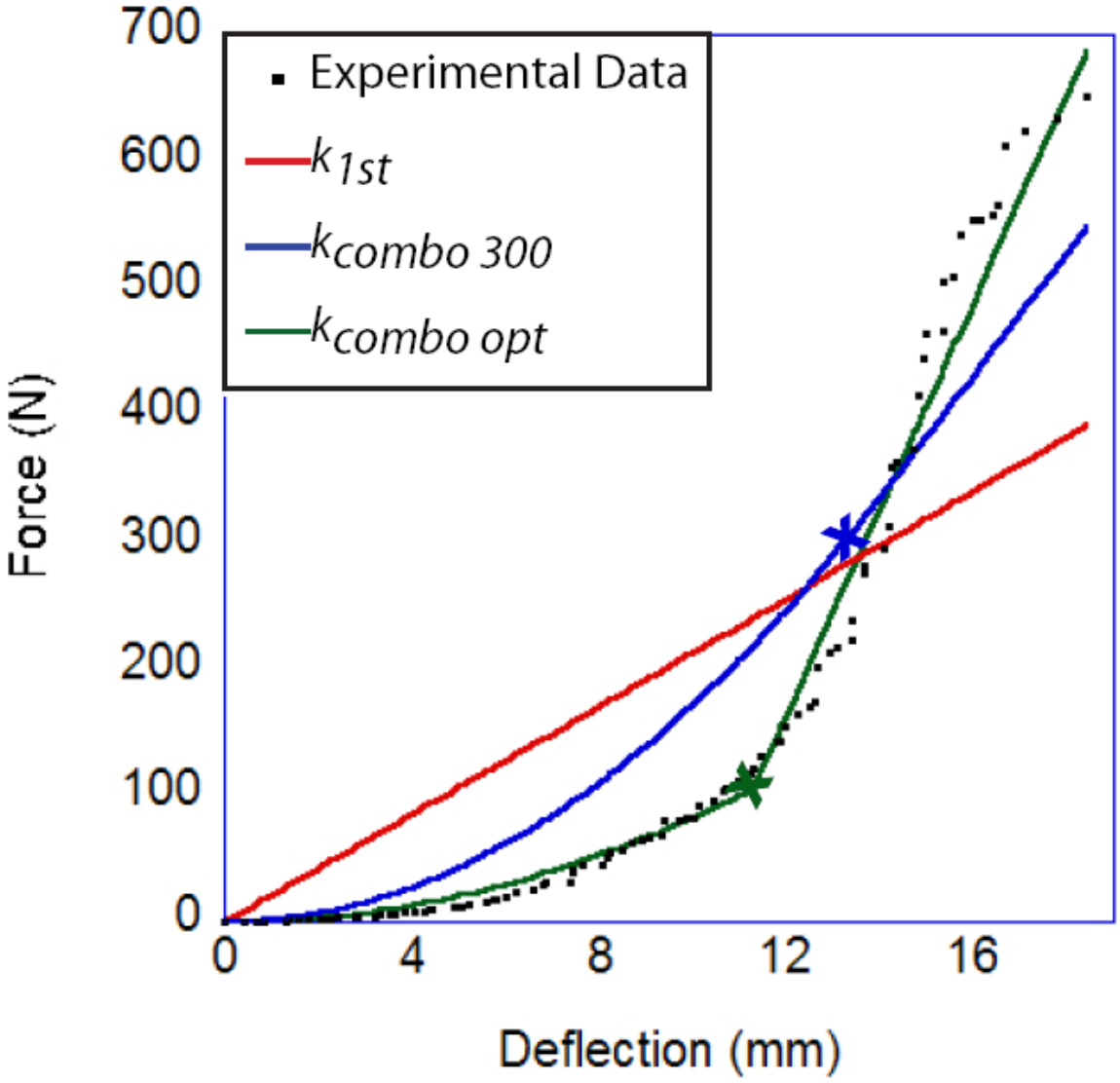

Figure 3.5 Force-deflection Stiffness Estimation Methods

The three force-deflection stiffness estimation methods are represented above. Stiffness comparisons between methods were made based on the linear region only. For k_{1st}, this is represented by the entire polynomial. For $k_{combo\ 300}$ and $k_{combo\ opt}$, this is represented by the portion to the right of the transition point, marked by an 'x'. The quality of fit of each method, and the peak (linear) stiffness estimate was compared between stiffness estimation methods.

Using a least squares regression approach, a first order polynomial (k_{1st}) was fit to the data for impacts between T_{imp} and T_{max}. An intercept of zero was selected for this method. This function was then differentiated to produce a single stiffness estimate, $k_{1st\ est}$.

I then incorporated potential non-linearities by using two piece-wise polynomials, which combined a second-order approach ($F=Bx^2+Ax$) for all force inputs between T_{imp} and $T_{transition}$, and a first order approach ($F= Lx$) for all force inputs greater than the transition. For the first piece-wise method, the second-order polynomial was fit to the entire range of the force-deflection data, using a least-squares approach. This function was forced to have an intercept of zero, and positive coefficients in order to prevent negative stiffness estimations at small deflection values. The transition point this method was selected to be 300 N for all participants, based on previous literature (Robinovitch, Hayes et al. 1991; Laing and Robinovitch 2010). The first-order portion of this polynomial was an extension, tangential to the second-order portion at the transition point, through to the maximum deflection in that trial.

The second piecewise method ($k_{combo\ opt}$) was determined based on an optimization routine (Figure 3.6). Specifically, the maximum deflection of each trial was divided to provide 100 potential transition points. For a set of one hundred iterations (i), a second-order polynomial was applied to data points with where deflection was less than, and including i%, using a least squares approach. This polynomial was constrained to an intercept of zero, and positive coefficients. A first-order portion was then applied to data points greater than i% of deflection, and was forced to intersect with the predicted point at i% of deflection. The transition point of the optimal fit minimized the mean squared error between the predicted polynomial and experimental force data. This method provides the 'optimal' transition point for the specific data set, but may not represent the optimal solution or optimal method of finding a transition point for other data sets, particularly when considering the large number of variations in how lateral impacts can occur.

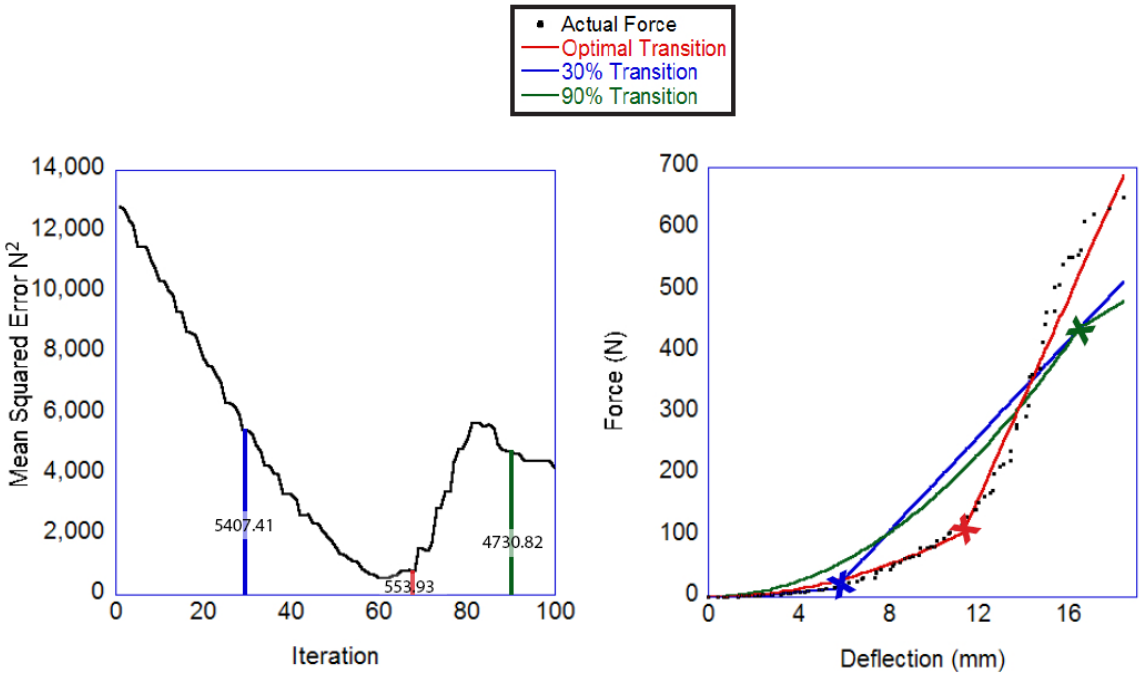

Figure 3.6 Method for Selecting Optimal Piece-wise Fit

For each trial, the force data was plotted against the deflection data (solid black marks) for all force inputs between T_{imp} *and* T_{max}. A set of possible transition points was created, ranging between one and one hundred percent of maximal trial deflection, in one percent increments. For a set of one hundred iterations (i), a second-order polynomial was fit to the low stiffness region (all data points with deflections less than i% maximal deflection), using a least-squares approach. This function was constrained to an intercept of zero and positive coefficients. A first-order polynomial was then applied to data points greater than i% of deflection, and was forced to intersect with the point at i% of deflection. The fit of this portion of the polynomial was determined using a least-squares approach. Transition points for iteration 30 (blue x), iteration 90 (green x) and the optimal transition point selected (red x) are shown above, along with the corresponding predicted polynomials. The optimal transition point was selected as that which minimized the error between the piece-wise polynomial and the experimental data, based on the mean squared error over the entire data set.

Table 3 Coefficients and Statistical Data Associated with Optimized Piece-wise Fit

Transition	A	B	Linear Stiffness Estimate (N/m)	MSE total	MSE high	R^2 total	R^2 high
30%	0.419	0.22	39090	5407.41	7947.17	0.852	0.852
61% (optimal)	0.820	0.00	81840	553.93	1461.7	0.985	0.986
90%	1.621	0.00	22020	4730.82	28404.93	0.870	0.968

The second piece-wise method was selected based on observations of the experimental data during processing, and similar methodology reported by Chandrashekar and colleagues (2008). When fitting the force-deflection data using the $k_{combo\ 300}$ method, it appeared that the fit could be improved by changing the point of transition between the low-deflection and high-deflection regions. The set transition point of 300 N was too high for some participants and too low for others (Figure 3.7).

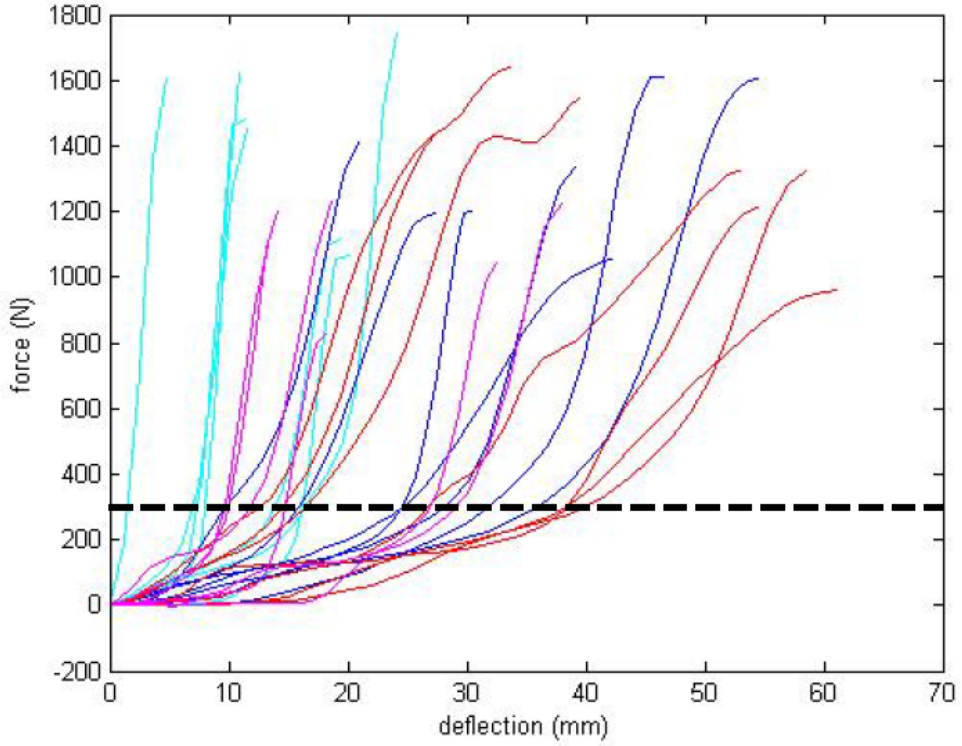

Figure 3.7 Force-Deflection Trace for All Participants (N=28)
One exemplary trial is represented for each participant from the five centimeter condition. The dashed line indicates the 300 N transition point utilized by the $k_{combo\ 300}$ method.

I observed that the transition between the low-deflection and high-deflection region appeared to occur at a point proportional to the maximum deflection or force, rather than a constant value across all participants. Upon normalizing the deflection data to the maximum trial deflection, a consistent pattern appeared. The transition appeared to occur at approximately 60% of maximum trial deflection during the zero centimeter condition, and 70% of maximum trial deflection during the five centimeter

condition (Figure 3.8). The optimization approach was selected in order to pinpoint the exact transition for each participant.

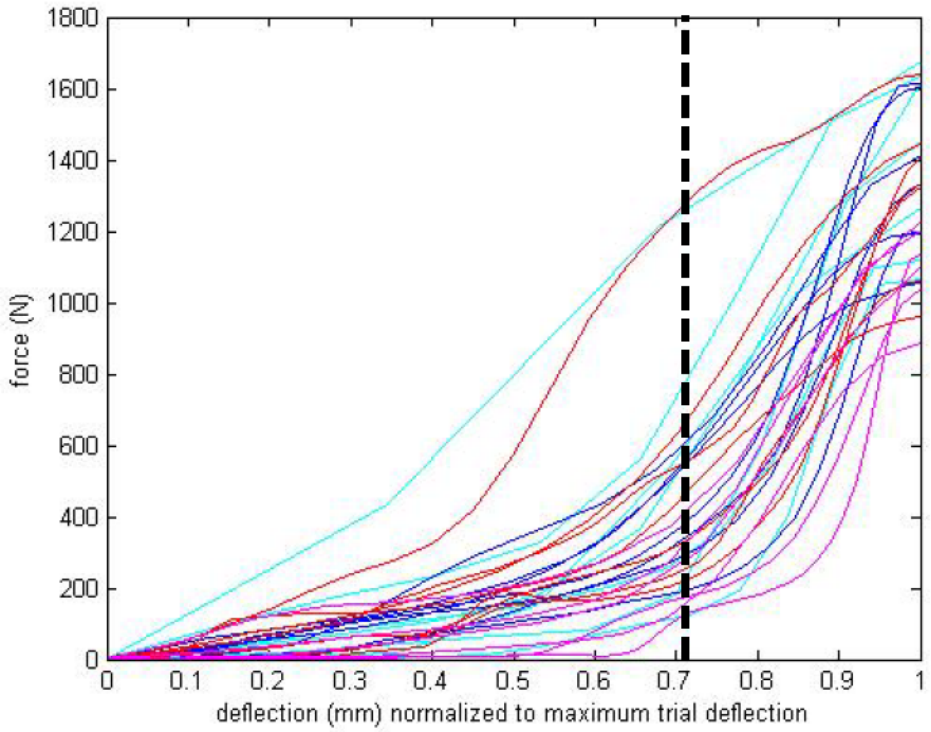

Figure 3.8 Force-Deflection Trace for All Participants (N=28), Normalized

The representative force-deflection traces for each participant, normalized to maximum trial deflection. The optimal transition point for the five centimeter condition appeared to occur at 70% of maximal trial deflection.

The transition points for the optimized polynomial were determined in several domains. The first transition, $L_{deflection}$ represents the transition in centimeters of deflection. The second transition, L_{force}, represents the transition in Newtons of force. A third transition, $L_{normmax}$, is the transition, normalized by the maximum trial deflection. $L_{soft\ tissue}$ represents the transition, normalized to the trochanteric soft tissue depth of the participant. A final transition normalizes the transition the effective mass of the pelvis, $L_{normpelvis}$.

The two portions of each polynomial for both piece-wise methods (the second-order portion applied to the low-deflection region, and the first-order portion applied to the high-deflection region) were then differentiated to produce stiffness estimates. The stiffness estimates based on the second-order portion took the form $k_{combo\ 300\ low} = dF/dx = 2*B*x + A$ and $k_{combo\ opt\ low} = dF/dx = 2*B*x + A$, resulting in a deflection-dependent stiffness estimate. The linear portion of the combination fits was set to the value of $k_{combo\ 300\ peak}$ and $k_{combo\ opt\ peak}$ at the appropriate transition point.

3.2.5 Statistics

All statistical analyses were performed with a software package using an α of 0.05 (SPSS version 17, Chicago, USA). The comparisons between stiffness estimation methods were performed using only the low BMI female group. This group was selected as the representative group because of the greater depth of literature relating to effective pelvic stiffness of this group (Robinovitch, Hayes et al. 1991; Laing and Robinovitch 2010).

3.2.5.1 Pelvic Stiffness Estimation Methods

Hypothesis One

Regarding the first hypothesis, I compared the quality of the fit of each force-deflection based stiffness estimation method (k_{1st}, $k_{combo\ 300}$, $k_{combo\ opt}$)(using a least-squares regression coefficient) with the experimental data. A comparison of these approaches, for one participant, is shown in Figure 3.5. The aim of this was to test whether the piece-wise combination methods provided a fit that was truer to the actual data than the simple linear fit (hypothesis 1a). Additionally, I aimed to show that the fit of the optimized model was an improvement on the model with only one possible transition point (hypothesis 1b). A simple r^2 was produced for the first model, k_{1st}. For the more complex models, separate r^2 values were developed for the entire force-deflection data set, as well as the high deflection region separately. The stiffness estimation methods tested, in order of complexity, were k_{1st}, $k_{combo\ 300}$,

and $k_{combo\ opt}$. The two piece-wise methods were compared to the simple linear method, and the most $k_{combo\ opt}$ was compared to the $k_{combo\ 300}$. An *a priori* increase of 0.05 was used to indicate a substantially enhanced fit.

Hypothesis Two

For the second hypothesis, k_{1st} was used as a 'gold standard' to test whether k_{vibe} is an appropriate surrogate for the estimation of pelvic stiffness. A fixed-effect-model ANOVA was performed, with stiffness estimation method (k_{1st} and k_{vibe}) as the repeated factor.

3.2.5.2 The Effect of BMI and Gender on Effective Pelvic Stiffness and Peak Forces During Lateral Falls

Based on the results of the analysis presented in section 3.2.4, $k_{combo\ opt}$ was selected as a 'gold standard' to compare the effects of BMI and gender on effective pelvic stiffness. The main focus of this analysis was the peak stiffness (i.e. the stiffness estimate in the linear region) rather than the stiffness in the toe-region or the entire force-deflection curve. This limitation was made for several reasons. Firstly, the stiffness in the linear region has greater implications when determining peak force following impact than the force-dependent low-stiffness region. Peak stiffness is greater than the stiffness in the toe-region. Use of this stiffness estimate would produce higher peak force estimates in a force-prediction model, which would provide more conservative (over-predicted peak force, i.e. worst-case scenario) predictions of fracture risk. Further, a single stiffness estimate is the simplest to implement in both mathematical and mechanical force prediction models.

Hypotheses Three and Four

Based on the results of the statistical tests regarding stiffness estimaton methods, $k_{combo\ opt\ peak}$ was selected as a 'gold standard' to test hypothesis three and four. These tests were performed determine whether the high BMI participants had lower estimated pelvic stiffness than low BMI participants. Because $k_{combo\ opt}$ is a force-dependent stiffness estimation, the estimate of pelvic stiffness at peak

force was determined for each participant. This variable is $k_{combo\ opt\ peak}$. A fixed-effect-model ANOVA, with BMI and gender as between-subject factors, were performed for the stiffness estimate. Regarding hypothesis five, a mixed model ANOVA was also used to test the influence of two between-subject factors, BMI and gender, on the optimal transition point selected by $k_{combo\ opt}$. This test was performed for $L_{deflection}$ and L_{force}.

Hypothesis Five

The transition points produced using the optimal piece-wise method, $k_{combo\ opt}$, were compared using a mixed-model ANOVA, with BMI and gender as between-subject factors. The specific transitions compared included $L_{deflection}$, L_{force}, $L_{normmax}$, $L_{normpelvis,}$ and $L_{soft\ tissue}$.

3.2.5.3 Peak Force Prediction

Hypothesis Six

Regarding hypothesis six, a mixed-model ANOVA, with BMI and gender as between-subject factors, and experimental drop height as the repeated measure, was used to test whether the stiffness estimate ($k_{combo\ opt\ peak}$) was influenced by drop height.

Hypothesis Seven

For hypothesis seven, a repeated-measures ANOVA, with BMI and gender as between-subject factors, was used to test the effect of BMI and gender on the five-centimeter condition peak force, and peak force normalized to the effective pelvic mass of the participant.

Hypothesis Eight

For hypothesis eight, the potential co-variates for the independent variables (height, body mass, effective mass of the pelvis, waist circumference, hip circumference, waist-hip ratio and soft tissue thickness) were compared to determine which measures were strong covariates. Using bivariate correlation tables, a significance level of $\alpha = 0.05$ and a minimum r^2 of 0.8 was used to determine

which variables could be eliminated. This was done to reduce the influence of any correlated variables (e.g. waist circumference, which is accounted for in waist-hip ratio and hip circumference). The continuous variables selected for inclusion into a backwards regression routine were height, body mass, hip circumference, and soft tissue thickness. A categorical variable, interaction group (high BMI females, low BMI females, high BMI males, low BMI males), was included due to the significant BMI-gender interactions outlined in the statistical methods for hypotheses one through four. Two regression models were produced to test the effect of these variables, as well as stiffness estimation method (i.e. one model including k_{1st} and one model including $k_{combo\ opt}$) on the five-centimeter condition peak force. The criterion for removal of a variable was a probability of F of 0.10.

3.3 Results

3.3.1 Pelvic Stiffness Estimation Methods

Overall, the four stiffness estimation methods were not statistically significant from one another ($F(1,1.091) = 3.736$, $p = 0.096$), which is likely due to the high amounts of variance associated with $k_{combo\ 300}$ (12877.394 N/m) and $k_{combo\ opt}$ (42384 N/m). Pairwise comparisons showed significant differences between k_{vibe}, k_{1st} and $k_{combo\ 300}$, but the greater between-subject variability produced by $k_{combo\ opt}$ resulted in no significant difference between the optimized stiffness estimation method and any other method. The two stiffness estimation methods which characterize the effective stiffness of the pelvis as a whole, k_{vibe} and k_{1st}, produced the lowest stiffness estimates (20034 (3508) N/m for k_{vibe} and 29964 (5930 N/m for k_{1st}) (Figure 3.9). The optimized piece-wise force-deflection stiffness estimation method, $k_{combo\ opt}$ produced the highest effective stiffness estimates (55709 (42384) N/m), but also the greatest between-subject variability.

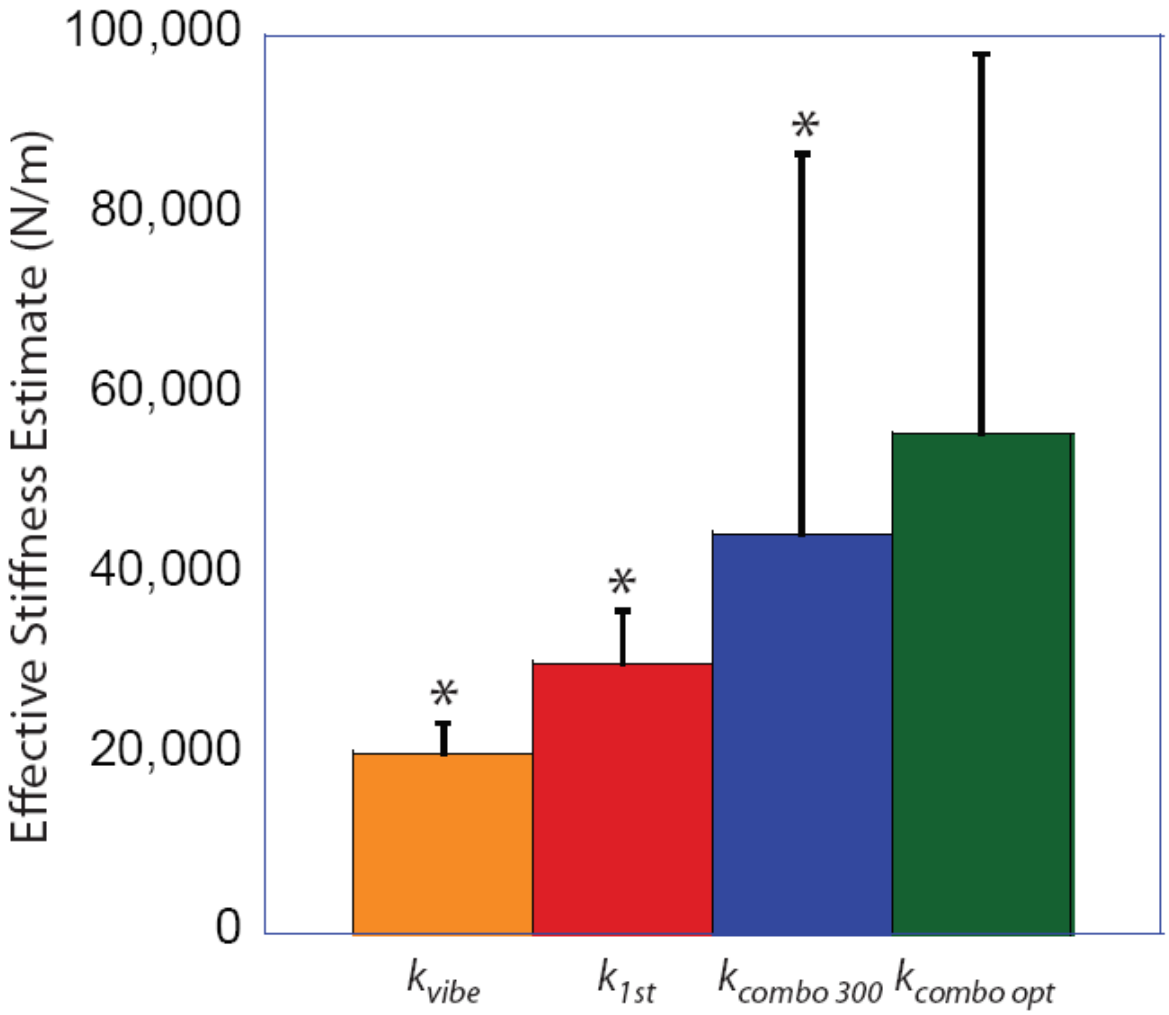

Significant pair-wise differences at $\alpha = 0.05$

Figure 3.9 Pair-wise Comparison of Effective Stiffness Estimation Methods

Pair-wise significant differences were found between k_{vibe}, k_{1st} and $\boldsymbol{k_{combo\ 300}}$, but not between $k_{combo\ opt}$ and any other method at $\alpha = 0.05$. The two stiffness estimation methods which characterize the effective stiffness of the pelvis as a whole, k_{vibe} and k_{1st}, produced the lowest stiffness estimates. The optimized piece-wise force-deflection stiffness estimation method, $k_{combo\ opt}$ produced the highest effective stiffness estimates, as well as the greatest between-subject variability.

The simpler piece-wise estimation method, $k_{combo\ 300}$, provided a substantial improvement (R^2 increase of 0.10207) in quality of fit to the experimental data over the linear approach, k_{1st}. (Table 4). The optimized approach produced an even stronger improvement (R^2 increase of 0.17282). In the linear, high-stiffness region, the best quality of fit was produced by $k_{combo\ 300}$. Because the number of

data points in the high stiffness region varies within each participant based on the transition used by each method, the R^2 calculated for each method is biased by the number of data points. Because of this, a comparison of decrease in mean squared error is a better comparison between stiffness estimation methods. The optimized method produced a mean squared error over the entire force-deflection curve 92.3% lower than that produced by k_{1st}, and 83.0% lower than that produced by $k_{combo\ 300}$. Within the high-stiffness region, the mean squared error was 90% lower for $k_{combo\ opt}$ than $k_{combo\ 300}$.

Table 4 Stiffness Estimation Method Quality of Fit Improvements

	R^2		Mean Squared Error (N^2)	
	Total Force-Deflection Curve	**High-Stiffness Region**	**Total Force-Deflection Curve**	**High-Stiffness Region**
k_{1st} (r^2)	0.81208	---	6119.86	---
$k_{combo\ 300}$ (r^2)	0.91415	0.96720	2601.28	5774.92
Improvement from k_{1st} (r^2)	0.10207*	---	3518.58	---
$k_{combo\ opt}$ (r^2)	0.98490	0.99236	441.10	577.52
Improvement from k_{1st} (r^2)	0.17282*	---	5678.76	---
Improvement from $k_{combo\ 300}$ (r^2)	0.07075*	0.02516	2160.18	5197.40

****Substantial improvement in quality of fit based on an a priori improvement of 0.05***

The average coefficients associated with each stiffness estimation method, determined for low-BMI females, are presented in Table 5.

Table 5 Coefficients Determined by Force-Deflection Stiffness Estimation Methods

		$k_{combo300}$	$k_{combo\ opt}$	k_{1st}
		For deflections 0cm-transition, $k_{combo} = Ax^2+Bx + C$, C=0; for deflections transition-peak, a single stiffness estimate $k_{combo\ peak}$		*A single stiffness estimate, k_{1st}*
A constant	**Mean**	156051	331442	---
	SD	159449	277084	---
B constant	**Mean**	14025	3896	---
	SD	15358	8345	---
Linear Region Stiffness (N/m)	**Mean**	44635	55709	20034
	SD	12877	42384	3508

3.3.2 Stiffness Estimates for BMI and Gender Groups

Strong main effects of BMI ($F(1,13) = 10.87$, $p = 0.003$) and gender ($F(1,13) = 5.97$, $p = 0.022$) were found for $k_{combo\ opt\ peak}$. Overall, the effective stiffness was 77% lower for the high BMI group than the high BMI group, and 63% lower for females than males. However, significant interactions were found between the BMI, gender, and the stiffness estimate, $k_{combo\ opt\ peak}$ (Figure 3.10) ($F(3,) = 5.31$, $p = 0.030$). This interaction was mainly driven by the low BMI males, for which the mean peak stiffness was twice as high as that of the high BMI males, the next highest group (Table 6).

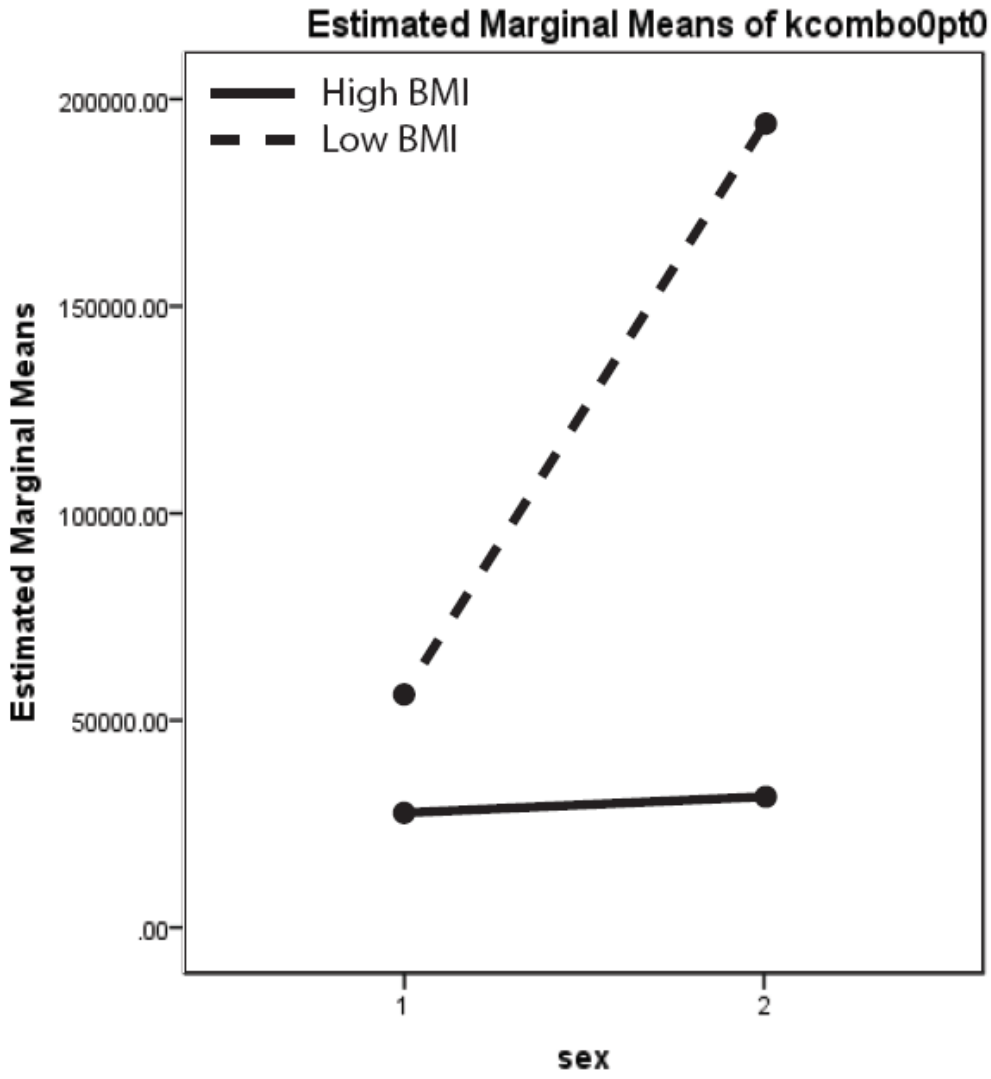

Figure 3.10 Main Effects of BMI and Gender for Stiffness Estimate

While main effects for both BMI and gender were evident, a strong interaction effect was found between these factors for the stiffness estimate, $k_{combo\ opt\ peak}$. BMI-related reductions in stiffness were much more substantial for males than females.

Table 6 Stiffness Estimates, by Group

		High BMI Females	Low BMI Females	High BMI Males	Low BMI Males
$k_{combo\ opt\ peak}$ N/m	Mean	36236	35525	47913	101985
	SD	5356	7089	12267	53440

Based on the evident interaction between BMI and gender, comparisons between groups were divided based on BMI-gender interaction groups (Figure 3.11). The gender-related reduction in effective stiffness was significant for low BMI females relative to low BMI males (t (6.988) = -2.379, p = 0.049) but not for high BMI females relative to high BMI males (t(12) = -1.130, p = 0.281). Effective stiffness was also much lower in high BMI males than low BMI males (t (6.026) = -2.917, p = 0.027), but this decrease was not found for high BMI females relative to low BMI females (t (6.297) = -1.78, p = 0.124).

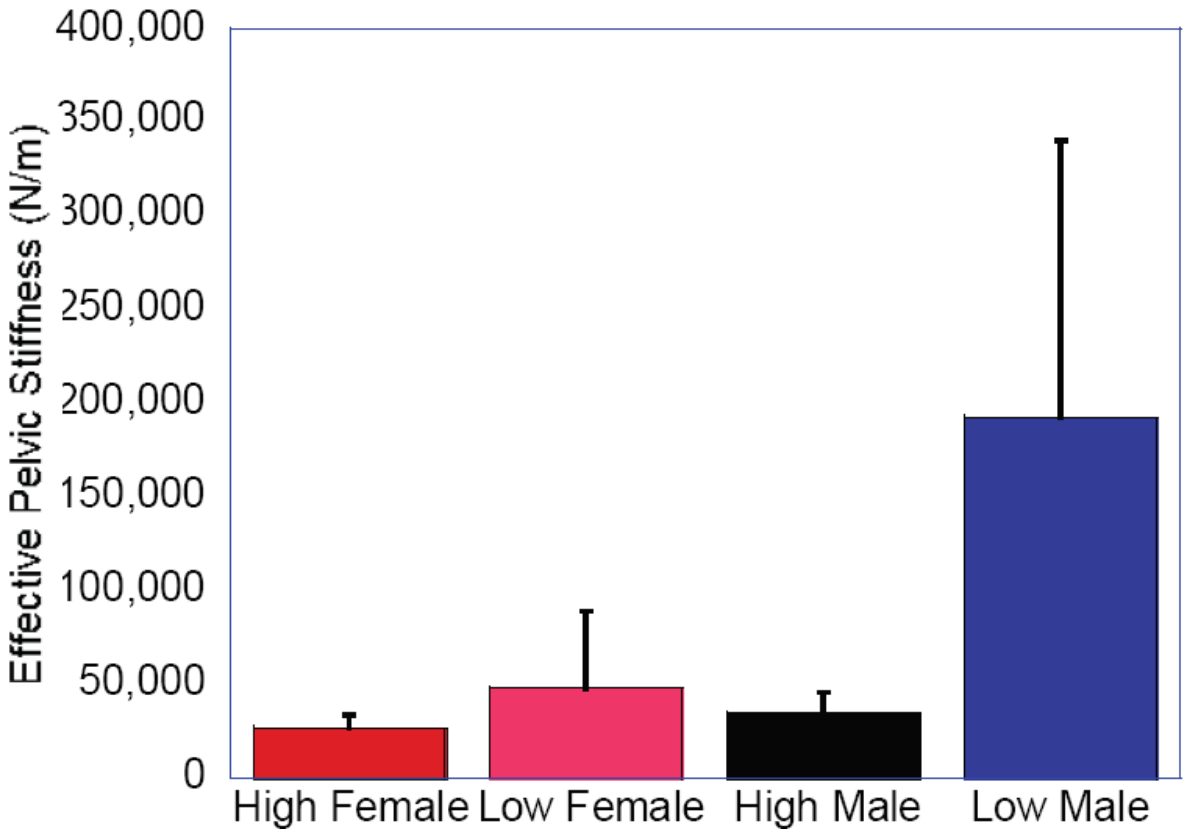

Figure 3.11 Effective Stiffness Estimate, by BMI-gender interaction group

The majority of the transition variables produced using the optimization routine were effected by BMI but not gender. The transition measured in Newtons, L_{force}, was 84% lower for low BMI (136.5 (142.0)N) participants than high BMI participants (838.66 (114.6)N) (F(1,13) = 221.84, p < 0.001)

(Figure 3.12). Normalized to the effective mass of the pelvis, this transition occurred at a significantly lower load per Newton of pelvis mass for low BMI participants (0.51 (0.54) N/N) than high BMI participants (1.65 (0.29) N/N) ($F(1,13) = 53.18$, $p<0.01$). Relative to deflection, the transition occurred at a magnitude of deformation three times higher for high BMI participants (1.87(0.53)cm) than for low BMI participants(0.56(0.43)cm) ($F(1,13)=62.74$, $p<0.001$), and 67% lower for males than females ($F(1,13)=7.597$, $p = 0.001$) (Figure 3.13). Normalized to soft tissue depth, this measurement was higher in high BMI participants (20.8 (6.5)%) than low BMI participants (14.7 (9.1)%) ($F(1,13)= 4.95$, $p = 0.036$). Finally, the transitions occurred at an overall average of 59.4 (16.5%) of maximum trial deflection, which is close to the estimated transition point of 60%. The transition point was higher for high BMI participants (69.9 (10.6)%) than for low BMI participants (49.0 (14.7)%) ($F(1,13)=18.840$), $p<0.001$).

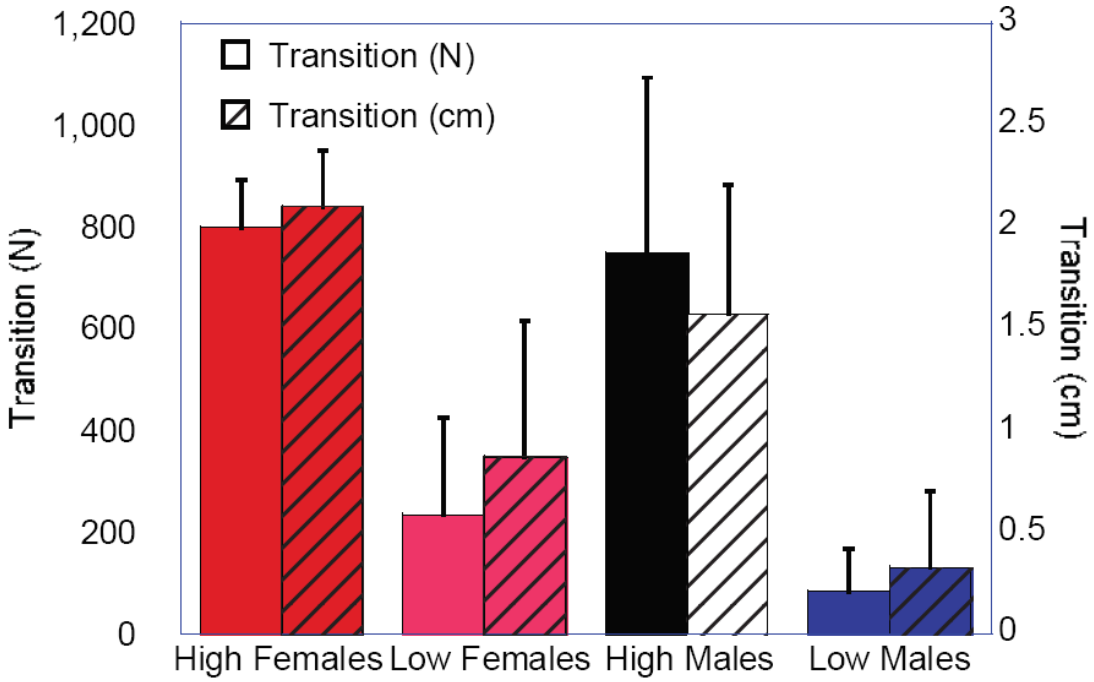

Figure 3.12 Absolute Transitions, by BMI-gender Interaction Group

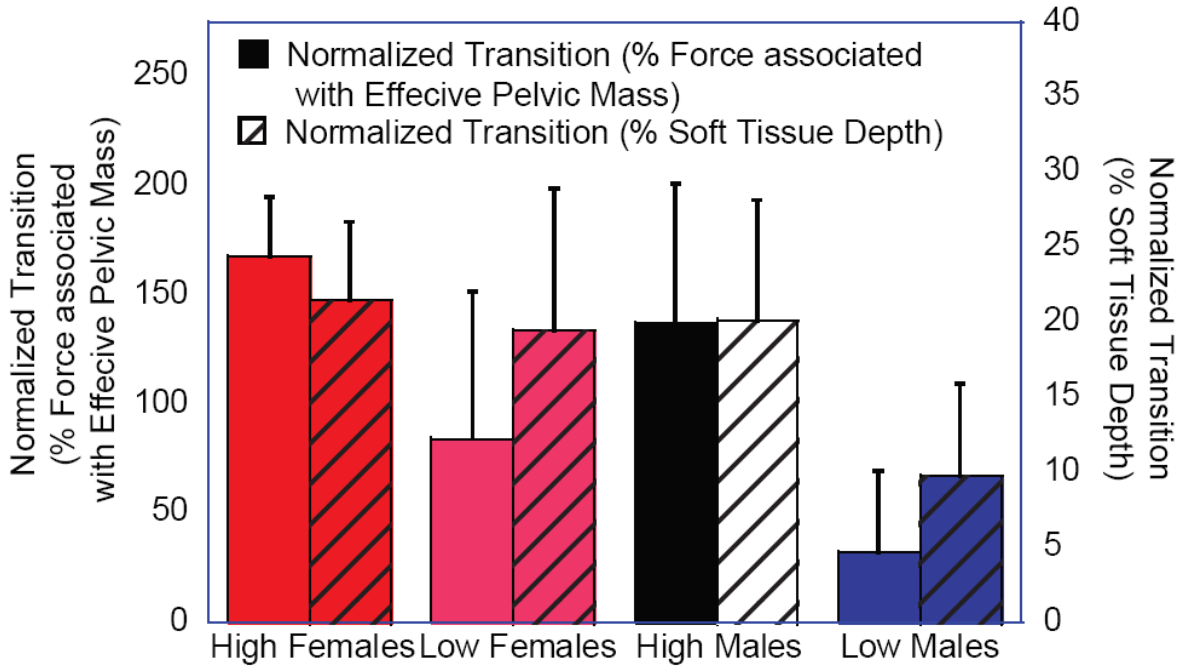

Figure 3.13 Normalized Transitions, by BMI-Gender Interaction Group

3.3.3 Peak Force Prediction

No significant differences were found between the stiffness estimates produced from the zero-centimeter drop-height condition and the five-centimeter drop-height condition ($F(1,27) = 0.135$, $p = 0.717$).

High BMI participants sustained peak forces (1415.2 (234.9) N) significantly higher than those sustained by low BMI participants (1154.5 (287.3) N) ($f(1,13)=0.7516$, $p=0.011$) during the five centimeter condition (Figure 3.14). No differences were found between males and females for this condition ($f(1,13)=3.641$, $p=0.068$). When the peak forces were normalized to the effective mass of the pelvis, the relationship between the low and high BMI participants was reversed. Low BMI participants sustained much higher normalized peak forces (4.09 (0.80) N/kg) than high BMI participants (2.82 (0.58) N/kg) ($f(1,13)=24.9$, $p<0.001$) (Figure 3.15). There were also no differences between males and females for the normalized peak force condition ($f(1,13)=1.225$, $p=0.279$).

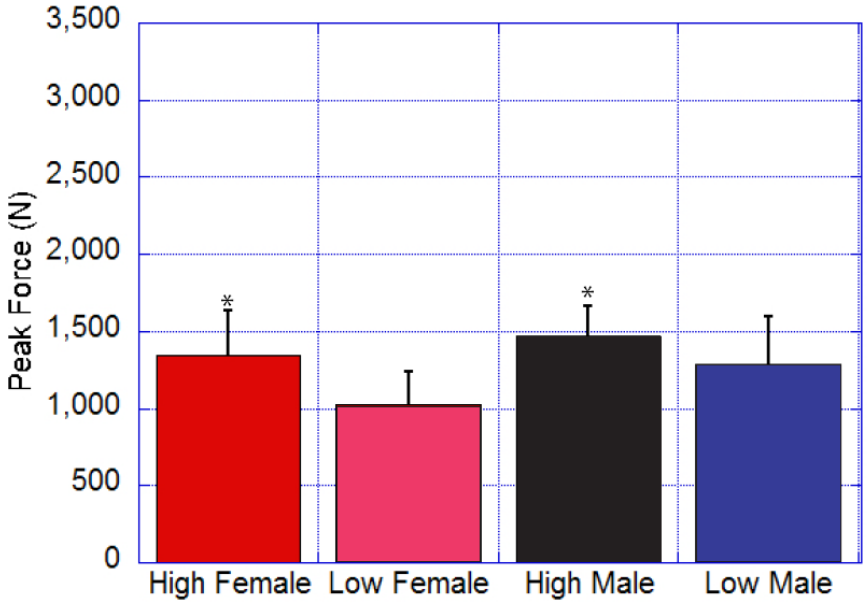

Figure 3.14 Peak Forces Sustained During the Five-centimeter Drop-height Condition

High BMI participants sustained significantly higher peak forces than low BMI participants ($f(1,13)=0.7516$, $p=0.011$) during the five centimeter condition.

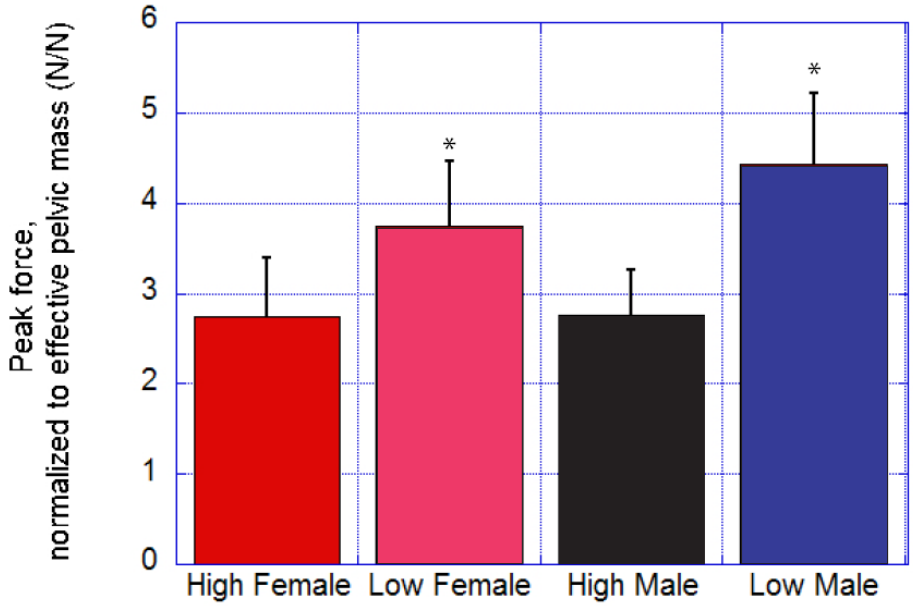

Figure 3.15 Peak Force Normalized by the Effective Pelvic Mass

Low BMI participants sustained much higher normalized peak forces than high BMI participants ($f(1,13)=24.9$, $p<0.001$)

The final regression model relating five-centimeter condition peak force to $k_{combo\ opt\ peak}$ and the selected variables produced a model for which $r^2 = 0.462$ ($F(2,25) = 8.717$, $p<0.001$). The predictors for this model are $k_{combo\ opt\ peak}$ ($\beta = 0.550$, $t(25) = 3.110$, $p=0.005$), height ($\beta = 0.326$, $t(25) = 2.119$, $p=0.045$) and soft tissue thickness ($\beta = 0.785$, $t(25) = 4.573$, $p<0.001$).

3.4 Discussion

This study adds depth to what is known about the force-deflection and resonance properties of the human pelvis during sideways falls. Regarding the first goal, I have found that selecting a more complex stiffness estimation method ($k_{combo\ opt}$) rather than a simpler approach (k_{1st}) can result in improvements in quality of fit of up to 17%. The optimized method also provided a 7% improvement over the $k_{combo\ 300}$, suggesting that method of fit has a substantial effect on how well effective stiffness is characterized. This supports hypothesis one. I also found discrepancies between the vibration-based stiffness estimation method and the force-deflection stiffness estimation methods, as well as between the stiffness estimates produced using k_{vibe} in this study. This supports hypothesis two. Evidence in the oscillations of force after peak impact force for several participants indicates that the impact dynamics of the pelvis may be a more complex system (e.g. one involving multiple modes of resonance) than previously estimated. While stiffness estimates produced using k_{1st} and $k_{combo\ 300}$ were within the range previously reported (Robinovitch, Hayes et al. 1991), some stiffness estimates produced by $k_{combo\ opt}$ were nearly double the previously reported maximum pelvic stiffness estimate of 70,000 kN/m.

Regarding the second goal, I have found that there is a strong effect of both BMI and gender on estimates of stiffness. The average effective pelvic stiffness of low BMI females was 65% lower than that of males, while the decrease in average effective pelvic stiffness between low BMI and high BMI males was 53%. These findings support hypotheses three and four, however, these differences were less evident between low BMI females and high BMI females, as well as high BMI females and high

BMI males. The transition point, which is key to the $k_{combo\ opt}$ mode of stiffness estimation, is mainly dependent on BMI, but is also affected by gender. This finding supports hypothesis five, and will enhance the predictive capability of methods that utilize a piece-wise force-deflection data fitting method. Relative to previous studies of pelvic stiffness, stiffness estimates for low BMI males ranged up to 280,000 N/m. This value is four times higher than the maximum effective stiffness previously reported, 70,000 N/m (Robinovitch, Hayes et al. 1991). The low BMI female and high BMI male groups also had members with stiffness estimates exceeding this previously reported maximal range.

Finally, related to the third aim, I found that there were no differences in stiffness estimates between the different experimental drop heights, which indicates that the stiffness estimates determined using a zero-centimeter drop height and $k_{combo\ opt}$ are acceptable estimates of effective pelvic stiffness for other drop heights and falls from standing height. This supports hypothesis six. Peak forces were an average of 261 N lower for low BMI participants than high BMI participants, but 45% higher when normalized to the effective mass of the pelvis. This supports hypothesis seven. This is evidence of some effect of soft tissue cushioning during impact. These peak forces were strongly related to height, trochanteric soft tissue depth and the stiffness estimates. This supports hypothesis eight, which relates these scientific findings to clinical applications.

3.4.1 Pelvic Stiffness Estimation Methods

The results regarding the quality of fit for stiffness estimation methods k_{1st}, $k_{combo\ 300}$, and $k_{combo\ opt}$ indicate that there is a substantial benefit to fitting the data with a piece-wise polynomial approach (Table 4). These results match the expected outcome of hypothesis 1a. This is also in line with the observations by Robinovitch et al. (1991) and Laing et al. (2010) regarding non-linearities of the force-stiffness relationship in the low force range, as well as what is known about the stress-strain relationship of biological tissues. The improvement between $k_{combo\ 300}$, and $k_{combo\ opt}$,, was also substantial, though in the high-stiffness region, this is only represented by a 2% increase. Because of

the varying number of data points included in the high-stiffness region, mean squared error may provide a less biased comparison between methods. In domain, $k_{combo\ opt}$ provided a 90% reduction in error over $k_{combo\ 300}$, a marked improvement in quality of fit. This adds to what is known about the multi-factorial effect of factors such as BMI and gender on the mechanical properties of other soft tissue components such as ligaments (Chandrashekar, Mansouri et al. 2006; Chandrashekar, Hashemi et al. 2008) and skin (Bader and Bowker 1983; Diridollou, Black et al. 2000). However, the added complexity of $k_{combo\ opt}$ on a person-by-person basis may not be justified for all purposes. Inclusion of a participant-specific transition point may not be practical for all applications, and could be limiting for modeling purposes.

The diminished quality of fit of k_{1st} relative to the more complex stiffness estimation methods does not remove it as a viable method for estimating effective pelvic stiffness, and ultimately predicting peak force. The linear estimation correlates strongly (r^2>0.8 for low BMI females) with the experimental data. Its simplicity is beneficial for modeling purposes because it is the simplest mode of stiffness estimation. The simple force prediction model in section 2.7 can only be used with linear stiffness estimates (i.e. those that follow Hooke's law regarding the relationship between applied force, spring stiffness and the change in spring length). Further, bio-fidelic mechanical systems utilizing a spring can also only be used with linear stiffness estimates. The low-deflection region non-linearities in the force-stiffness relationship are too complex for these force prediction models.

The benefit of $k_{combo\ opt}$ may be in its ability to compartmentalize the separate components of effective pelvic stiffness in realistic, *in vivo* conditions, rather than an isolated *in vitro* set-up. It is likely that the stiffness in the non-linear toe region of the force-deflection curve is related to soft tissue stiffness. This is supported in several ways. First, soft tissue stiffness is much lower than skeletal stiffness (Best, McElhaney et al. 1994). Second, the stiffness of a spring is determined by the relationship $k=AE/L$. The increase in stiffness in the toe region is likely to be associated with an

increase in contact area between the participant and the force plate. This increase is most likely related to the increased radius of soft tissue contacting the force plate increases, and would be relatively constant once the soft tissue is compressed enough that the contact area is constrained by the skeletal components. The linear elastic region is then dominated by the deformation of the skeletal pelvis. Because much less deflection occurs in this region, and the contact area is relatively constant, there is a large increase in stiffness. The ability of $k_{combo\ opt}$ to determine the transition point between these two regions is useful in several ways. First, it allows a more accurate characterization of stiffness in both the overall force-deflection curve, as well as the high-stiffness region, as shown by the improvement in quality of fit between $k_{combo\ 300}$ and $k_{combo\ opt}$. Second, this allows for the development of more complex force-prediction models, which may be more accurate as a result. Third, characterization of the properties of each component separately could provide more accurate knowledge of how each tissue reacts during impact than what is known based on *in vitro* research.

For many participants, stiffness estimates based on the k_{vibe} were lower than expected based on previous reports and other estimations of stiffness in this study. Analysis of the raw data revealed that this method could produce low estimates of effective pelvic stiffness for trials in which it appeared that the pelvis oscillated at a very low frequency after impact (Figure 3.16). This could be explained by two or more modes of vibration following impact, rather than the single mode of vibration assumed in a simple mass-spring model. Multiple modes of vibration, superimposed, could cause result in interference, changing the apparent frequency of vibration. If a higher frequency of oscillation is observed (Figure 3.16 b), the stiffness estimate increases. Statistical analysis showed a significant effect of BMI on the stiffness estimate produced by this method. Due to the error that is apparent with this method, this may not be an accurate analysis of the effect of either BMI or gender on k_{vibe}. If the k_{vibe} stiffness estimation method were to be changed to account for multiple modes of vibration, the analysis of

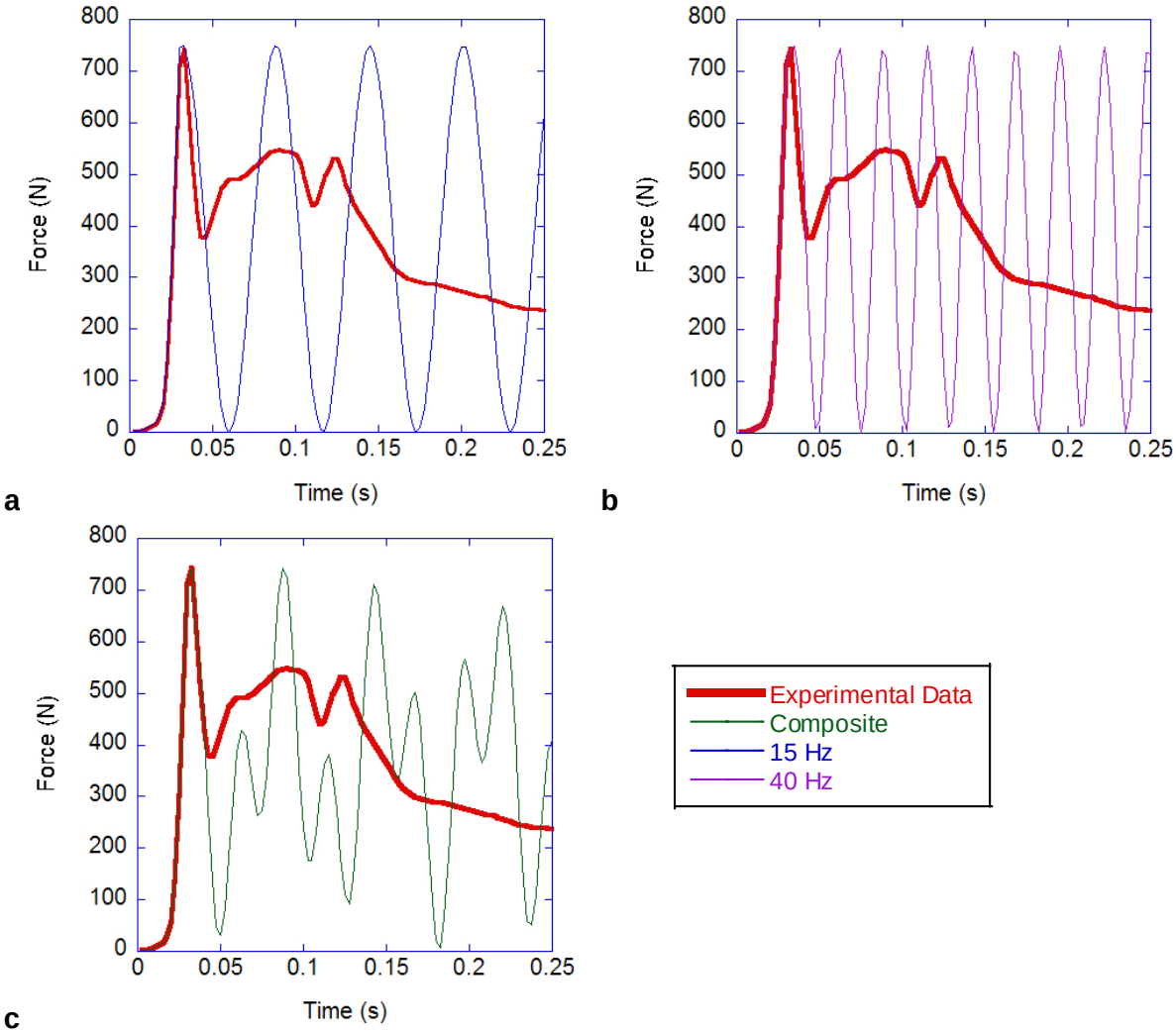

Figure 3.16 k_{vibe} Frequency Estimation Error

Relative to the actual force (dark red) observed during impact, the procedure for calculating k_{vibe} resulted in low estimations of the natural frequency of the pelvis (Figure 3.16a, blue). This could be due to multiple modes of vibration in the pelvis during impact. A prediction of the natural frequency of vibration based on the force-deflection method stiffness estimate is shown in Figure 3.16b (violet). This was found by determining a frequency of oscillation, ω, from the stiffness estimate at peak force, determined by the $k_{combo\ opt}$ approach. A second mode of vibration, offset by 0.0125 seconds, was then introduced to produce a composite vibration (Figure 3.16c, green).The interference of two or more modes of vibration would cause both destructive and constructive interference. This would cause distortion in the observed force amplitude after impact, which would obscure the selection of the true T_{min}. This would result in an incorrect period of oscillation, which would then produce an incorrect estimation of k_{vibe}. *All force values in* Figure 3.16 *have been scaled to the peak force of the actual force observed during impact to highlight the change in frequency of force oscillation rather than the change in force that would be associated with constructive and destructive interference.*

variance results may change to show effects of BMI and gender that are more in line with the results of the force-deflection methods.

The most significant limitation when comparing the relative qualities of the four modes of stiffness estimation is that the results have not been used to predict peak forces. Predictions of peak forces from a height of five-centimeters, based on the stiffness parameters characterized at zero centimeters, would allow the comparison of each approach to a separate data set. Predictions of peak forces from standing height would allow a comparison of the estimated impact forces to the known fracture tolerances of the proximal femur. Based on the results of the comparison between the zero- and five-centimeter drop-height conditions, the stiffness estimates determined in this study would be acceptable characterizations of stiffness at higher energy levels.

The peak stiffness estimates (i.e. $k_{combo\ 300\ peak}$ and $k_{combo\ opt\ peak}$, the stiffness estimates in the high-deflection region) found in this study are only applicable to un-braced, directly lateral impacts to the greater trochanter, with the hip flexed to 75˚. It is currently unknown how well this would match true falls from standing height in older adults. Given the number of possible combinations of impact velocity, hip flexion angle, and rotations about all of the local axes of the pelvis, it may be a better strategy to find the component stiffness of trochanteric soft tissue and the rest of the pelvis and develop a model that can predict peak force based on these variables. However, in research by Laing et al. (Laing, Tootoonchi et al. 2006), a torso-upright position produced significantly lower peak forces than a side-lying position similar that which was employed in this study. This indicates that the positioning used for this study may provide 'worst-case scenario' peak stiffness and peak force estimations. This would be a safer, more conservative approach, to estimating peak forces in the elderly.

The limitations of the resonance-based stiffness estimation, k_{vibe}, show that it is of limited use relative to the models which incorporate deflection data. Expansion of this method to incorporate the

multiple modes of vibration would make it a more useful technique for the study of hip impacts where the ability to use kinematic markers is limited. Of the force-deflection methods, k_{1st} is most beneficial in its simplicity. This makes it the most straightforward approach to select a stiffness input to a peak-force prediction model. On the other hand, $k_{combo\ opt}$ is most useful in its ability to partition effective pelvic stiffness into low-force and high-force regions. This may, in the long run, be more useful in determining how pelvic stiffness modifies the peak forces resulting from a lateral impact to the hip. For example, $k_{combo\ opt}$ provides a transition point which may represent how much energy is absorbed by the soft tissue prior to the impact of the greater trochanter. Knowledge of the stiffness in the low-deflection region may also be useful for determining peak forces during very low, but clinically significant falls. There may be a secondary benefit to the study of balance control. Characterization of the force attenuation properties of soft tissue thickness at very low forces may be beneficial in determining their effect on modulating perturbations (e.g. colliding with a chair or moving object) during standing or walking tasks. Because the benefits of these two stiffness estimation methods are so different, they should both be the subject of continued research.

The stiffness estimates provided by $k_{combo\ opt}$ are higher than the previously reported stiffness estimation range of 15,000 to 70,000 N/m (Robinovitch, Hayes et al. 1991; Robinovitch, Hayes et al. 1997; Laing and Robinovitch 2008), which is likely due to the location of the transition. This is particularly exaggerated in low BMI males—the mean stiffness estimate produced by $k_{combo\ opt}$ is approximately 68% greater than the mean stiffness estimate produced by k_{1st}. This is strong evidence that there should be careful consideration in the selection of stiffness estimates for peak force prediction for groups based on differing body habitus characteristics.

The transition selected by $k_{combo\ opt}$ partitions the stiffness estimate into two regions, but what factors (e.g. soft tissue depth, skeletal components) dominate each region is not known. One explanation is that as soft tissue compresses from initial impact to transition, the contact area increases. After the

transition point is reached, soft tissue reaches maximal compression, and *A* is related to the height and width of the pelvis in the sagittal plane. The contact area and soft tissue compression would cease to increase, causing a plateau in stiffness. Soft tissue would therefore have a limited effect on effective stiffness in the high force region.

3.4.2 Stiffness Estimates for BMI and Gender Groups

Overall, there were significant main effects of BMI and gender, which supports hypotheses three and four. The effective stiffness of the pelvis is dependent on several components such as skeletal structure and soft tissue depth, which vary with BMI and gender. There was also a significant BMI-gender interaction, as well as two comparisons where the distinctions between BMI-gender interaction groups were not as distinct.

There were no differences found in the estimates of pelvic stiffness for females between the high and low BMI group. This is contrary to the prediction of hypothesis three, and does not appear to follow the theoretical estimation of stiffness, $k=AE/L$, where L would be the depth of trochanteric soft tissue. A difference was found between the high and low BMI males, but only using $k_{combo\ opt}$. If the transition point selected by $k_{combo\ opt}$ is based on the point at which A is maximized, a theory presented in section 3.4.1, this may explain why a difference was not found for females. The maximal contact area is not based solely on the dimensions of the sagittal plane cross-section of the pelvis and proximal femur, but also a portion of the soft tissue surrounding it. The high BMI participants had greater depth of soft tissue directly over the greater trochanter, but also anterior and posterior to the hip. Therefore, the amount of maximal contact area was likely greater for high BMI participants than low BMI participants. This was not measured in this study. Including this information may show that the $k=AE/L$ adequately describes the relationship between peak force, soft tissue depth, and the maximal area of the hip in the sagittal plane.

Significant differences in pelvic stiffness were found between low BMI males and females. The males in this group do have significantly higher effective pelvic stiffness than females, as predicted in hypothesis four. This matches the results published by Robinovitch et al. (Robinovitch, Hayes et al. 1991) regarding gender-related differences in pelvic stiffness. The trochanteric soft tissue thickness was not significantly different between males and females for the low BMI group ($F(1,6) = 0.278$, $p = 0.608$), which indicates that the difference in peak stiffness is not related to the depth of soft tissue. Several anatomical components, particularly the structure of the pelvis and proximal femur, likely contribute to the decreased peak stiffness in females.

Based on epidemiological data, the effective pelvic stiffness of low BMI males is extremely high relative to the relative frequency of hip fracture in this population. Effective stiffness has been shown in this study, as well as others (Robinovitch, Hayes et al. 1991; Robinovitch, Hayes et al. 1997; Laing and Robinovitch 2008), to correlate positively with peak force. This discrepancy is likely due to other factors regarding hip fracture. Older adult males suffer fall-related injuries at a much lower frequency than older adult females (Nevitt, Cummings et al. 1991). Older adult males have significantly higher BMD (a measure of bone strength) than older adult females (Gjesdal, Halse et al. 2008). Finally, older adult males have greater upper body strength (Frontera, Hughes et al. 1991), a factor which is hypothesized to be protective against hip fracture in exchange for a higher incidence of wrist fracture and other upper extremity injuries (Nevitt and Cummings 1993).

In contrast to the evidence presented for low BMI participants, no difference was found between high BMI males and females. This contrary to what was predicted in hypothesis 4. The expected differences between the peak pelvic stiffness of males and females were based mostly on the skeletal components rather than soft tissue. High BMI participants had a significantly greater depth of trochanteric soft tissue than low BMI participants ($F(1,26) = 54.023$, $p<0.001$). The lower soft tissue thickness associated with low BMI participants would be associated with less energy absorption in

the low-stiffness region, and higher energy applied during the high-stiffness region. It is likely that peak effective stiffness was reached for the low BMI participants.

The non-linear region is theorized to be related to soft-tissue deformation. This is expected to occur to a greater extent in the high BMI group due to their greater depth of trochanteric soft tissue. A potential consequence of this is that the linear (peak) stiffness is never reached for these participants at the within the range of impact energy in this study. An example of this is participant BAL (Appendix 3, HM 3 BAL). For this participant, the transition occurred at 95% of maximal deflection, with the low-stiffness second-order portion of the polynomial accounting for 84 out of 86 experimental data points. It is not clear from this specific data set if a true peak effective pelvic stiffness was found. Therefore, further studies are required to determine if the stiffness in the high-deflection region is different for high BMI males and females at higher impact energies. Regardless, it appears that gender-related differences in effective pelvic stiffness are attenuated for high BMI participants in the impact scenarios used in this study. If there were further non-linearities in this relationship, it is possible that peak stiffness was not reached for these groups. Therefore the comparison between high BMI males and females would not produce significant differences.

BMI had a much stronger effect on the transitions selected by $k_{combo\ opt}$ than gender. This produces mixed results for hypothesis five. There appears to be a strong relationship between the optimized transition point, L_{force} and the weight of the participant. L_{force} occurred at a much higher force for high BMI participants than low BMI participants. The amount of deflection at the transition, $L_{deflection}$ is also distinctly different between the two BMI groups, but how this is related to the covariates measured in this study is not as clear. The transition consistently occurred at 60% of maximal trial deflection, with slightly higher in the high BMI participants, and slightly lower in the low BMI participants. The point at which $L_{deflection}$ occurs is most likely dependent on the depth of trochanteric soft tissue, however, this relationship was not tested in this study. This could explain why gender did not have a significant influence on $L_{deflection}$ and L_{force}. For low BMI participants, the amount of soft

tissue overlying the hip was not significantly different between males and females ($F(1,12) = 0.639$, $p = 0.421$). For high BMI participants, males had slightly thinner soft tissue than females ($F(1,6) = 7.792$, $p = 0.016$), a difference of approximately 20%, or less than two centimeters. If the relationship between $L_{deflection}$ and soft tissue thickness is significant (this was not tested in this thesis), this could explain why there was no effect of gender on the transition points associated with $k_{combo\ opt}$.

The relationship between BMI and the transition point may clarify what was previously observed regarding the transition point. The effective mass of the pelvis is approximately half the total body mass, the 300 N transition point previously observed may be due to the population studied. The average weight for participants reported by Robinovitch et al. (Robinovitch, Hayes et al. 1991) is 683.3 N, while Laing et al. (Laing and Robinovitch 2008) reports a mean weight of 553.3 N. A transition at 300 N may not have been significantly different from a transition point selected by $k_{combo\ opt}$, for these participants. While $k_{combo\ opt}$ may not have had a significantly improved fit compared to $k_{combo\ 300}$, a transition point of 300 N may be too low to estimate effective pelvic stiffness in morbidly obese fallers. Selection of a transition point at lower forces results in lower stiffness estimates. A demonstration of this effect is shown for participant ATH in Figure 3.17. This participant had the highest effective pelvic mass, at 652.3 N. The optimal transition point for this participant, selected by $k_{combo\ opt}$, was 731.3 N, a 431.3 N increase over the transition point used for $k_{combo\ 300}$. For fallers with very low body weight, selection of a 300 N transition point would result in higher predictions of effective pelvic stiffness than those produced by $k_{combo\ opt}$. Because the transition point appears to be highly related to the effective mass of the pelvis, $k_{combo\ opt}$ is therefore not much more complex than $k_{combo\ 300}$. Based on the tradeoff between method simplicity and accuracy of stiffness estimation, it may be beneficial to use the more complex method.

A potential limitation of this study is that the hormonal influence on peak pelvic stiffness was not investigated. In theory, cyclic hormonal fluctuations would cause more variance in the compliance of ligaments in the pelves and hips of females. This would cause more variance in the peak pelvic

stiffness estimations. This was not found to be the case. Both low BMI and high BMI females had less variance in the stiffness estimate than their male counterparts BMI males. Further, this hormonal influence is not as strong for post-menopausal women, the group of older adults at highest risk for hip fracture (Cummings and Melton 2002). It is not likely, therefore, that the hormonal influence of the female participants would limit the applicability of these stiffness estimates to older adult females.

Strong conclusions about the pelvic stiffness of high BMI fallers cannot be made until a true peak stiffness is reached for these participants. This can be explored either through continued pelvis release experiments (using higher drop heights) or, more safely, using soft tissue attached to a mechanical indentor. This second method was utilized by Robinovitch and colleagues (1995), however, the soft tissue depth was limited to a maximum of five centimeters. The results of this study show that males do have greater pelvic stiffness than females. More research of the pelvis, in an isolated and de-fleshed state, could add depth to the explanation of why this difference exists.

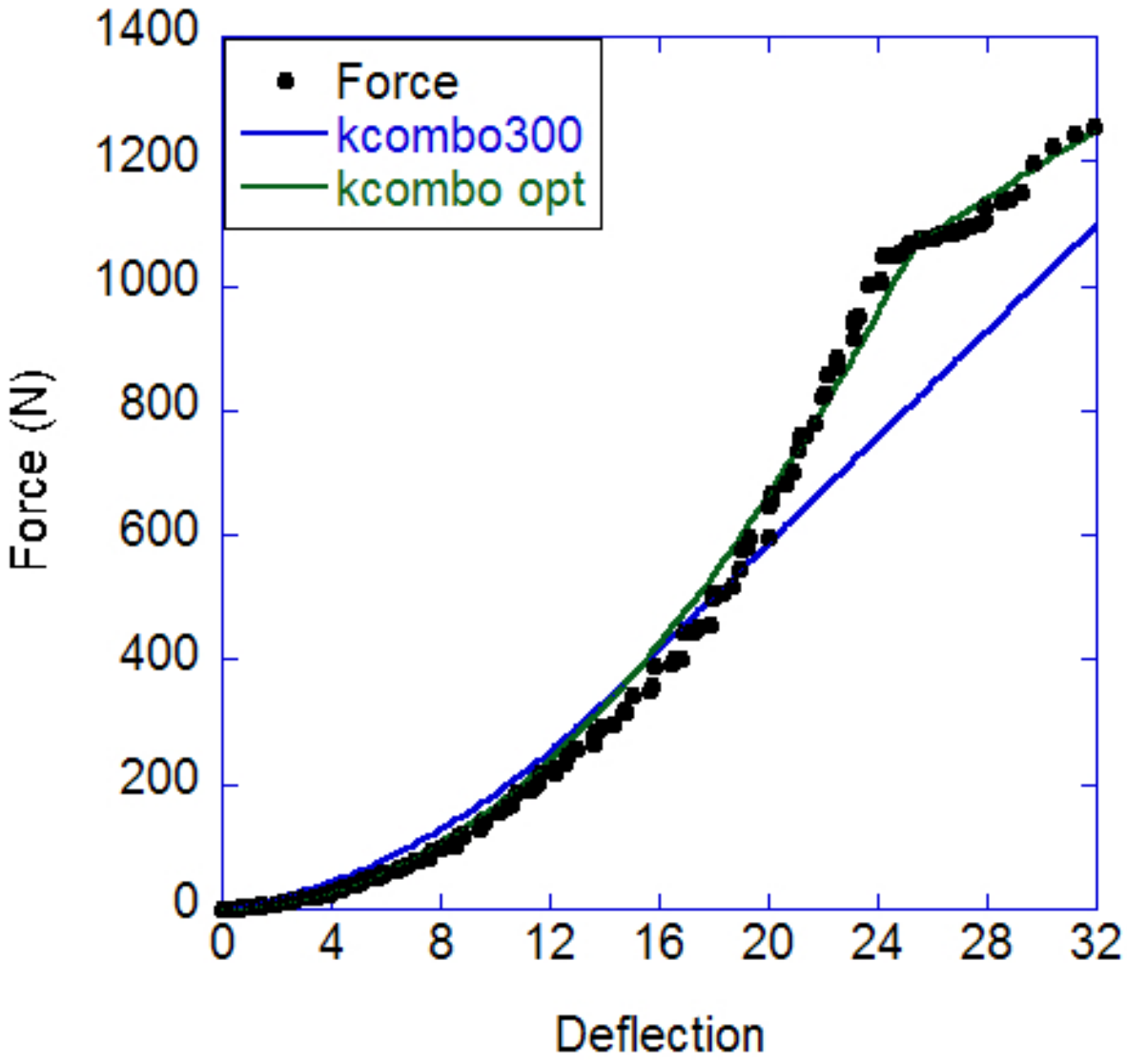

Figure 3.17 Stiffness Method Comparison for Participant ATH

The quality of fit (determined by R^2) improves by 0.12 between $k_{combo\ 300}$ and $k_{combo\ opt}$. The transition point selected by the $k_{comboopt}$, 1082.4 N, is a 782.4 N increase from the transition point used by $k_{combo\ 300}$.

3.4.3 Peak Force Predictions

The stiffness estimates derived from the five-centimeter drop-height data do not differ from those derived from the zero-centimeter drop-height data (Figure 3.18). This data suggests there are no further non-linearities in the force-stiffness relationship that may not have been captured with these

experimental conditions. This matches results from Robinovitch et al. and Laing et al. (Robinovitch, Hayes et al. 1991; Laing and Robinovitch 2010), who reported no further non-linearities in the force-stiffness relationship at forces greater than 300 N. The potential for non-linearities in the force-stiffness relationship is related to the stiffness of the soft tissue. Further non-linearities in the force-stiffness relationship were not observed in this study, and the referenced studies because the soft tissue stiffness was limited by the maximum trochanteric soft tissue depth, however, this may not be true for more morbidly obese fallers.

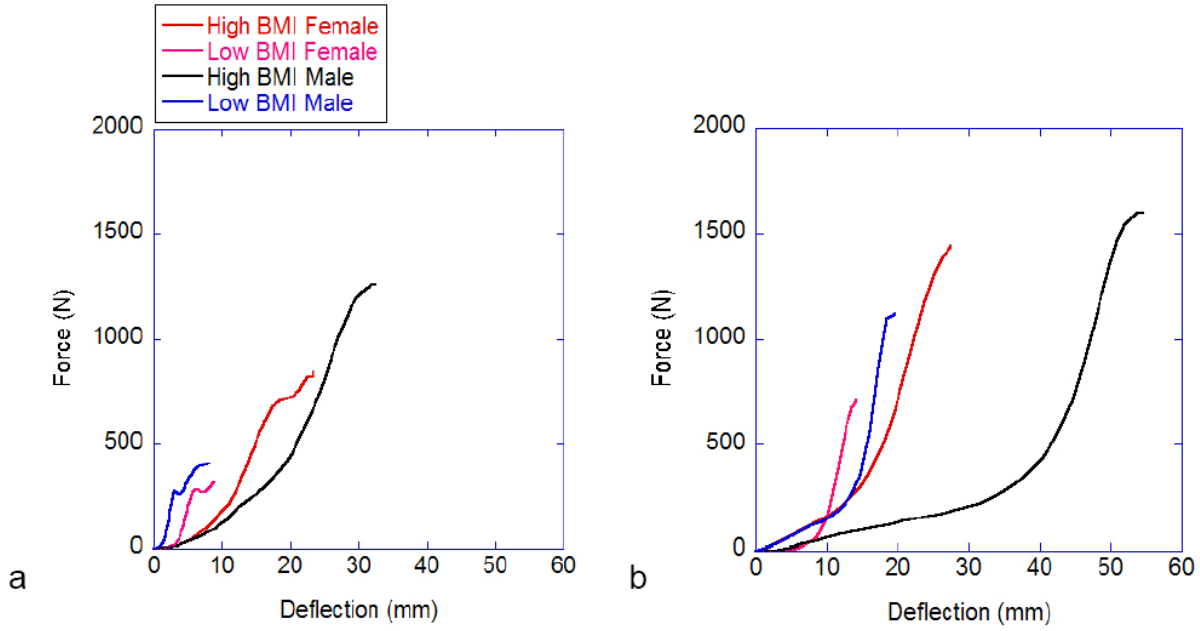

Figure 3.18 Force-Deflection Curves for Four Representative Participants

Figure 3.18a represents the resulting force-deflection curves from a zero-centimeter drop height condition for four participants. Figure 3.18b represents the resulting force-deflection curves from a five-centimeter drop height condition for four participants. The slope of the force-deflection curve does not vary between drop-heights in the high-stiffness region.

For morbidly obese fallers, pelvis release experiments from the heights used in this study may show further non-linearities in the force-stiffness relationship. This would indicate that pelvis release experiments from a higher drop height may be justified in order to reach peak stiffness. Ethical considerations, however, may prevent such experimentation. The peak force for high BMI

participants during the five-centimeter drop-height condition ranged up to a maximum of 1784.5 N. The reported fracture tolerance of the proximal femur is as low as 2,000 N in older adults (Bouxsein, Courtney et al. 1995). While the fracture tolerance in young adults is normally closer to 8,000 N (Courtney, Wachtel et al. 1994), higher energy pelvis release experiments may push peak forces closer to the fracture tolerance. At minimum, higher energy pelvis release experiments would cause significantly more bruising, discomfort, and soft tissue changes. Because this has not been shown to be an issue in this study, it is likely that effective stiffness estimates derived from the zero-centimeter drop-height data are a suitable representation for the majority of low and high BMI people.

The low BMI participants experienced higher normalized peak forces than the high BMI participants. While this measure has little bearing on actual fracture outcomes, it indicates that the soft tissue does provide a cushioning impact for high BMI participants during impact. This suggests that low BMI fallers may benefit from interventions such as protective hip padding, which reduces the effective stiffness of the pelvis by providing an in-series very low stiffness component. These protective measures may not be as useful for high BMI fallers, as the change in overall effective stiffness introduced by a compliant hip protector may be less for high BMI persons (with low pelvic stiffness) than for low BMI persons (with high pelvic stiffness).. Relative to the effective stiffness of the pelvis, the effective stiffness of the pelvis and low-stiffness padding or flooring, in-series, may not be significantly different.

Ultimately, however, peak force has greater bearing on clinical fracture risk than normalized peak force. In this case, the high BMI participants experienced much higher peak forces than those sustained by low BMI participants. The effective mass of the pelvis, for these participants, is high enough that it outweighs the benefit of the soft tissue cushioning. This may provide a significant load-tolerance mismatch for subpopulations of the high BMI population. Even though obesity is generally linked with high bone mineral density, cyclic dieting (Lainglois, Mussolino, et al. 2001) and weight-loss surgeries (Meyer, Tverdal et al. 1998; Carrasco, Ruz et al. 2009), along with poor diet are

associated with low bone density. As the rate of older adults that are obese increases, a higher incidence of hip fracture could occur due to these mechanical factors.

To estimate whether the current effective stiffness and mass characteristics combined to produce impact forces that are above the fracture threshold of the proximal femur during realistic fall scenarios, it would be necessary to simulate falls using impact velocities expected during a fall from standing height. These simulations were not included as a part of this thesis. Relative to the peak forces observed in this study, high BMI participants reached 46% of the average fracture tolerance of the proximal femur in older adults, while low BMI participants reached 37% from the five centimeter experimental drop height (Lochmüller, Groll et al. 2002). For both groups, this shows that fallers in both BMI groups could experience hip fractures from starting heights much lower than standing height.

Ideally, the estimated peak stiffness value can be used to predict the peak force of a fall from standing height. A moderate relationship was found between $k_{combo\ opt}$ ($r^2 = 0.550$), trochanteric soft tissue depth ($r^2 = 0.785$), participant height ($r^2 = 0.326$), and the peak force associated with a five-centimeter freefall. These results match what was expected based on theoretical relationships between stiffness and peak force, and support further research to develop predictive models of impact loads that incorporate both effective stiffness and soft tissue thickness.

The third factor which proved to be a significant predictor of peak force was participant height. This could be related to a potential relationship between body height and dimensions of the pelvis such as the interspinous distance (Ridgeway, Arias et al. 2011). Increase in total body height may therefore increase the size of the contact area during impact, which would increase effective pelvic stiffness. Height is the weakest of the three predictive variables, however, which is likely due to the variability in the relationship between height and pelvic dimensions. More accurately measured pelvic dimensions would likely result in a stronger predictive capability.

The last variable excluded from the backwards regression analysis was the effective mass of the pelvis. This resulted in an R^2 decrease of 0.007, and a slight increase in standard error. The significance of this variable prior to exclusion, however, was 0.258, which is substantially over the exclusion criterion of 0.100. This variable was expected to be included in the final regression model, based on the relationship between force, impact velocity and participant characteristics ($F_{peak} = v_{impact}\sqrt{mk}$, described in section 2.7). This may be due to a strong correlation between the neutral mass of the pelvis and soft tissue depth ($r(26) = 0.709$, $p<0.001$).

The results of the regression analysis are limited by two factors. The first is sample size and distribution. While peak force was normally distributed in terms of skew, the kurtosis of the sample was very low (-0.983). This was a result of using two distinctly different BMI groups, and would be improved by the inclusion of a normal BMI group to strengthen what is known about the characteristics of the force-stiffness relationship. The second limiting factor is that peak effective stiffness was potentially not captured for high BMI participants, using the current methods. Finding a true peak stiffness for these participants would likely change results of the regression analysis. Standardized residuals were within the expected range for all predicted values using the current data, but it is unclear if this would change if stiffness estimates for the high BMI participants increases.

The results of the regression analysis, as they currently stand, add evidence that interventions focused on reducing effective stiffness would be a mechanically effective method of reducing the peak force suffered following a fall from standing height. The peak forces observed in the high BMI participants, however, are very concerning. The effective mass of the pelvis, for these participants, exceeds the cushioning capability of their increased soft tissue depth.

3.4.4 Limitations and Sources of Error

There are several further limitations to this study. Statistically, the sample size and population studied are a significant limitation. A larger sample may reduce the variance in the stiffness estimates,

particularly for groups with a large amount of variance (such as the low BMI males). This would increase the effect size of stiffness estimation method. Particularly for $k_{combo\ 300}$ and $k_{combo\ opt}$, this could provide us with more confidence in determining whether the methods provide different results, and aid in determining whether one approach is a more appropriate measure to focus on in future studies. The effect of sample size and range of body composition characteristics would have the greatest effect on the regression analysis. While the skew of the sample used in the regression analysis was minimal (-0.149) the kurtosis (-0.983) shows that there is a lack of values close to the mean. This is related to the exclusion of normal BMI participants. The sample population was large enough to provide a substantial effect (the post-hoc effect size was 0.859), and no significant errors were observed in the residual plots. The regression model, however, may be improved by the inclusion of normal BMI participants, which would provide more peak forces close to the mean.

Technical limitations include marker migration, soft tissue pre-compression and the lack of data related to pressure distribution. Marker migration and soft tissue pre-compression are two factors that were carefully considered during the development of this study. Placement of the marker overlying the greater trochanter was inspected between trials to ensure consistent location. The marker was also visually observed during each pelvis release experiment. When studying normal-weight and under-weight participants, a small amount of migration of the skin and marker relative to the skeletal landmark is expected. When studying obese participants, this effect is magnified. It is unknown what effect marker migration has had on the results for these participants. It is likely that this effect is limited by the fact that only the vertical movement of the marker was analyzed. Further research about the technical limitations of kinematic analysis would be useful for continued study of this growing population.

Soft tissue pre-compression is a limiting factor, however, care was taken to ensure that the effect would be consistent across all participants and conditions. It is unknown how much soft tissue pre-compression occurred during the pelvis release experiments. The maximal deflections from each trial

ranged up to 96.6% of the soft tissue thickness measured by ultrasound. This shows that the pre-compressed tissue likely reached a point during free-fall at which the effect of compression in the sling was negated. Pilot testing showed that the pre-compression effect of the spandex shorts caused minimal changes to the peak force and impact characteristics relative to a pair of loose shorts. Despite this, care was taken to ensure that the spandex shorts selected for each participant were neither too loose for consistent marker placement, nor too tight and compressive. If movement of the marker overlying the greater trochanter was observed (i.e. the marker moved to any place other than the palpated greater trochanter between trials), a smaller size of shorts was selected. If a large amount of soft tissue bulging was observed, particularly around the waist and leg bands, a larger size of shorts was selected.

The lack of data about pressure distribution between the start of impact and peak force is a limiting factor given the current results. It is unknown what effect the dimensions of the pelvis (height, width and depth) have on the stiffness characteristics of the pelvis. It is also unknown how these dimensions are modified by the volume of soft tissue. While only trochanteric soft tissue depth was measured, the effect is not limited to this dimension. Soft tissue surrounds the pelvis, and may change the peak contact area during impact. This factor could be determined using a pressure plate.

The most clinically significant limitation is the position of the pelvis during impact. Research by and Laing et al. (Robinovitch, Hayes et al. 1997; Laing, Tootoonchi et al. 2006) shows that changing the body position during pelvis release experiments from side-lying to a torso-upright position decreased peak force at the hip by 30%. Nankaku and colleagues reported that changing from a lateral impact to a backwards impact results in a 1000 N increase in impact force following a fall from standing height (Nankaku, Kanzaki et al. 2005). Hip flexion angle and bracing by the upper limbs are also factors which would change the positioning and magnitude of force applied to the pelvis during impact. This study focuses on only one configuration. Further research which focuses on the stiffness of each component of the pelvis, combined with the results from this study, may produce stiffness

estimations that would be useful for predicting peak forces resulting from a greater variety of falling configurations.

Another deficit that electromyography was not collected as part of the current studies. Robinovitch and colleagues (1997) reported no effect of trunk muscle activation on peak force and stiffness outcomes during lateral pelvis release experiments. While care was taken to ensure the participants were relaxed (psychologically and physically) before each trial, this was not monitored. Participants who were more nervous than they reported could have used strategies such as bracing to limit the pain of impact during the pelvis release trial. This would have an effect on the peak forces recorded. Varying levels of bracing attempts using hip stabilizing muscles (such as gluteus medius) would certainly have an effect on the effective pelvic stiffness determined in this study. Nankaku and colleagues reported moderate gluteus medius EMG activity (25-30% maximal voluntary contraction) during a voluntary fall from standing height. If this level of muscle activation is present during falls in the elderly, then muscle-relaxed pelvis release experiments may produce lower stiffness estimates than those that occur during actual falls. A measure of cardiovascular stress, using a heart rate monitor, and activation of gluteus medius, using electromyography, may be of benefit to further pelvis release experiments.

Finally, the age of the population studied is a significant limitation. It is unknown how well these estimations of pelvic stiffness in young adults will correspond to the effective pelvic stiffness of older adults. Hormonal influence on soft tissue tensile properties, level of hydration and muscle tone are all factors that are likely to be different in older adults. Stiffness of the proximal femur has been shown to be lower in older adults than young adults during high rates of loading (Courtney, Wachtel et al. 1994), but it is likely that there are may more structural effects that have not yet been studied. Further cadaveric study and modeling of impacts would likely be the safest approach of estimating peak force and impact characteristics in this population.

3.5 Implications

This thesis has demonstrated that body habitus and gender have significant effects on the stiffness of the pelvis during lateral falls. These differences are likely related to a combination of soft tissue and pelvic anatomical differences between BMI and gender groups. Different approaches may be required for each of these BMI and gender groups in order to reduce the risk of fall related injury.

3.5.1 For Clinicians

Pelvic stiffness, along with other easily collected variables, may be helpful in predicting peak forces resulting from lateral falls in the elderly. The creation of this type of tool may be beneficial for clinicians and residential care facilities attempting to determine the best approach for limiting fracture risk amongst their patients. This information would also be useful for the development of new interventions to reduce the effect of force during lateral falls.

Most relevant to clinicians is that while high BMI fallers may in some cases have lower pelvic stiffness, this may not be effective in reducing peak forces. The effective mass of the pelvis is great enough in this sub-population to outweigh the reduction in pelvic stiffness. Clinically, this means that fall prevention and mechanical risk reduction techniques should not be ignored for obese older adults. Unfortunately, there are several limitations in the implementation of these mechanical risk-reduction interventions, such as the maximum size and increased fitting diffculties associated with wearable protective hip padding in obese adults (Choi, Hoffer et al. 2010). Additionally, compliant impact surfaces have a theoretically more limited mechanical effectiveness for high BMI fallers than low BMI fallers. Increasing populations of obese older adults (Arterburn, Crane et al. 2004) may result in a greater incidence of fall-related injury in this sub-population than what has been previously observed in epidemiological study.

3.5.2 For Research

The data presented in this thesis will aid in selecting the most appropriate pelvic stiffness parameters when modeling impact dynamics for higher energy falls. In order to produce these tools, however, further research is necessary. The benefit of each of the stiffness estimation methods described in this thesis, relative to actual falls, cannot be known until the stiffness estimates are used in a force prediction model. Related to the limitations of this thesis, further investigations of the component properties of the pelvis and soft tissue should be completed. This will build on the research of Hayes and colleagues, Robinovitch and colleagues, Lauritzen and Askegaard, and Beason and colleagues. Particularly, focus on the changes in BMD, and pelvic and trochanteric soft tissue thickness, as they relate to aging, obesity, and changes in body habitus would be particularly beneficial. Additionally, further pelvis release experiments, utilizing a pressure plate, would be extremely useful in determining factors such as the peak contact area of the pelvis following a lateral impact. These investigations would fine-tune the pelvic stiffness estimation approach, and make its applications more versatile.

Finally, while this study shows some benefit of dividing the force-deflection curve into distinct low-stiffness and high-stiffness regions, the effect of this separation on estimating peak force is not known. Additionally, while it can be theorized that stiffness in the low-force region is dominated by soft tissue characteristics, and that stiffness in the high-force region is dominated by skeletal components. Whether or not this is the case should be the focus of more research in both the *in vivo* and *in vitro* realms. The transition between these two regions appears to have some relationship with weight and soft tissue depth. While it is unclear what this transition represents, more study of this transition point and the high-stiffness region may provide more insight into how the hip is loaded during impact.

3.6 Conclusions

The research presented in this thesis provides valuable information regarding impact related injuries. Relating to the first goal, method of stiffness estimation method has been shown to have a significant impact on the stiffness estimate produced, and the quality of fit to the experimental data. There is a clear effect of both BMI and gender on effective pelvic stiffness, but this difference is less clear between some BMI-gender interaction groups. Finally, knowledge of effective pelvic stiffness may be useful for prediction of peak force following a lateral fall.

Appendix 1: Ultrasound Technique

An ultrasound device (M-Turbo Ultrasound System, SonoSite, Bothell, Washington, USA) with a C60x 5-2MHz, curved array (30cm scan depth), was used to determine the two-dimensional soft tissue depth over the greater trochanter.

The ultrasound technique of two raters was tested to maximize the validity and repeatability of these measures. Eight short lengths of plastic pipes were measured by a lab member via calipers and submerged into gelatin ultrasound phantoms. The dimensions of the pipes were unknown to the raters, who collected three two-dimensional images of each pipe dimension (length, width, height). Agreement between the raters was moderate for all three dimensions (interclass correlation of 0.749, 0.660, 0.727 for length, width and height, respectively), and reliability within the main rater was high (interclass correlation of 0.998, 0.866 and 0.995). Measurements determined by ultrasound were all within 0.1 cm of the measurements previously determined via calipers. Both raters had an average error of 3.5%.

The technique was also tested *in vivo*, with six female participants, using the same methods and controls as the main study. Participants were asked to stand with the medial edges of their calcaneus and first metatarsal fifteen centimeters apart. This foot position was marked on a tape affixed to the floor in order to maintain a consistent stance during and between ultrasound measurements. The participant was asked to stand with their weight evenly distributed through each foot, with their upper body braced against a wooden box (122 x 61 x 20 centimeters) to reduce movement of the hip and spine during the ultrasound collection (Figure 3.1). This limited changes in angle of the femur with respect to the pelvis, as well as variation in the amount of soft tissue overlying the greater trochanter. After exposing the skin over the left hip by lifting up the leg of the participant's shorts, the greater trochanter was identified through palpation, and ultrasound gel was applied to the skin over the

landmark. With the ultrasound transducer aligned perpendicular to the femur, three coronal plane ultrasound images were collected (Figure 3.2). Care was taken to limit compression of the soft tissue by the transducer head. For each image, the built-in software caliper function was used to measure the distance between the surface of the skin and the greater trochanter.

The results from this in-vivo pilot study supported the reliability of this approach. For each participant, all soft tissue thickness measurements were within 0.5 cm of each other. Inter-rater reliability for the pilot study were fairly strong (interclass correlation of 0.779 for the right hip), as was intra-rater reliability (interclass correlation of 0.942).

Appendix 2: Sling Selection

The sling supporting the pelvis is made of a thin piece of rip-stop nylon, 51cm wide (corresponding to the distance from the waist to mid-thigh of the participant) by 137cm long (evenly cradling the pelvis, with 5cm double-layer channels on each short end for the passage of a height-adjustable set of strong nylon climbing ropes and a turnbuckle; this unit was in turn connected to an electromagnet (custom model, AEC Magnetics, Cincinnati, Ohio, USA) affixed to the ceiling.

Sling selection was based on minimizing pre-compression of the soft tissue while maximizing participant comfort and reproducibility of the participant position within the sling. In a pilot study related to sling selection, the full nylon sling was compared to one which had a 15cm by 30 cm oval hole removed from the center of the sling to allow the pelvis to suspend freely, with no tissue compression. Previously, the sling with the hole had been rejected for the purpose of the pelvis release experiments based on predictions of soft tissue bulging over the uncompressed region (the portion of the pelvis and thigh exposed by the hole), but from the pilot data, this was not consistent (Figure A.1). While in some cases, tissue did bulge over the greater trochanter, in others, the femur was allowed to adduct, stretching the tissue directly over the greater trochanter, and causing it to bulge in other areas. Despite consistent marking of landmarks on the participant, and attempts to position the pelvis consistently with respect to the hole, tissue bulging and stretching effects were not consistent. Ultrasound was used to determine the two-dimensional soft tissue depth over the greater trochanter in both the standing position defined previously (Figure 3.1), and while the participant was suspended in the modified sling. These two measurements were not significantly different for the two pilot participants. Peak forces from a five-centimeter pelvis release were also not significantly different. Reproducibility of the participant position was much more difficult with the modified sling than the full sling, due to the variability in the amount of soft tissue bulging and stretching through

the hole. The full sling was also much more comfortable for the participant, which allows for a more relaxed state prior to the pelvis release. For all of these reasons the full sling was adopted.

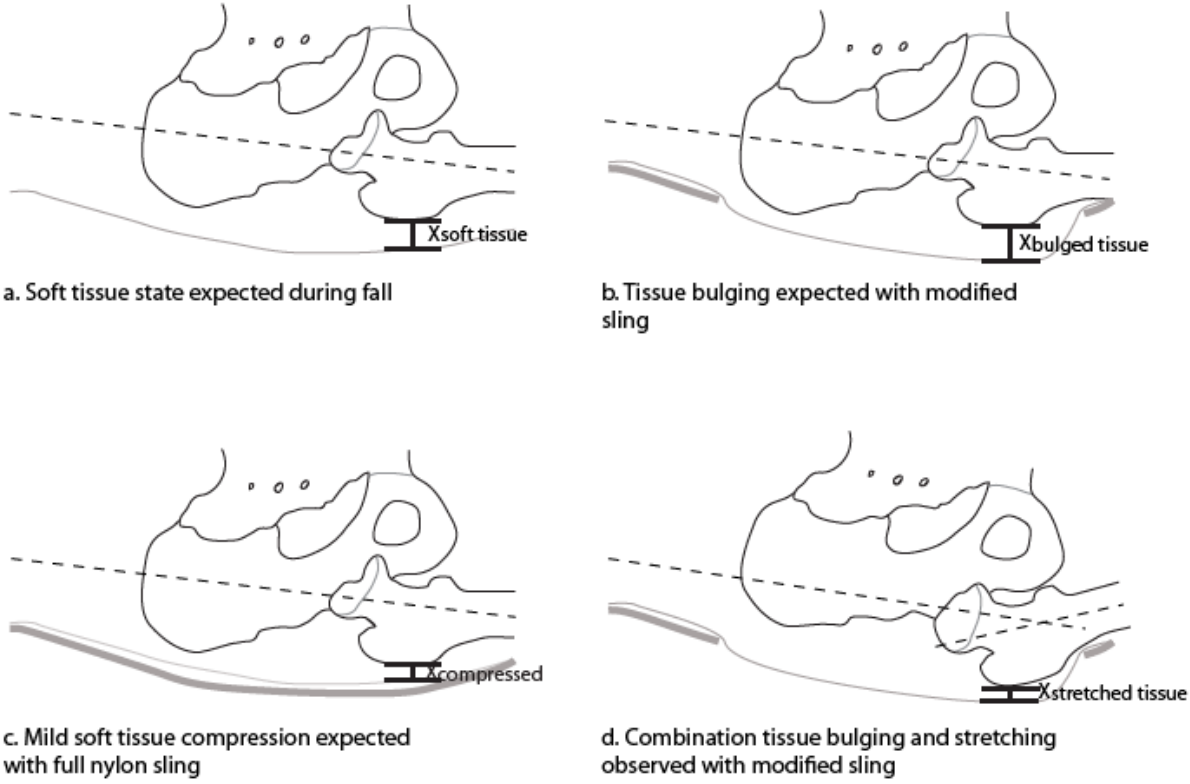

Figure A.1 Expected and observed soft tissue pre-compression

Several trials of a pilot study were completed in order to investigate the effect of sling type on soft tissue pre-compression and impact characteristics. It was expected that the modified sling type (with a 15cm by 30 cm oval hole removed from the center of the sling) would reduce the pre-compression observed during experiments using the full sling (image c). The modified sling (images b and d), however, resulted in more variable pre-impact positioning, despite the extra care required to reproduce placement between trials. In some cases, the skin and soft tissue was stretched within the opening, causing more compression of the soft tissue. In others, the soft tissue bulged out of the opening in the sling. Further, the modified sling allowed changes in the position of the femur with respect to the pelvis, which was not consistent or predictable.

Appendix 3: Force-Deflection Curves for All Participants

The following set of images represents the force-deflection curves for four pooled trials, one image per participant. The participant codes for the images below indicate the BMI-gender grouping, following the following scheme:

Code	Group
HF	High BMI Females
HM	High BMI Males
LF	Low BMI Females
LM	Low BMI Males

This code is then followed by a number and a three-letter code indicating the specific participant. The experimental data points are represented by the black circles. The curve fit to the experimental data is represented by a black line.

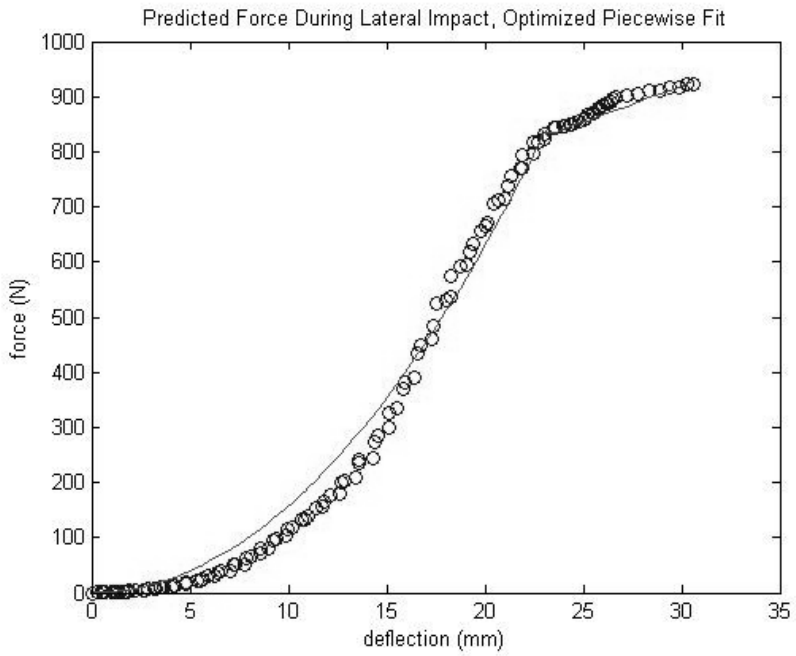

HF 1 KMD

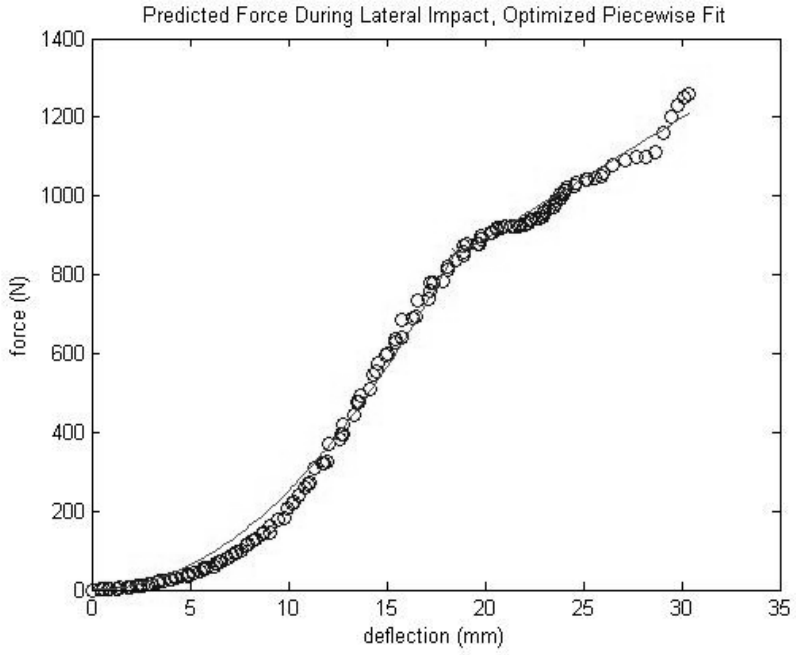

HF 2 MAA

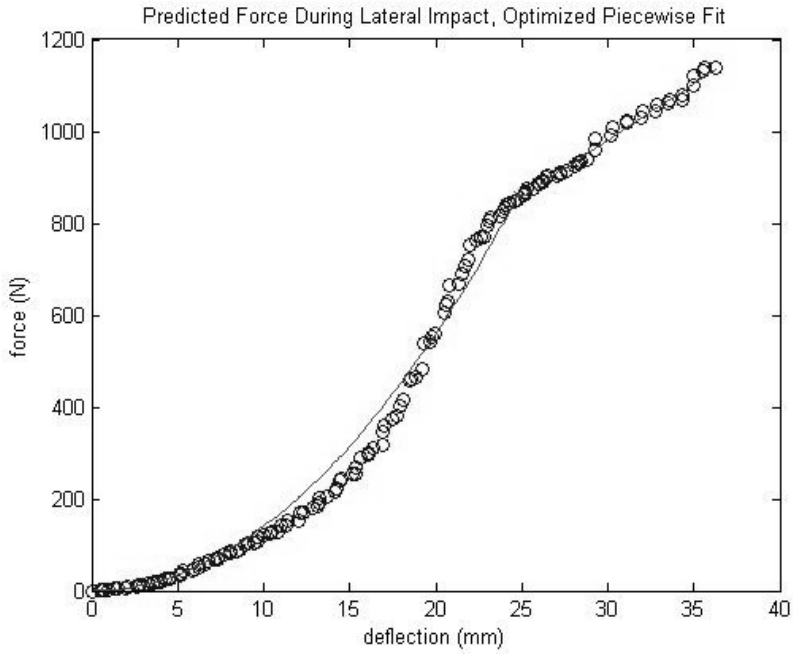

HF 3 MDC

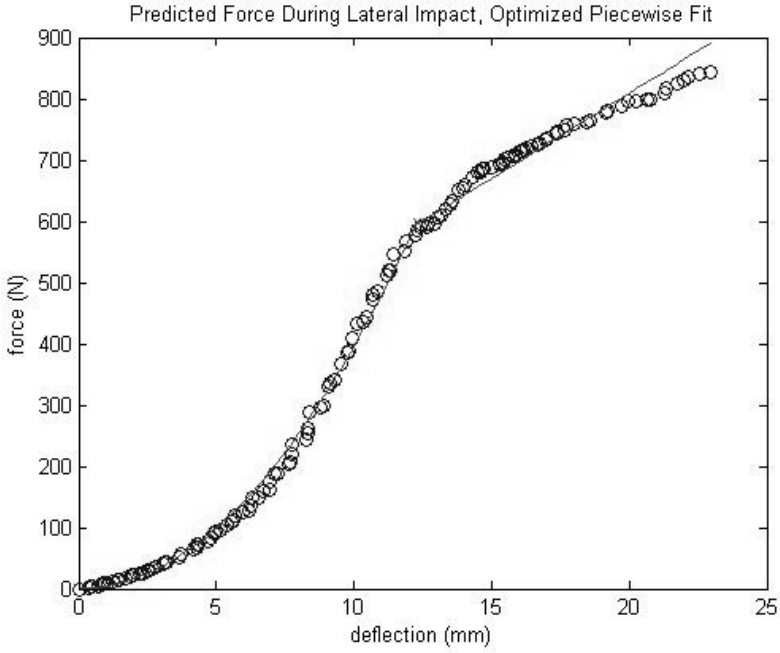

HF 4 CAT

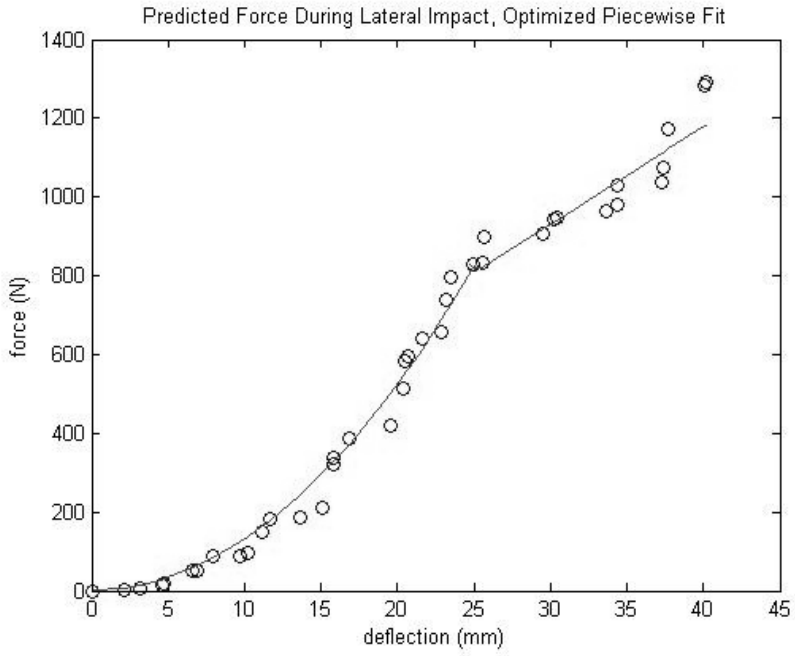

HF 5 CBM

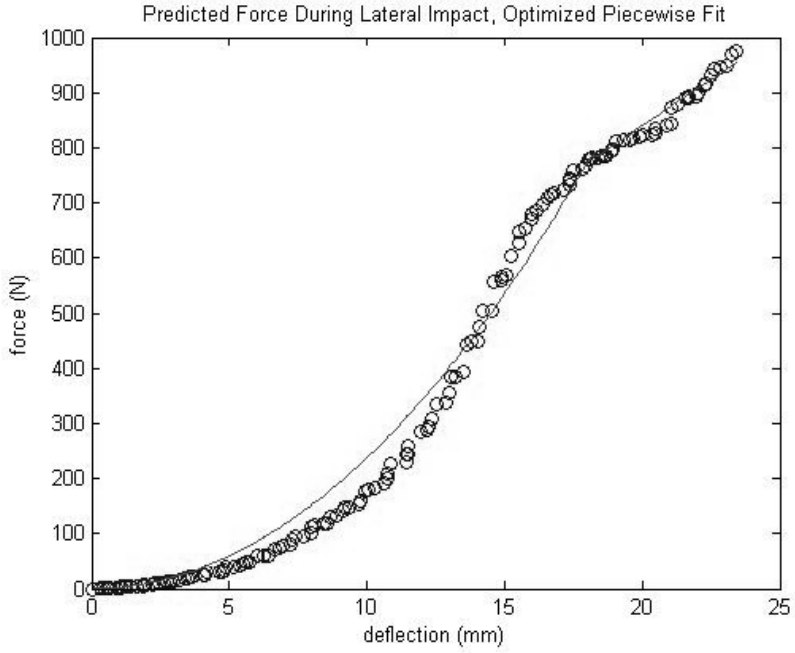

HF 6 CVB

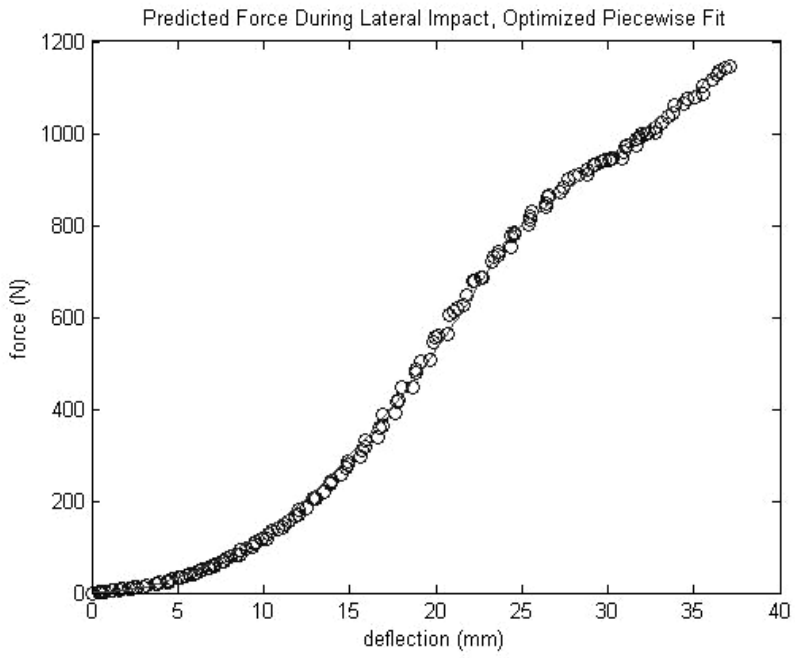
Predicted Force During Lateral Impact, Optimized Piecewise Fit
force (N)
deflection (mm)
0
200
400
600
800
1000
1200
0
5
10
15
20
25
30
35
40

HF 7 DCM

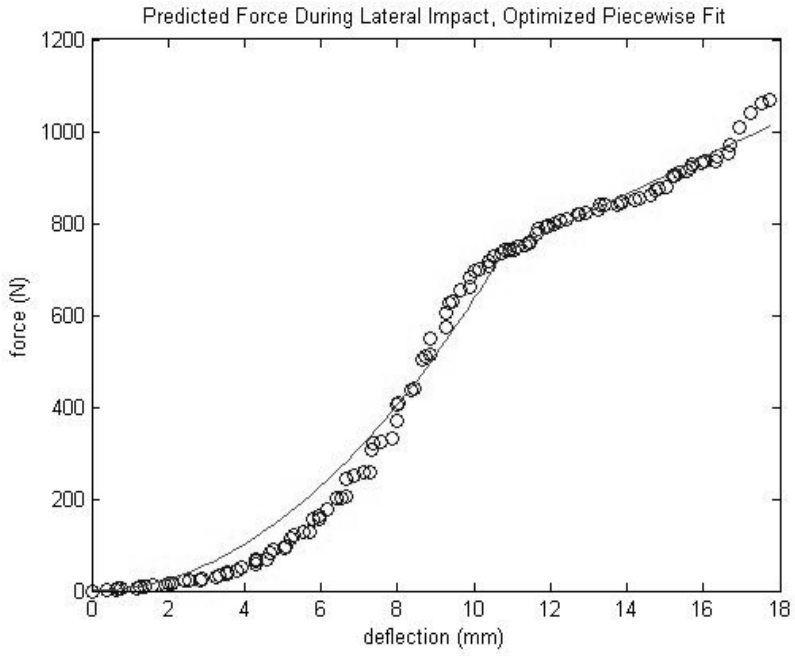

HM 1 ACC

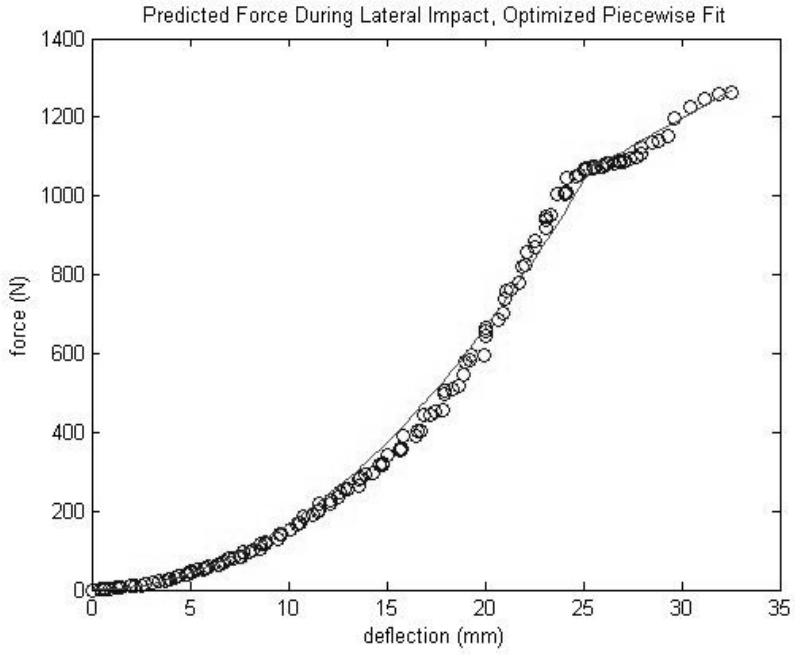

HM 2 ATH

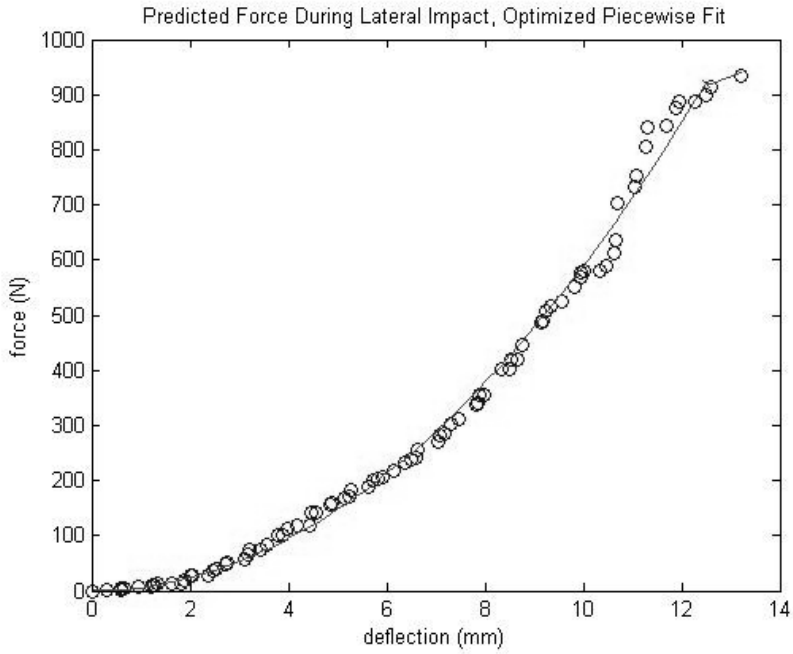

HM 3 BAL

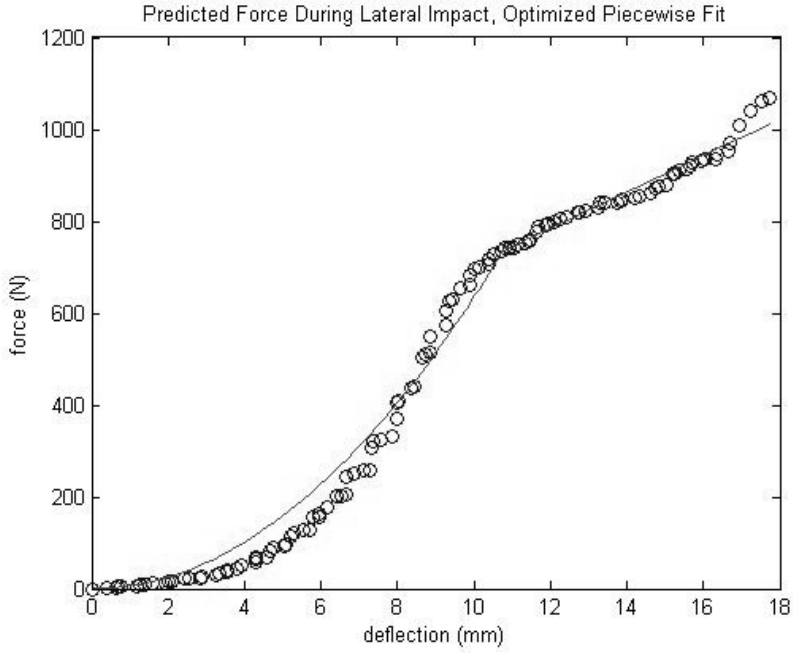

HM 4 BRP

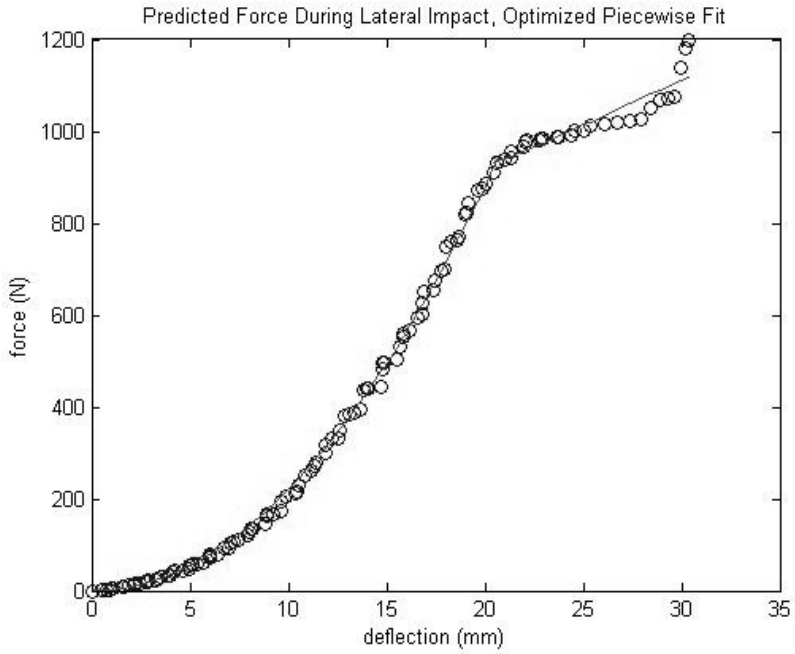

HM 5 KSC

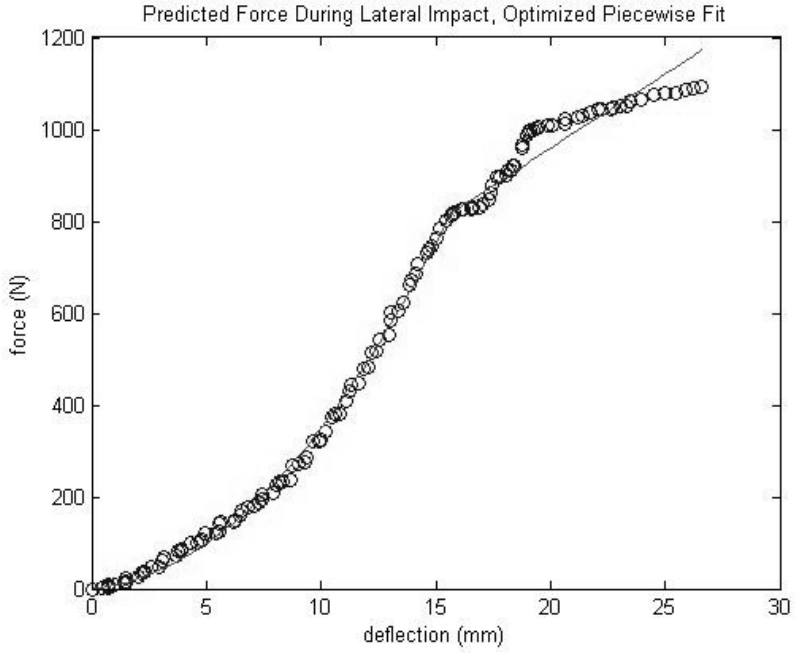

HM 6 MEJ

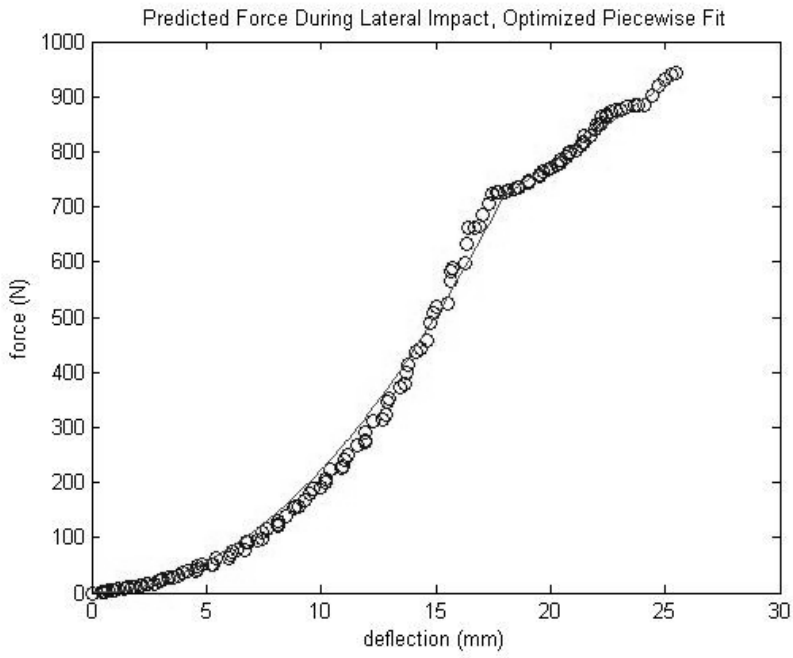
Predicted Force During Lateral Impact, Optimized Piecewise Fit
force (N)
deflection (mm)
0
100
200
300
400
500
600
700
800
900
1000
0
5
10
15
20
25
30

HM 7 YKJ

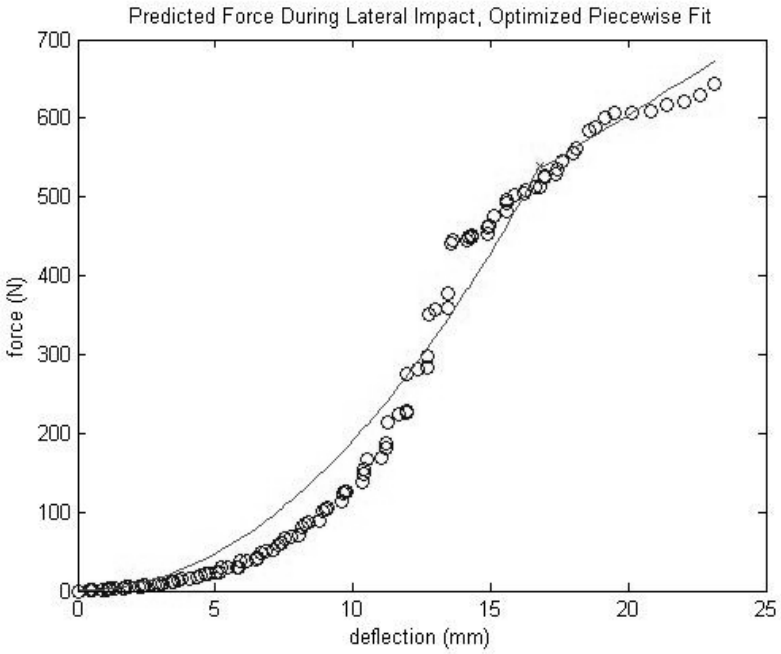

LF 1 EMB

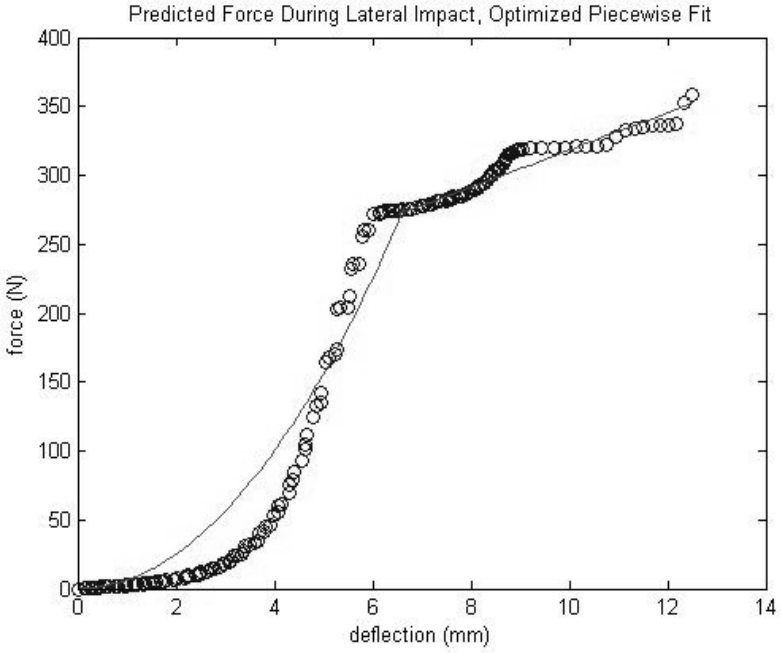

LF 2 FYC

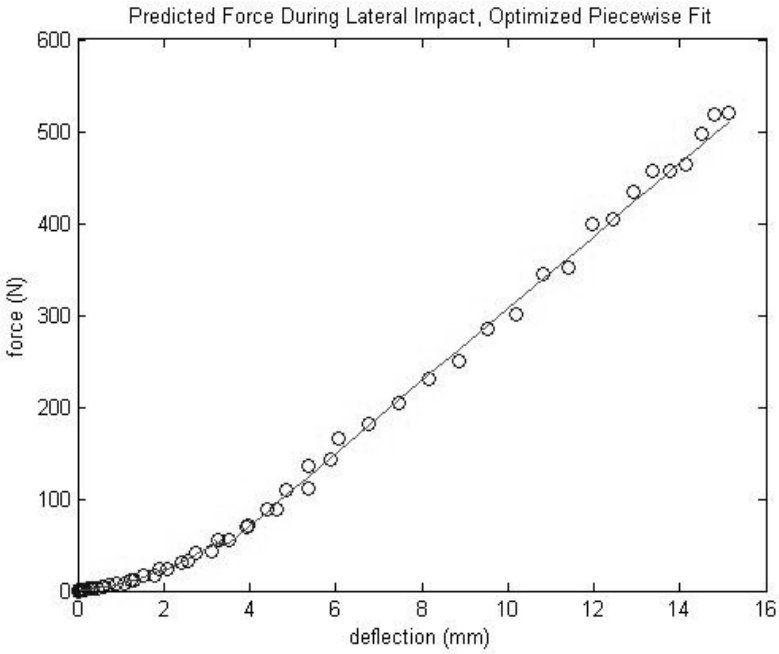

LF 3 JAC

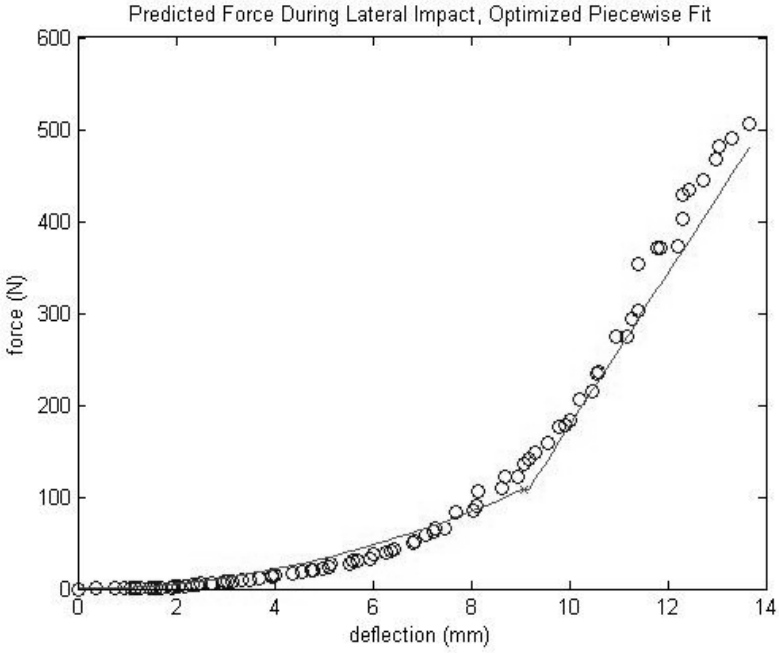

LF 4 JLH

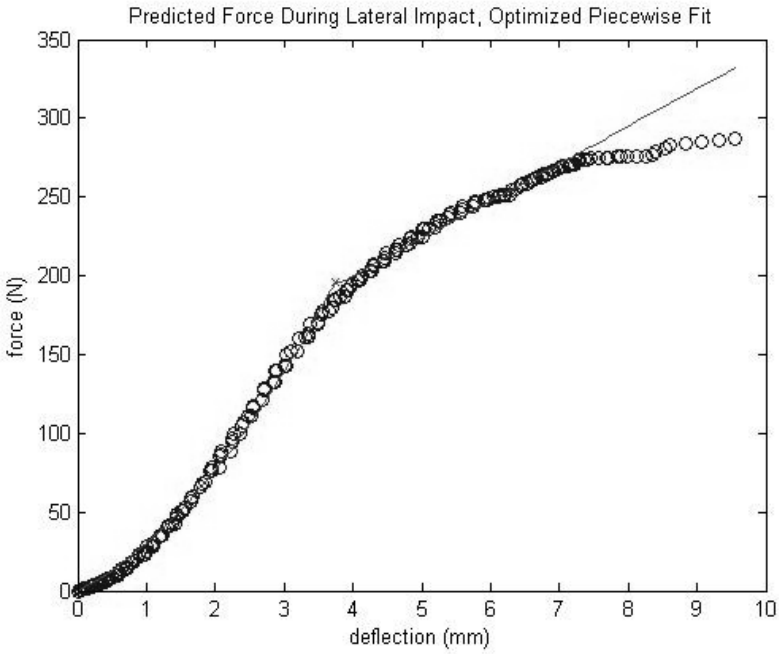

LF 5 LEM

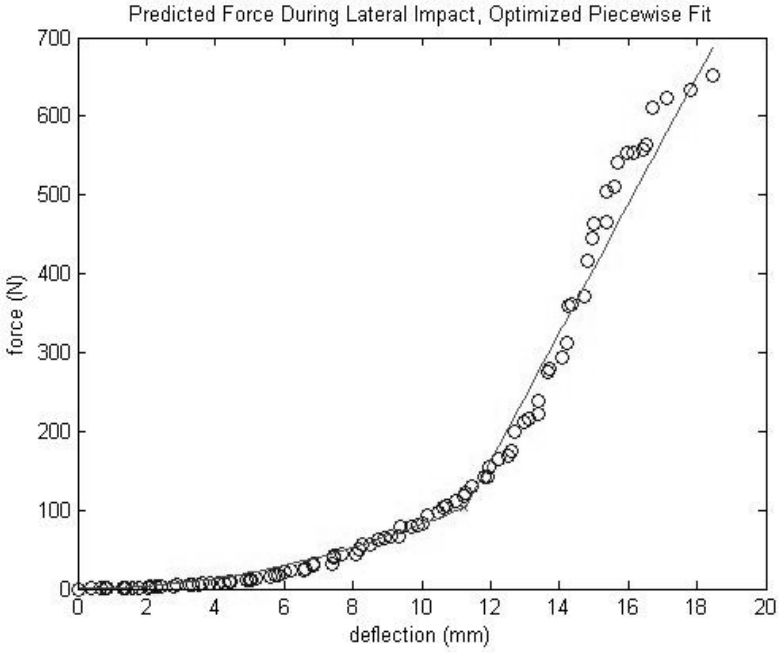

LF 6 TAL

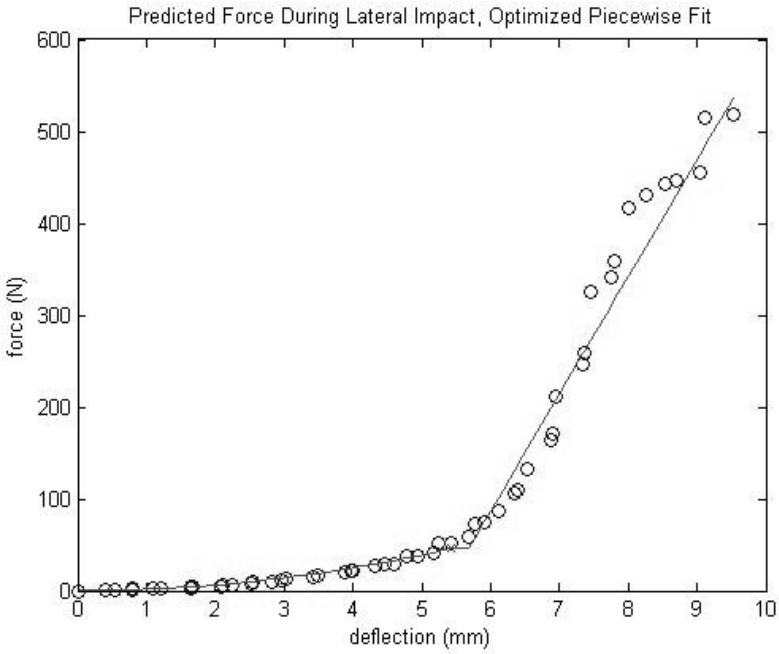
Predicted Force During Lateral Impact, Optimized Piecewise Fit
force (N)
deflection (mm)
0
100
200
300
400
500
600
0
1
2
3
4
5
6
7
8
9
10

LF 7 TMT

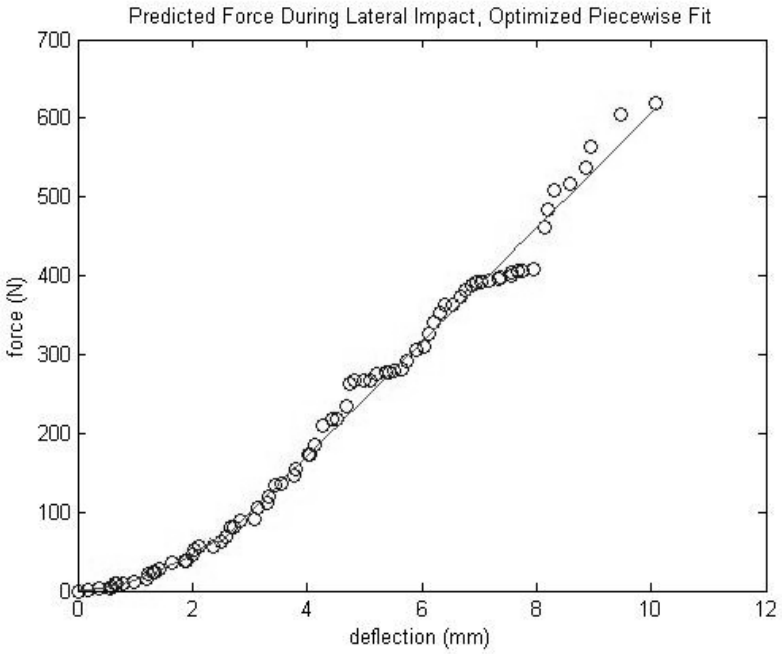

LM 1 AAY

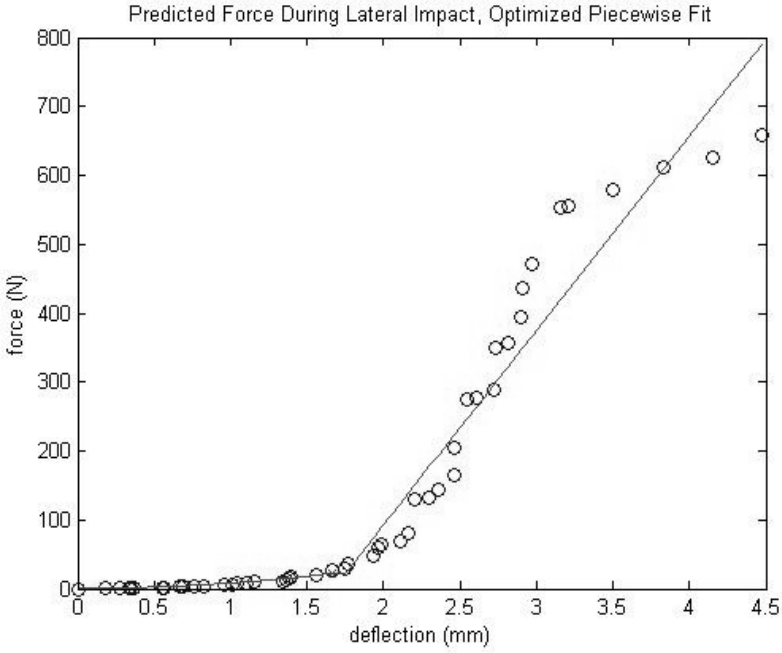

LM 2 ADT

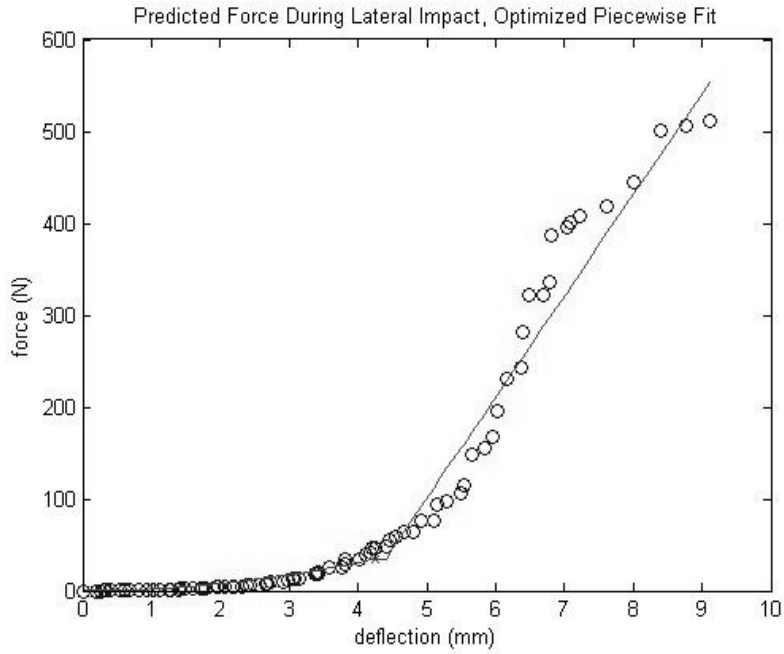

LM 3 DAT

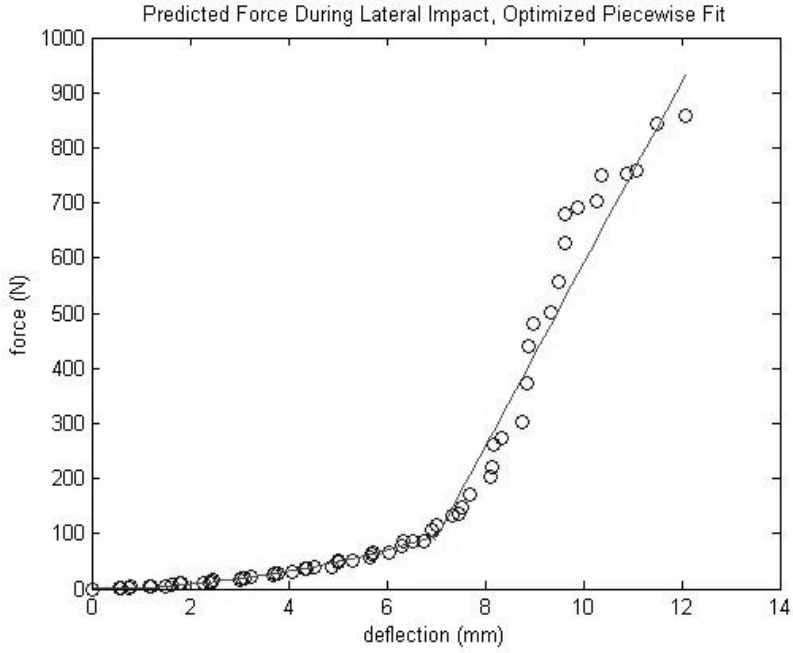

LM 4 KSL

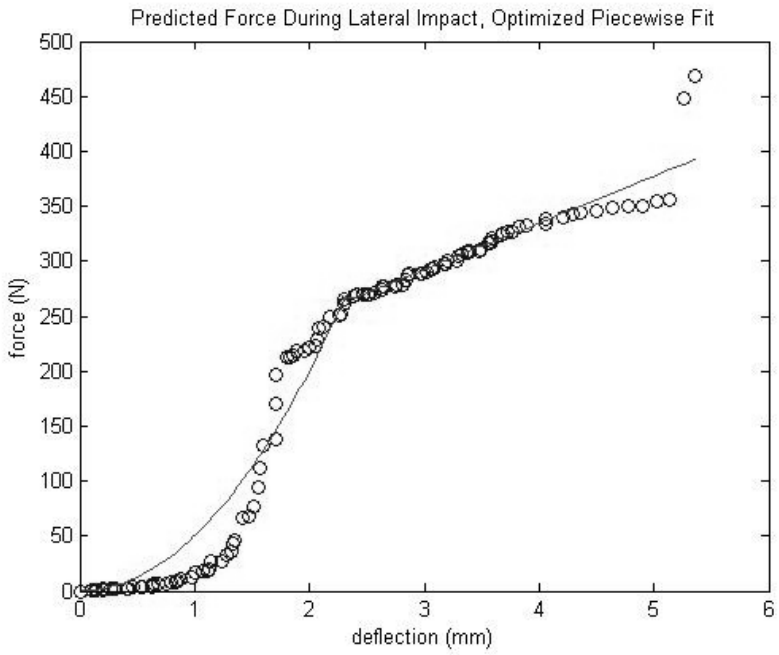

LM 5 MAD

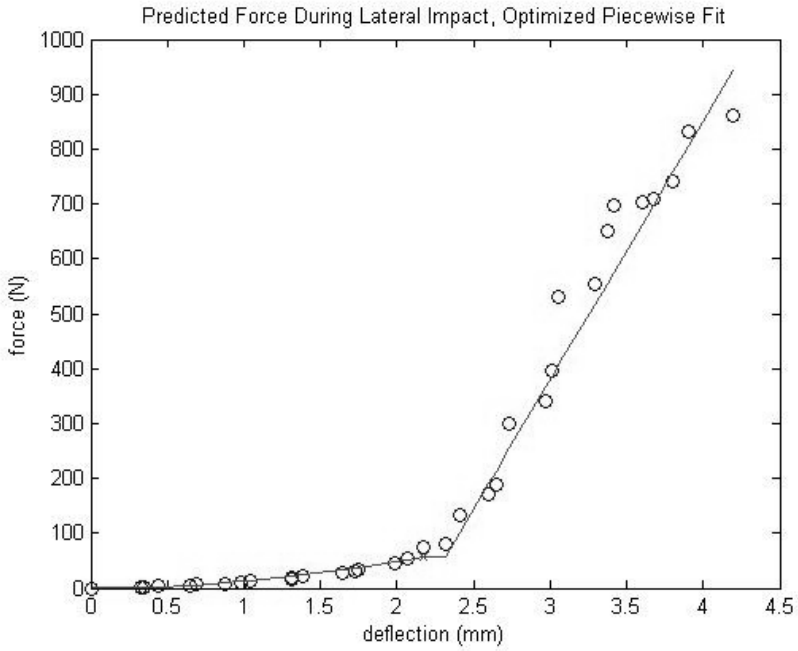

LM 6 NSF

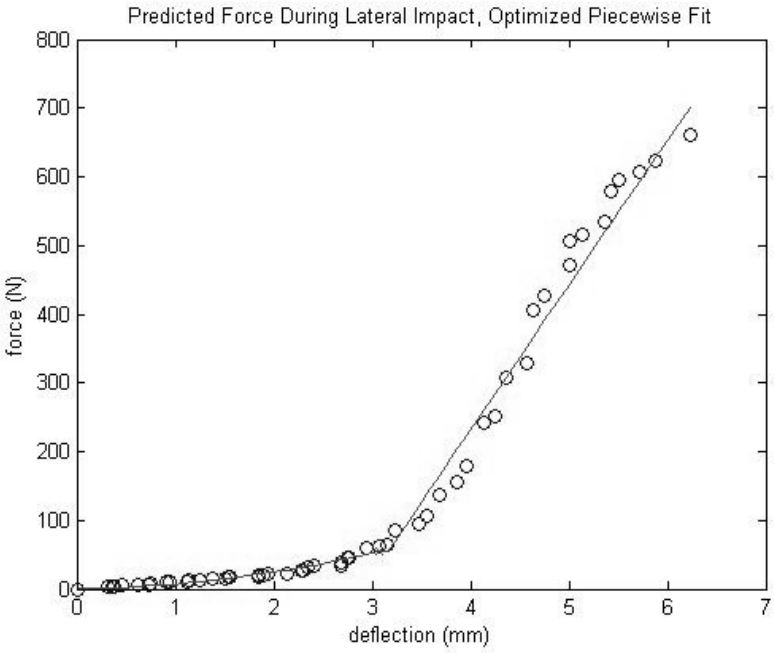
Predicted Force During Lateral Impact, Optimized Piecewise Fit
force (N)
deflection (mm)
0
100
200
300
400
500
600
700
800
0
1
2
3
4
5
6
7

LM 7 TAS

References

Arterburn, D. E., P. K. Crane, et al. (2004). "The coming epidemic of obesity in elderly Americans." Journal of the American Geriatrics Society **52**(11): 1907-1912.

Bader, D. and P. Bowker (1983). "Mechanical characteristics of skin and underlying tissues in vivo." Biomaterials **4**(4): 305-308.

Beason, D., G. Dakin, et al. (2003). "Bone mineral density correlates with fracture load in experimental side impacts of the pelvis." Journal of biomechanics **36**(2): 219-227.

Belanger-Ducharme, F. and A. Tremblay (2005). "Prevalence of obesity in Canada." Obesity Reviews **6**(3): 183-186.

Best, T. M., J. McElhaney, et al. (1994). "Characterization of the passive responses of live skeletal muscle using the quasi-linear theory of viscoelasticity." Journal of biomechanics **27**(4): 413-419.

Bouxsein, M., A. Courtney, et al. (1995). "Ultrasound and densitometry of the calcaneus correlate with the failure loads of cadaveric femurs." Calcified tissue international **56**(2): 99-103.

Bouxsein, M., P. Szulc, et al. (2007). "Contribution of Trochanteric Soft Tissues to Fall Force Estimates, the Factor of Risk, and Prediction of Hip Fracture Risk*." Journal of Bone and Mineral Research **22**(6): 825-831.

Cameron, I., S. Robinovitch, et al. (2010). "Hip protectors: recommendations for conducting clinical trials—an international consensus statement (part II)." Osteoporosis International **21**(1): 1-10.

Carrasco, F., M. Ruz, et al. (2009). "Changes in bone mineral density, body composition and adiponectin levels in morbidly obese patients after bariatric surgery." Obesity surgery **19**(1): 41-46.

Chandrashekar, N., J. Hashemi, et al. (2008). "Low-load behaviour of the patellar tendon graft and its relevance to the biomechanics of the reconstructed knee." Clinical Biomechanics **23**(7): 918-925.

Chandrashekar, N., H. Mansouri, et al. (2006). "Sex-based differences in the tensile properties of the human anterior cruciate ligament." Journal of biomechanics **39**(16): 2943-2950.

Cheng, X., G. Lowet, et al. (1998). "Prediction of Vertebral and Femoral Strength In Vitro by Bone Mineral Density Measured at Different Skeletal Sites*." Journal of Bone and Mineral Research **13**: 1439-1443.

Choi, W., J. Hoffer, et al. (2009). "The effect of positioning on the biomechanical performance of soft shell hip protectors." Journal of biomechanics.

Choi, W., J. Hoffer, et al. (2010). "Effect of hip protectors, falling angle and body mass index on pressure distribution over the hip during simulated falls." Clinical Biomechanics.

Choi, W., J. Hoffer, et al. (2010). "Effect of hip protectors, falling angle and body mass index on pressure distribution over the hip during simulated falls." Clinical Biomechanics **25**(1): 63-69.

Cooper, C., E. Atkinson, et al. (1992). "Incidence of clinically diagnosed vertebral fractures: a population-based study in Rochester, Minnesota, 1985-1989." Journal of Bone and Mineral Research **7**(2): 221-227.

Corbeil, P., M. Simoneau, et al. (2001). "Increased risk for falling associated with obesity: mathematical modeling of postural control." IEEE Transactions on Neural Systems and Rehabilitation Engineering **9**(2): 126-136.

Courtney, A., E. Wachtel, et al. (1994). "Effects of loading rate on strength of the proximal femur." Calcified tissue international **55**(1): 53-58.

Cummings, S. and L. Melton (2002). "Epidemiology and outcomes of osteoporotic fractures." The Lancet **359**(9319): 1761-1767.

Diridollou, S., D. Black, et al. (2000). "Sex and site dependent variations in the thickness and mechanical properties of human skin in vivo." International journal of cosmetic science **22**(6): 421-435.

Etheridge, B., D. Beason, et al. (2005). "Effects of trochanteric soft tissues and bone density on fracture of the female pelvis in experimental side impacts." Annals of biomedical engineering **33**(2): 248-254.

Feldman, F. and S. Robinovitch (2007). "Reducing hip fracture risk during sideways falls: evidence in young adults of the protective effects of impact to the hands and stepping." Journal of biomechanics **40**(12): 2612-2618.

Feldman, F. and S. N. Robinovitch (2007). "Reducing hip fracture risk during sideways falls: Evidence in young adults of the protective effects of impact to the hands and stepping." Journal of biomechanics **40**(12): 2612-2618.

Fleischer, J., E. Stein, et al. (2008). "The decline in hip bone density after gastric bypass surgery is associated with extent of weight loss." Journal of Clinical Endocrinology & Metabolism **93**(10): 3735.

Frick, K., J. Kung, et al. (2010). "Evaluating the Cost-Effectiveness of Fall Prevention Programs that Reduce Fall-Related Hip Fractures in Older Adults." Journal of the American Geriatrics Society **58**(1): 136-141.

Frontera, W. R., V. A. Hughes, et al. (1991). "A cross-sectional study of muscle strength and mass in 45-to 78-yr-old men and women." Journal of Applied Physiology **71**(2): 644.

Gjesdal, C., J. Halse, et al. (2008). "Impact of lean mass and fat mass on bone mineral density: The Hordaland Health Study." Maturitas **59**(2): 191-200.

Gjesdal, C. G., J. I. Halse, et al. (2008). "Impact of lean mass and fat mass on bone mineral density: The Hordaland Health Study." Maturitas **59**(2): 191-200.

Grisso, J., J. Kelsey, et al. (1991). "Risk factors for falls as a cause of hip fracture in women. The Northeast Hip Fracture Study Group." New England Journal of Medicine **324**(19): 1326.

Hayes, N., J. Close, et al. (2008). "What predicts compliance rates with hip protectors in older hospital in-patients?" Age and ageing **37**(2): 225.

Hayes, W., E. Myers, et al. (1996). "Etiology and prevention of age-related hip fractures." Bone **18**(1): S77-S86.

Hayes, W., S. Piazza, et al. (1991). "Biomechanics of fracture risk prediction of the hip and spine by quantitative computed tomography." Radiologic Clinics of North America **29**(1): 1.

Ioannidis, G., A. Papaioannou, et al. (2009). "Relation between fractures and mortality: results from the Canadian Multicentre Osteoporosis Study." Canadian Medical Association Journal **181**(5): 265.

Kempson, G. (1982). "Relationship between the tensile properties of articular cartilage from the human knee and age." Annals of the Rheumatic Diseases **41**(5): 508.

Keyak, J., H. Skinner, et al. (2006). "Effect of force direction on femoral fracture load for two types of loading conditions." Journal of Orthopaedic Research **19**(4): 539-544.

Kuwahata, A., Y. Kawamura, et al. (2008). "Non-weight-bearing effect of trunk and peripheral fat mass on bone mineral density in pre-and post-menopausal women." Maturitas **60**(3-4): 244-247.

Laing, A. and S. Robinovitch (2008). "The Force Attenuation Provided by Hip Protectors Depends on Impact Velocity, Pelvic Size, and Soft Tissue Stiffness." Journal of biomechanical engineering **130**: 061005.

Laing, A. and S. Robinovitch (2009). "Low stiffness floors can attenuate fall-related femoral impact forces by up to 50% without substantially impairing balance in older women." Accident Analysis & Prevention **41**(3): 642-650.

Laing, A. and S. Robinovitch (2010). "Characterizing the effective stiffness of the pelvis during sideways falls on the hip." Journal of biomechanics.

Laing, A. C., I. Tootoonchi, et al. (2006). "Effect of compliant flooring on impact force during falls on the hip." Journal of Orthopaedic Research **24**(7): 1405-1411.

Langlois, J., M. Mussolino, et al. (2001). "Weight loss from maximum body weight among middle-aged and older white women and the risk of hip fracture: the NHANES I epidemiologic follow-up study." Osteoporosis International **12**(9): 763-768.

Lauritzen, J. and V. Askegaard (1992). "Protection against hip fractures by energy absorption." Danish medical bulletin **39**(1): 91.

Lauritzen, J., M. Petersen, et al. (1993). "Effect of external hip protectors on hip fractures." The Lancet **341**(8836): 11-13.

Lloyd, B., D. Williamson, et al. (2009). "Recurrent and injurious falls in the year following hip fracture: A prospective study of incidence and risk factors from the Sarcopenia and Hip Fracture study." The Journals of Gerontology Series A: Biological Sciences and Medical Sciences **64**(5): 599.

Lochmüller, E., O. Groll, et al. (2002). "Mechanical strength of the proximal femur as predicted from geometric and densitometric bone properties at the lower limb versus the distal radius." Bone **30**(1): 207-216.

Lochmüller, E. M., O. Groll, et al. (2002). "Mechanical strength of the proximal femur as predicted from geometric and densitometric bone properties at the lower limb versus the distal radius." Bone **30**(1): 207-216.

Maitland, L., E. Myers, et al. (1993). "Read my hips: measuring trochanteric soft tissue thickness." Calcified tissue international **52**(2): 85-89.

Majumder, S., A. Roychowdhury, et al. (2007). "Simulation of hip fracture in sideways fall using a 3D finite element model of pelvis-femur-soft tissue complex with simplified representation of whole body." Medical engineering & physics **29**(10): 1167-1178.

Maki, B. and G. Fernie (1990). "Impact attenuation of floor coverings in simulated falling accidents." Applied Ergonomics **21**(2): 107-114.

Marks, R., J. Allegrante, et al. (2003). "Hip fractures among the elderly: causes, consequences and control." Ageing research reviews **2**(1): 57-93.

Marshall, D., O. Johnell, et al. (1996). "Meta-analysis of how well measures of bone mineral density predict occurrence of osteoporotic fractures." British Medical Journal **312**(7041): 1254.

Melton, J. L. (1990). "A “Gompertzian” view of osteoporosis." Calcified tissue international **46**(5): 285-286.

Melton, L. (1993). "Hip fractures: a worldwide problem today and tomorrow." Bone **14**: 1-8.

Meyer, H., A. Tverdal, et al. (1998). "Weight Variability, Weight Change and the Incidence of Hip Fracture: A Prospective Study of 39000 Middle-aged Norwegians." Osteoporosis International **8**(4): 373-378.

Nankaku, M., H. Kanzaki, et al. (2005). "Evaluation of hip fracture risk in relation to fall direction." Osteoporosis International **16**(11): 1315-1320.

Nevitt, M. and S. Cummings (1993). "Type of fall and risk of hip and wrist fractures: the study of osteoporotic fractures. The Study of Osteoporotic Fractures Research Group." Journal of the American Geriatrics Society **41**(11): 1226.

Nevitt, M. C., S. R. Cummings, et al. (1991). "Risk factors for injurious falls: a prospective study." Journal of gerontology **46**(5): M164.

Nielson, C. M., M. L. Bouxsein, et al. (2009). "Trochanteric soft tissue thickness and hip fracture in older men." Journal of Clinical Endocrinology & Metabolism **94**(2): 491.

Pande, I., D. Scott, et al. (2006). "Quality of life, morbidity, and mortality after low trauma hip fracture in men." British Medical Journal **65**(1): 87.

Papadimitropoulos, E., P. Coyte, et al. (1997). "Current and projected rates of hip fracture in Canada." Canadian Medical Association Journal **157**(10): 1357.

Pulkkinen, P., F. Eckstein, et al. (2006). "Association of geometric factors and failure load level with the distribution of cervical vs. trochanteric hip fractures." Journal of Bone and Mineral Research **21**: 895-901.

Pulkkinen, P., T. Jämsä, et al. (2008). "Experimental hip fracture load can be predicted from plain radiography by combined analysis of trabecular bone structure and bone geometry." Osteoporosis International **19**(4): 547-558.

Ridgeway, B., B. E. Arias, et al. (2011). "The relationship between anthropometric measurements and the bony pelvis in African American and European American women." International Urogynecology Journal: 1-6.

Robinovitch, S., W. Hayes, et al. (1991). "Prediction of femoral impact forces in falls on the hip." Journal of biomechanical engineering **113**: 366.

Robinovitch, S., W. Hayes, et al. (1997). "Distribution of contact force during impact to the hip." Annals of biomedical engineering **25**(3): 499-508.

Robinovitch, S., W. Hayes, et al. (1997). "Predicting the impact response of a nonlinear single-degree-of-freedom shock-absorbing system from the measured step response." Journal of biomechanical engineering **119**: 221.

Robinovitch, S., T. McMahon, et al. (1995). "Force attenuation in trochanteric soft tissues during impact from a fall." Journal of Orthopaedic Research **13**(6): 956-962.

Sran, M. and S. Robinovitch (2008). "Preventing fall-related vertebral fractures: Effect of floor stiffness on peak impact forces during backward falls." Spine **33**(17): 1856.

Sran, M. M. and S. N. Robinovitch (2008). "Preventing fall-related vertebral fractures: effect of floor stiffness on peak impact forces during backward falls." Spine **33**(17): 1856.

Van den Kroonenberg, A., W. Hayes, et al. (1995). "Dynamic models for sideways falls from standing height." Journal of biomechanical engineering **117**: 309.

van den Kroonenberg, A., W. Hayes, et al. (1996). "Hip impact velocities and body configurations for voluntary falls from standing height." Journal of biomechanics **29**(6): 807-811.

Wiktorowicz, M., R. Goeree, et al. (2001). "Economic implications of hip fracture: health service use, institutional care and cost in Canada." Osteoporosis International **12**(4): 271-278.

Woo, S., K. Ohland, et al. (1990). "Aging and sex-related changes in the biomechanical properties of the rabbit medial collateral ligament." Mechanisms of ageing and development **56**(2): 129-142.